DEVELOPMENT OF OPTICAL SENSOR BASED ON COLORIMETRIC DYE ARRAY AND DIVERSITY ORIENTED FLUORESCENCE LIBRARY APPROACH

KRISHNA KANTA GHOSH

(M. Sc., Indian Institute of Technology Madras, Chennai, India)

A THESIS SUBMITTED

FOR THE DEGREE OF DOCTOR OF PHILOSOPHY

DEPARTMENT OF CHEMISTRY

NATIONAL UNIVERSITY OF SINGAPORE

2012

Thesis Declaration

The work in this thesis is the original work of Krishna Kanta Ghosh, performed independently under the supervision of Professor Young Tae Chang, (in the Chemical Bioimaging Lab, S9-03-03), Chemistry Department, National University of Singapore, between 08/08/2008 and 04/08/2012.

The content of the thesis has been partly published in:

1) Ghosh, K. K., Yap, E., Kim, H., Lee, J. S., and Chang, Y. T. (2011) A colorimetric pH indicators and boronic acids ensemble array for quantitative sugar analysis. *Chem. Commun. 47*, 4001-3.
2) Ghosh, K. K., Ha, H. H., Kang, N. Y., Chandran, Y., and Chang, Y. T. (2011) Solid phase combinatorial synthesis of a xanthone library using click chemistry and its application to an embryonic stem cell probe. *Chem. Commun. 47*, 7488-90.

Name	Signature	Date

ACKNOWLEDGEMENTS

Foremost, I would like to express my heartfelt gratitude to my supervisor, Professor Young-Tae Chang for his thoughtful guidance, lots of patience, motivation, and enthusiasm during the last four years. His encouragement always facilitate me to learn innovative things in the scientific field and to overcome difficult challenges.

I would also to express my sincere gratitude to Dr. Ha Hyung-Ho for his valuable guidance, great support, and continuous help during my graduate study. There are no sufficient words to express my gratitude to him. My sincere appreciation also goes to Dr. Marc Vendrell, Dr . Jun-Seok Lee, Dr. Kaustabh Kumar Maiti and Dr. Kang Nam-Young, for their kind support, guidance and continuous encouragement.

I am thankful to all the past and present members of our lab whose contribution made this journey really enjoyable in each and every step of my research life. Words are insufficient to express my sincere thanks for being such helpful and cooperative lab-mates to Dr. Yun Seong Wook ,Dr. Sung Chan Lee, Dr. Yun-Kyung Kim, Dr. Kim Hanjo, Feng Suihan, Kelly, Dr. Sung Jin Park, Dr. Junyoung Kim, Dr. Woo Sirl Lee, Dr. Satoshi Arai, Dr. Li Xin, Dr. Yoo Jung Sun, Dr. Jiyeon Ock, Dr. Kim Jinmi, Dr. Taslima Khanam, Dr. Teoh Chai Lean, Chang Liang, Dr. Kale, Dongdong, Xu Wang, Samira, MyungWon, Yoges, Meiling, Cheryl, Emmiline, Jow Zhi Yen, Chee Geng, Physilia, Jimmy, Pamela, Fronia, Eunice and Keenth.

My special thanks go to Dr. Animesh Samanta, Duanting, Raj Kumar, and Bikram who always support me like my family member during my Phd. These memorable days will remain as a sweet memory forever.

I take this opportunity to thank all of my friends and juniors who helped my dreams come true. I am thankful to Tanay, Mainakda, Pasarida, Gautam, Pradipta, Kausik, Sadanandada, Amarenduda, Subhankar, Srimanta, Asim, Hriday, Sudiptada, Sabyasachi, Nimai, Bijay and Jhinukdi who made my stay at NUS so pleasant.

Financial and technical support from the Department of Chemistry of the National University of Singapore (NUS) is greatly acknowledged. I would like to thank all the staffs in chemistry administrative office, Lab-supplies for their immense support.

Finally, I would like to express my deepest gratitude towards my parents, my brother, sister, brother in-law. I think that without their continuous support and constant inspiration this thesis would not have been completed.

At last I would like to heartily thank God for giving me the patience, faith and strength to complete my thesis.

Table of Contents

Summary

Depending on the nature of the optical sensors this thesis is accomplished in three main chapters: (a) strategies of single molecule sensor development for biological application, (b) strategies of combined fluorescent molecules i.e. FRET based sensor development and (c) combinatorial sensing approach to discriminate highly cross reactive analytes.

In chapter 2, the synthesis of two diversity-oriented fluorescent xanthone libraries (CX and AX) is explored. For the rapid and efficient synthesis of these xanthone libraries a solid phase methodology was successfully adopted. These libraries were further diversified to their corresponding acetyl (CXAC and AXAC) and chloroacetyl (CXCA and AXCA) derivatives. In order to evaluate their photophysical properties, full spectral characterisations were carried out for all the library compounds. With the interest to develop a stem cell selective blue fluorescent probe we screened the CX, CXCA and CXAC libraries against mouse embyronic stem cells and identified one compound CXAC 59, that selectively stains mESC over MEF and other differentiated cells. This novel stem cell selective blue fluorescent probe was thereby named CDb8 (compound of designation blue).

The synthesis of three FRET based fluorescent libraries were demonstrated in Chapter 3. CX and AX compounds are coupled with suitable green and yellow fluorescence emitting BODIPY compounds to generate their corresponding FRET libraries - CXBD, AXBD and AXBY. In this synthetic design, a solid phase activated ester chemistry was implemented for the facile synthesis of FRET libraries. After evaluation of their photo-physical properties we observed that these molecules possess

mega stock shifts with an average energy transfer of 95% from xanthone (donor) to BODIPY (acceptor).

In the chapter 4, we utilized the concept of combinatorial sensing strategy to develop an artificial tongue for discrimination of three different sugars- glucose, fructose and sucrose quantitatively. This artificial tongue was constructed with an ensemble of 11 pairs of probes selected from the initial combination of 39 off-the-shelf dyes and 7 commercially available boronic acids. Each probe consists of a dye molecule coupled to a boronic acid. One particular probe is not sensitive or specific enough to discriminate all the sugars. However, the combined response from the dye array provides an indicative fingerprint to discriminate glucose, fructose and sucrose quantitatively. Furthermore, these colorimetric dyes and boronic acids ensemble array were used to quantify the glucose level in real sample-saline. This result demonstrates the practical applicability of the combinatorial sensing approach.

List of Tables

List of Figures

Chapter 1

Chapter 2

Chapter 3

Chapter 4

List of Charts

Chapter 2

List of Schemes

Abbreviation of symbols

AcOH	Acetic acid
Ac_2O	Acetic anhydride
ACN	Acetonitrile
BSA	Bovine serum albumin
BuOH	Butanol
$CDCl_3$	Deuterated chloroform
$CHCl_3$	Chloroform
CO_2	Carbondioxide
D_2O	Deuterated oxide
DAD	Diode array detector
DCC	N,N'-Dicyclohexylcarbodiimide
DCM	Dichloromethane
DIC	N,N'-Diisopropylcarbodiimide
DIEA	Diisopropyl ethylamine
DMAP	Dimethylaminopyridine
DMF	N, N-Dimethylformamide
DMSO	Dimethyl sulfoxide
DMSO-d6	Deuterated dimethyl sulfoxide
DOS	Diversity oriented synthesis
DOFLA	Diversity oriented fluorescence library approach
EA	Ethyl acetate
ESI	Electrospray ionization
Ex	Excitation

Em	Emission
FRET	Fluorescence resonance energy transfer
HATU	2-(1H-7-Azabenzotriazol-1-yl) 1,1,3,3-tetramethyl uronium hexafluorophosphate methanaminium
HCl	Hydrochloric acid
HEPES	4-(2-Hydroxyethyl)-1-piperazineethanesulfonic acid
HPLC	High-performance liquid chromatography
HPLC-MS	High-performance liquid chromatography mass spectrometry
HTS	High throughput screening
MEF	Mouse Embryonic Fibroblast
mESC	Mouse Embryonic Stem Cell
MeOH	Methanol
MeOD	Deuterated methanol
MeCN	Acetonitrile
MS	Mass spectrometry
NMR	Nuclear magnetic resonance
Q	Quantum yield
RT	Room temperature
TFA	Trifluoroacetic acid
THF	Tetrahydrofuran
TLC	Thin layer chromatography
TOS	Target oriented synthesis
TRITC	Tetramethylrhodamine-5-isothiocyanate
UV	Ultraviolet

List of publications

1. **Ghosh, K. K.,** Yap, E., Kim, H., Lee, J. S., and Chang, Y. T. (2011) A colorimetric pH indicators and boronic acids ensemble array for quantitative sugar analysis. *Chem. Commun. 47*, 4001-3.
2. **Ghosh, K. K**., Ha, H. H., Kang, N. Y., Chandran, Y., and Chang, Y. T. (2011) Solid phase combinatorial synthesis of a xanthone library using click chemistry and its application to an embryonic stem cell probe. *Chem. Commun. 47*, 7488-90.
3. Vendrell, M., Krishna, G. G., **Ghosh, K. K**., Zhai, D., Lee, J. S., Zhu, Q., Yau, Y. H., Shochat, S. G., Kim, H., Chung, J., and Chang, Y. T. (2011) Solid-phase synthesis of BODIPY dyes and development of an immunoglobulin fluorescent sensor. *Chem. Commun. 47*, 8424-6.
4. Das, R. K.; Samanta, A.; **Ghosh, K. K**; Zhai, D.; Xu, W.; Su, D.; Leong, C.; Chang, Y. T.(**2011)** Target Identification: A Challenging Step in Forward Chemical Genetics *Interdiscip. Bio Central*, *3*, 1-16.

Chapter 1

1.1 Overview of optical sensor

A sensor[1] is an analytical device for monitoring the concentration or any other physical quantity of an analyte in a continuous and reversible manner. To date, three major classes of sensors are widely used- mechanical, electrochemical and optical sensors. Although the use of mechanical and electrochemical sensors has been demonstrated for a long time, the application of optical sensors is more recent. Several research groups have demonstrated the potential application of optical sensing in a variety of research fields including environmental monitoring[2], process control[3], and *in vivo* sensing[4]. Presently, industries and universities are placing significant efforts into developing sensitive and specific optical sensors. According to the nature of the signal used for optical sensing, these sensors are classified as absorbance, reflectance, fluorescence, Raman, and Infrared sensors. The signal of optical sensors is usually derived from intrinsic or extrinsic optical signals. In intrinsic optical signal detection, the spectral properties of an analyte itself are used for its determination. For example, the colour of blood was used to measure the oxygen level in blood or the fluorescence of chlorophyll was used to determine the rate of photosynthesis. If the analyte does not show any changes in optical properties, an indicator or label is used to transduce the analyte concentration into an useful optical signal (e.g. pH and oxygen sensors). Usually, optical sensors have several advantages over the electrochemical and mechanical sensors.

- Optical sensors are insensitive towards high pressure and magnetic fields. Besides, the optical sensors have no electrical interferences and no additional reference element is required like an electrode.

- Optical sensors have a small dynamic range but they have a much higher resolution compared to their mechanical or electrochemical counterparts. In addition, the optical signals can transmit more information than electrical signals.
- An optical sensor can be used to analyse multicomponent samples by using an array of sensors.
- Optical sensors are usually non-invasive and also they can be used as disposable sensors.

This thesis is mainly focussed on the development of fluorescent and colorimetric (absorbance) based optical sensors.

1.2 Fluorescent spectroscopy and fluorophores

Fluorescent molecules have drawn considerable interest due to their huge application in the development of chemosensors[5], luminenescence devices[6] and bio-imaging agents[7]. Fluorescence[8] is a phenomena in which a dye molecule absorbs a light of a specific wavelength in the UV-visible region. Upon reaching an electronically excited singlet state, it emits a part of the excess energy in the form of radiation at a longer wavelength. Most of the molecules cannot emit their excess energy in the form of radiation upon excitation due to the loss of energy through non-fluorescent mechanisms (e.g. vibrational relaxation, collision with the media etc). However, some molecules are able to decay their excess energy in the form of radiation, thus showing the fluorescent properties. Among these molecules the most representative fluorescent scaffolds are BODIPY[9], rosamine[10], fluorescein[11], coumarin[12], dapoxyl[13], dansyl[14], NBD[15], cyanine[16], pyrene[17], styryl[18], xanthone[19], and oxazine[20]. Interestingly, these limited number of fluorescent scaffolds cover almost all colours in the spectrum from UV-visible to near-infrared (NIR).(Figure 1.1)

The most important properties of fluorescent small molecules are their exceptionally high sensitivity and specificity. As such, fluorescent sensor molecules are now widely used in chemistry, biology and environmental sciences. There are two different ways for the development of fluorescent sensor. 1) Target Oriented Approach 2) Diversity Oriented Approach.

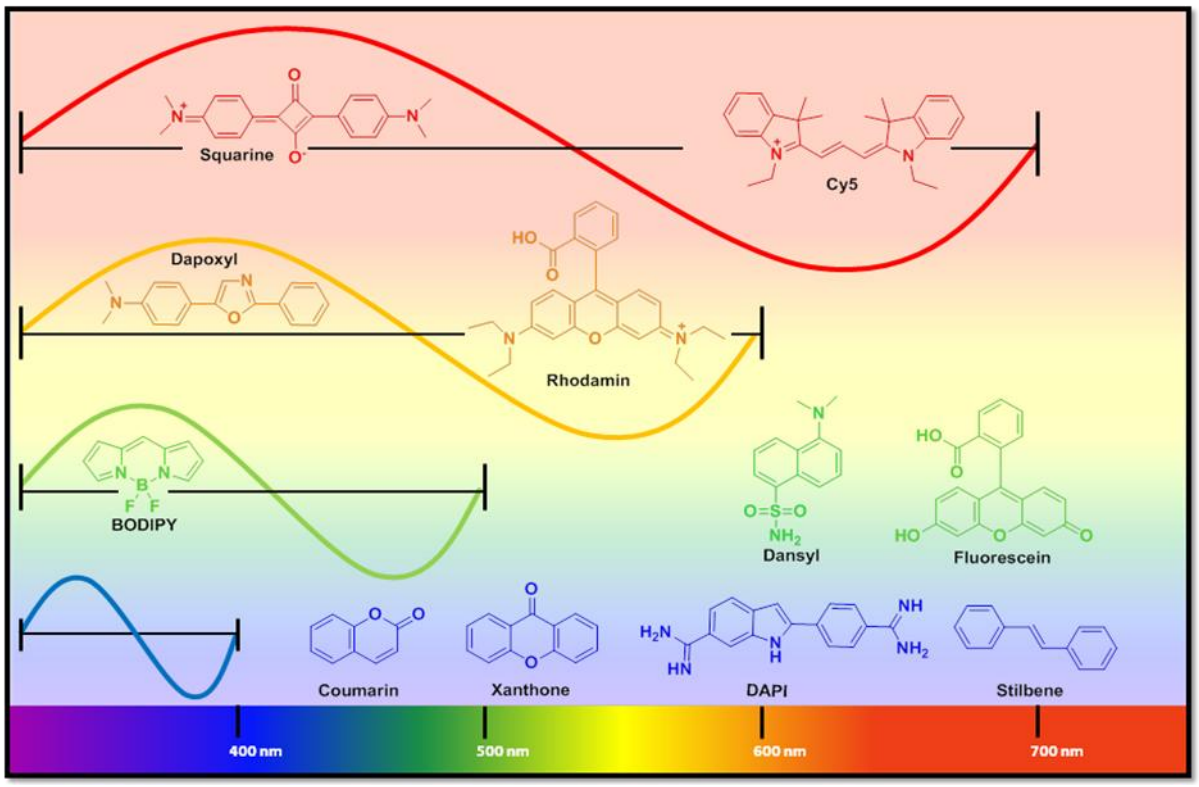

Figure 1.1. Emission spectral range of representative fluorophores.

1.3 Synthetic strategies for novel fluorescent sensors

1.3.1 Target oriented synthesis of fluorescent sensors

A general strategy for probes development is the target-oriented approach[21-22] (TOS), based on the concept of known molecular recognition mechanisms for an individual analyte. In this conventional approach, the target recognition moiety of the molecule is designed on the basis of empirical knowledge and the fluorophore is simply used as a signal amplifier (Figure 1.2). Using this knowledge-based architecture, numerous fluorescent sensors have been developed for metal ions [23-24], nitric oxide[25], H_2O_2[26], peroxynitrile[27], highly reactive oxygen species[28], singlet oxygen[29] etc (Figure 1.3). However the speed and the scope of this method of sensor development is limited as this conventional design of the probes often fails when applied to the complex biological systems. To date, only a few recognition moieties have been reported, such as derivatives of crown esters, ethylenediamines, acetates, and pyridines, amongst others[30].

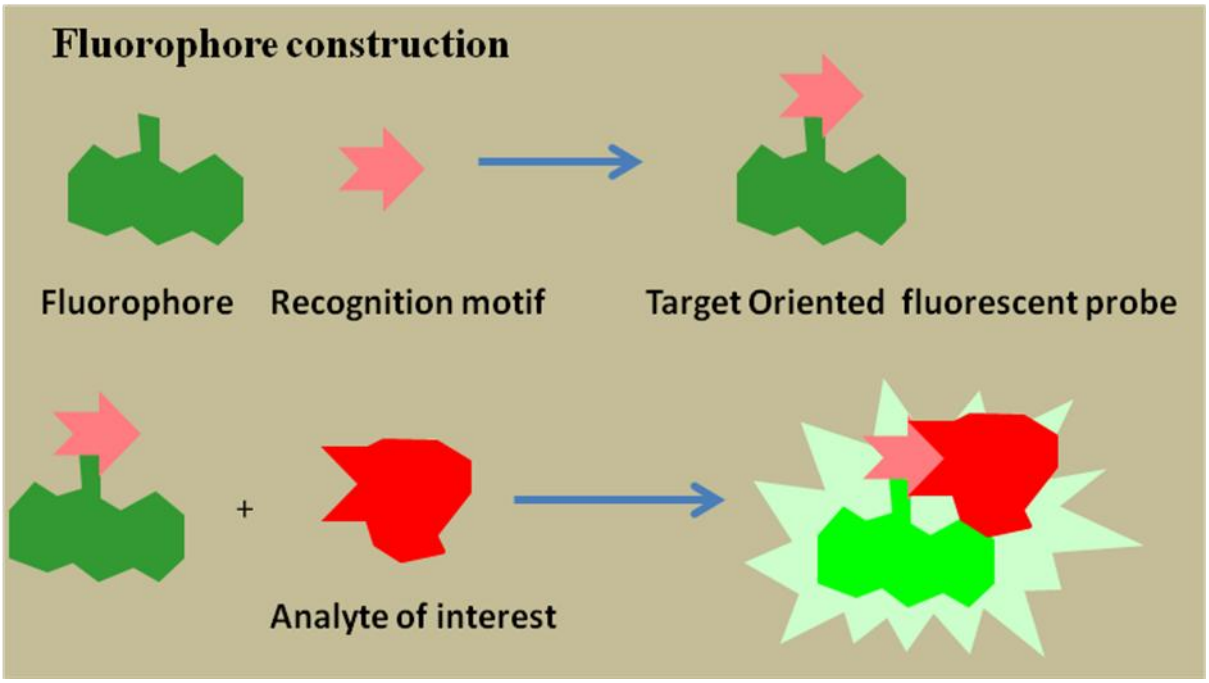

Figure 1.2. Schematic diagram for Target oriented fluorescent sensor design

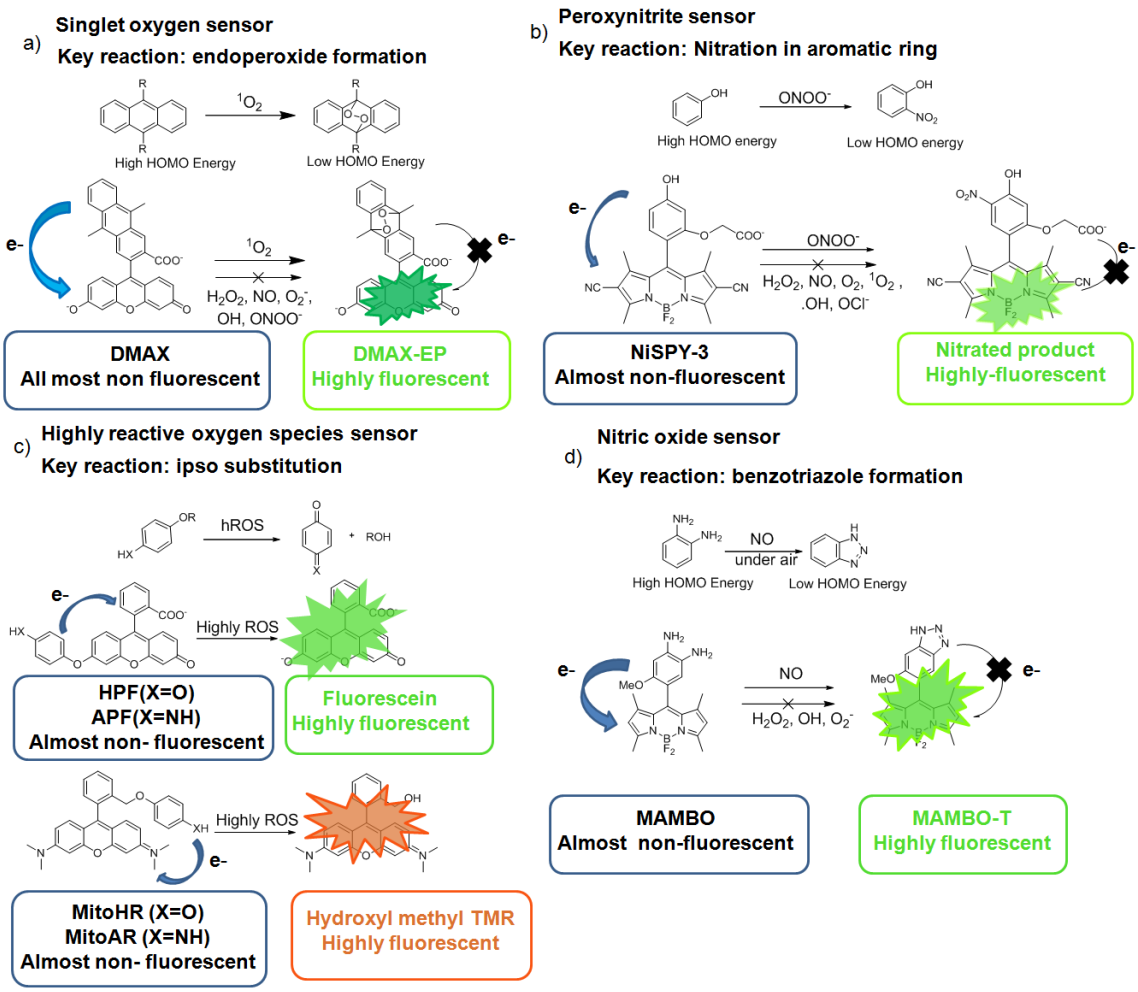

Figure 1.3. Representative examples of Target oriented fluorescent sensor development. (a) singlet oxygen[29] sensor (b) peroxynitrile[27] sensor (c) highly reactive oxygen species[28] sensor (d) nitric oxide[25] sensor

1.3.2 Diversity-oriented synthesis of fluorescent sensors

To overcome these limitations of TOA, several research groups have started working on diversity-oriented fluorescence library approaches[31] (DOFLA) for the development of fluorescent optical sensors. In DOFLA, new fluorescent probes are developed without prior knowledge about the target recognition mechanism and the fluorescent dye library is unbiased to any specific target analyte. These fluorescent libraries are designed and synthesized in a short time, either by solution or solid phase

organic synthesis (SPOS). Once the libraries are synthesized, individual analyte molecules are tested in a high-throughput screening manner. DOFLA introduces structural diversity into the fluorescent scaffolds[32] so that the fluorescence properties of the final products are affected by the diversity of the substituent. Since a broad chemical diversity can be incorporated, a large number of molecular interactions can be potentially identified. Additionally, multiple sensors can be discovered from a single library. (Figure 1.4)

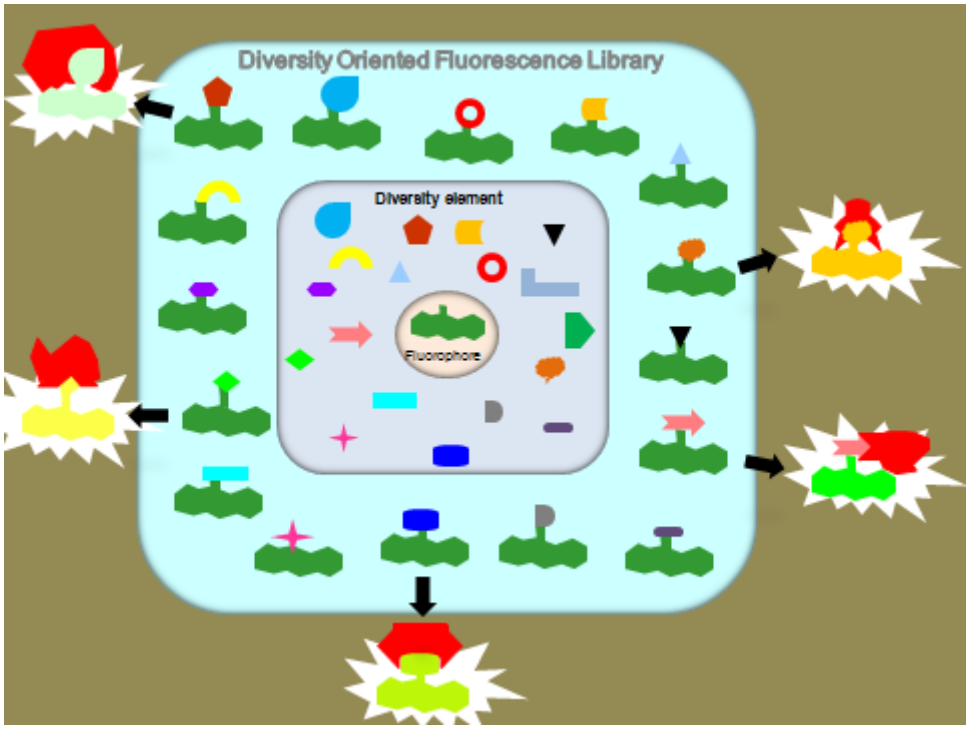

Figure 1.4. Schematic diagram for Diversity oriented fluorescent sensor design

Bäuerle and co-workers first synthesized the diversity oriented fluorescent libraries by derivatizing a coumarin scaffold using palladium-catalyzed cross coupling reactions[33]. These derivatives not only have structural differences but also have different photo physical properties like excitation, emission wavelengths, extension coefficients and quantum yields. A separate diversity oriented rhodol library was reported by Peng and Yang as having a very diverse photophysical properties[34]. A styryl and a BODIPY

library have been also been reported by Chang and co-workers with the potential to serve as live cell imaging probes. In addition to this Chang et al. have also synthesized several diversity oriented libraries including rosamine, cyanine, chalcone, dapoxyl, bemzimidazol, libraries and evaluated their photophysical properties as well as their applications in optical sensors development. Recently, the supremacy of DOFLA has been demonstrated by several research groups by further developing the optical probes for a variety of target analytes including glucagon[35], DNA[36], GTP[37], β-amyloid[38], Heparin[39], glutathione[40], human serum albumin[41], embryonic stem cell probe[42], etc.

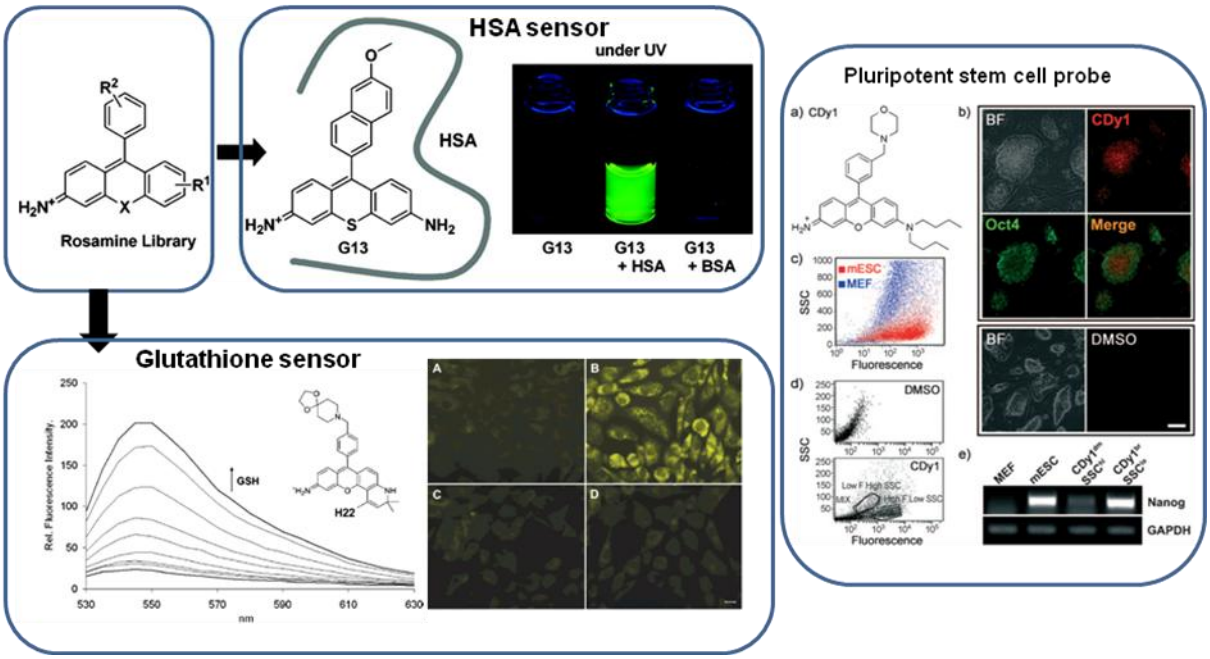

Figure 1.5. Synthesis of Diversity-oriented fluorescent rosamine library and development of optical sensor for HSA[41], Glutathione[40] and pluripotent stem cell probe[42].

1.4 Solid phase synthesis of fluorescent molecules

To synthesize a library of fluorescent molecules in a highly efficient manner, it is required to develop an efficient synthetic methodology. Several solution phase parallel synthesis of dye molecules have already been reported in the literature, however this includes tedious purification steps with typically low recovery yields. This limitation can be overcome for the synthesis of individual compounds, but it would seriously hamper the combinatorial derivatization of the fluorescent scaffold, which require labour intensive purification processes. In order to overcome these challenges, solid-phase methodologies[43] have been successfully applied for the diversification of fluorescent scaffolds that involve challenging purification steps. Solid phase synthesis is a methodology where one of the reactant molecule that is attached to an insoluble material i.e., the solid support, undergoes a transformation to form the products. This solid phase synthesis was first developed by Merrifield for peptide synthesis[44], later it was used for oligonucleotide synthesis[45]. Now solid phase synthesis is widely used in combinatorial chemistry for the development of large number of molecules in a relatively short time. Solid phase synthesis helps to overcome the technical difficulties associated with the solubility and purification. In this synthetic strategy, purification is simply done by washing the resin with a variety of solvents. By using suitable solvents or solvent mixtures all the unbound impurities and the excess solution phase reagent can be washed away completely. Another advantage of this solid phase synthesis is that by using an excess amount of reagent, the reaction can be driven to completion to provide higher yields. Recently, several combinatorial fluorescent dye libraries have been synthesized using solid support. Chang et al. have published combinatorial fluorescent libraries including rosamine[40], styryl[38], BODIPY[46] and dapoxyl[47] using solid phase chemistry. Encouraged by these, we have adopted the solid phase synthesis for the combinatorial diversification of fluorescent xanthone scaffold using click chemistry.

1.5 Click Chemistry for fluorescent library synthesis

Click chemistry[48] is a concept rather than a single reaction. A click reaction usually follows relatively simpler reaction conditions but has a broader range of applications. Click reaction has high yield and produces a minimum amount of easily removable by-products[49-50]. There are four major classes of reactions that are known to follow the criteria of click chemistry: nucleophilic ring opening reactions, non-aldol type carbonyl chemistry, additions to carbon–carbon multiple bonds and cycloaddition reactions. Among these reactions the Huisgen 1,3-dipolar cycloaddition[51] between an azide and a terminal alkynes is one of the most popular click reactions due to its high yield, superior stereoselectivity and biocompatibility[52-53]. One of the most important features of the reaction is the formation of 1,2,3- triazole moiety. The triazole moiety is quite stable in both acidic and basic conditions. It is also resistant to metabolic degradation which is an important feature of a probe[54]. Due to the simplicity and biocompatibility of the click reaction, it is also widely used in different research field, including dendrimer and polymer grafting,[55–57] synthesis[58-59] and in chemical ligation[60-61]. In addition, click chemistry is also used in the synthesis of peptidomimetics [62- 63], in bioconjugations[64–66], surface chemistry[67], metal chelating system[68]. In recent times, numerous combinatorial fluorescent dye libraries including coumarins,[69] carbostyrils,[18] anthracenes,[70] naphthalimides[71] and pyridyloxazoles[72] have been published where the click chemistry has been used to introduce the diversity in the molecules.

1.6 Combinatorial sensing strategy and colorimetric sensor array

As discussed earlier, the most conventional approaches for chemical sensor discoveries consist of the designing of a 'Lock-and-Key' system where a specific receptor is attached to the sensor molecule which can strongly and selectively bind to the analyte of interest[73]. In this approach the selectivity is achieved through the recognition of the analyte at the receptor site. A similar approach for the sensor discoveries involves the use of a physicochemical effect that is selective for a particular target analyte. An example of this approach is the construction of a pH electrode using the selective ionic effect. In this design, the selectivity is obtained through the transduction process in which the method of detection dictates which species are sensed. Both the above approaches are useful when a fixed target is to be analysed in the presence of controlled backgrounds and interferences. However, this type of approach requires the synthesis of a separate, highly selective sensor for the detection of an individual analyte. In addition, this is not particularly useful for analyzing and classifying a complex mixtures or some highly cross reactive analytes because in these cases the ‘lock’ could able to fit with a number of similar kind of ‘keys’. As an alternative to the conventional sensing strategy, many researchers are now using an array of sensors instead of a single sensor[74-75]. In this alternative sensor architecture, an array of different sensors is used, with every element in the sensor array chosen to respond to a number of different chemicals or classes of chemicals. The collection of sensors should contain as much chemical diversity as possible, so that the array responds to the largest possible cross-section of analytes[76]. In this design, the response of a single sensor was unable to identify and classify the analytes of interest but the response of the collection of sensors in the array can provide an unique fingerprint for each analyte which allows the further classification and identification of these analytes

(Figure 1.6). However most of chemical sensors suffer in selectivity due to the interference from a number of structurally or chemically similar analytes. Series of chemical sensor arrays has been reported in last decade which serves for the analysis and classification of different classes of analytes. In particular, Suslick group developed a conventional optical sensor array by immobilizing dyes on a hydrophobic membrane which was able to discriminate various chemicals including amines[77-78]. As a simple detection platform, Sessler and co-workers demonstrated a colorimetric anion sensor composed of commercial dyes which can discriminate anions simply by naked eye color change detection[79]. These reports successfully demonstrate the potential discrimination power of colorimetric sensors. Although there are several reports where the sensor array can discriminate several different sugars, till date no sensor array that is capable of discriminating the sugars quantitatively has been reported. Here, in chapter 3, we embarked on a challenge to develop methods with the potential to discriminate three different sugars, glucose, fructose and sucrose quantitatively using a combinatorial sensing strategy.

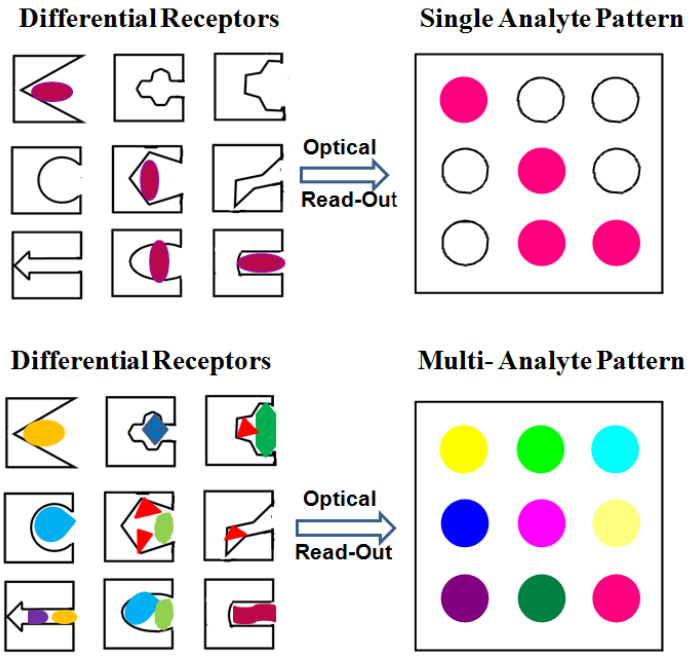

Figure 1.6. Schematic diagram of combinatorial sensing strategy of differential sensory

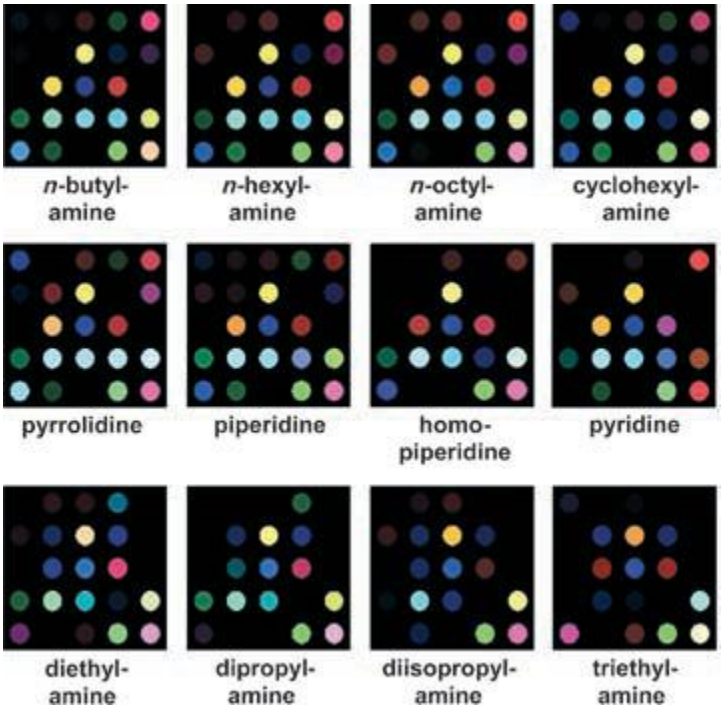

Figure 1.7. Representative example of cross reactive sensor array for discrimination of amines[79]

1.7 Scope and Outline of the thesis

We discussed earlier the different strategies to develop the optical sensors. We have also highlighted diverse applications of the optical sensors. In this thesis, our main focus is to develop *in vitro* optical sensors and live cell imaging probes based on a diversity-oriented fluorescent library approach and colorimetric sensor array.

The aims for this thesis project are-

- To develop a novel synthetic strategy for the construction of a diversity-oriented fluorescent xanthone library (CX). In this synthetic strategy, click chemistry has been used for the combinatorial diversification of the fluorescent xanthone core. A solid phase methodology was successfully applied for the facile synthesis of a large number of compounds in a relatively short time. The incorporation of an acetyl or a chloroacetyl moiety to the CX library generates its corresponding CXAC and CXCA library. In order to explore the photo physical properties of CX, CXCA and CXAC compounds, full spectral characterisation was also carried out. To facilitate the identification of new blue fluorescent bioimaging probes CX, CXAC and CXCA compounds were then screened against mouse embryonic stem cells (mESC). One of the compounds, CDb8 was identified as a probe that selectively stains in mESC over MEF (mouse embryonic fibroblast).
- To systematically evaluate xanthone's photophysical properties and its applications in bio imaging, we have developed a second generation of xanthone library (AX) using acid chloride diversity. 80 AX compounds were synthesized using solid phase chemistry. This library is also further diversified to AXAC and AXCA libraries.
- To design and synthesize the first FRET based fluorescent libraries using CX and AX compounds. We have adopted a solid phase methodology to construct

the FRET based green fluorescent libraries namely AXBD and CXBD. 78 members AXBD and 70 members CXBD compounds were synthesized by combining a common BODIPY compound with respective AX and CX compounds. Utilising the same synthetic strategy as AXBD or CXBD, another FRET based library was developed which shows fluorescence in the yellow colour region. In order to demonstrate the photophysical properties, spectral characterisation were carried out. These mega stock shift dyes have almost more than 95% energy transfer from donor to acceptor.

- To develop an artificial tongue for the sugars which can quantitatively discriminate among glucose, fructose and sucrose. This tongue was successfully applied for the qualitative discrimination of sugar mixtures. With the interest to evaluate the practical applications of this artificial tongue, a real sample saline was tested and its exact sugar content quantified.

1.8 References

1. Stetter, J. R., Penrose, W. R., and Yao, S. (2003) Sensors, Chemical Sensors, Electrochemical Sensors, and ECS. *Journal of The Electrochemical Society 150*, S11-16

2. Clifford K. Ho., Robinson, A., Miller D. R., and Davis. M J. (2005) Overview of Sensors and Needs for Environmental Monitoring. *Sensors* 5, 4-37.

3. Wold, J. P., Jorgensen, K., and Lundby, F. (2002) Nondestructive measurement of light-induced oxidation in dairy products by fluorescence spectroscopy and imaging. *Journal of dairy science 85*, 1693-704.

4. Samanta, A., Vendrell, M., Yun, S. W., Guan, Z., Xu, Q. H., and Chang, Y. T. (2011) A photostable near-infrared protein labeling dye for in vivo imaging. *Chemistry, an Asian journal 6*, 1353-7.

5. Martinez-Manez, R., and Sancenon, F. (2003) Fluorogenic and chromogenic chemosensors and reagents for anions. *Chemical reviews 103*, 4419-76.

6. Electrogenerated Chemiluminescence and Proton-Dependent Switching of Fluorescence: Functionalized Difluoroboradiaza-*s*-indacenes Kollmannsberger, M., Gareis, T., Heinl, S., Breu J., and Daub, J. (1997) *Angew Chem Int Edit 36*, 1333-35

7. Que, E. L., Domaille, D. W., and Chang, C. J. (2008) Metals in neurobiology: probing their chemistry and biology with molecular imaging. *Chemical reviews 108*, 1517-49.

8. Lakowicz, J.R. (2006) Principles of fluorescenc spectroscopy, *Third Edition. Springer*

9. Wang, T. Y., and Silvius, J. R. (2000) Different sphingolipids show differential partitioning into sphingolipid/cholesterol-rich domains in lipid bilayers. *Biophysical journal 79*, 1478-89.

10. Tokimoto, T., Tsukahara, S., and Watarai, H. (2005) Lactone cleavage reaction kinetics of rhodamine dye at liquid/liquid interfaces studied by micro-two-phase sheath flow/two-photon excitation fluorescence microscopy. *Langmuir : the ACS journal of surfaces and colloids 21*, 1299-304.

11. Pham, W., Xie, J., and Gore, J. C. (2007) Tracking the migration of dendritic cells by in vivo optical imaging. *Neoplasia 9*, 1130-7.

12. Fischer, D., Theodorakis, E. A., and Haidekker, M. A. (2007) Synthesis and use of an in-solution ratiometric fluorescent viscosity sensor. *Nature protocols 2*, 227-36.

13. Petchprayoon, C., Suwanborirux, K., Tanaka, J., Yan, Y., Sakata, T., and Marriott, G. (2005) Fluorescent kabiramides: new probes to quantify actin in vitro and in vivo. *Bioconjugate chemistry 16*, 1382-9.

14. Davies, P. J., Cornwell, M. M., Johnson, J. D., Reggianni, A., Myers, M., and Murtaugh, M. P. (1984) Studies on the effects of dansylcadaverine and related compounds on receptor-mediated endocytosis in cultured cells. *Diabetes care 7 Suppl 1*, 35-41.

15. Yang, S., Feng, G., and Williams, N. H. (2012) Highly selective colorimetric sensing pyrophosphate in water by a NBD-phenoxo-bridged dinuclear Zn(ii) complex. *Organic & biomolecular chemistry 10*, 5606-12.

16. Mujumdar, R. B., Ernst, L. A., Mujumdar, S. R., Lewis, C. J., and Waggoner, A. S. (1993) Cyanine dye labeling reagents: sulfoindocyanine succinimidyl esters. *Bioconjugate chemistry 4*, 105-11.

17**.** Halleux, V.de, Mamdouh, W., Feyter, S. De., Schryver, F. De., Levin, J., Geerts, Y. H.(2006) Emission Properties of a Highly Fluorescent Pyrene Dye in Solution and in the Liquid State. *J. Photochem. Photobiol. A 178*, 251-257

18. Rubner, M. M., Holzhauser, C., Bohlander, P. R., and Wagenknecht, H. A. (2012) A "clickable" styryl dye for fluorescent DNA labeling by excitonic and energy transfer interactions. *Chemistry 18*, 1299-302.

19. Li, J., Hu, M., and Yao, S. Q. (2009) Rapid synthesis, screening, and identification of xanthone- and xanthene-based fluorophores using click chemistry. *Organic letters 11*, 3008-11.

20. Vogelsang, J., Cordes, T., Forthmann, C., Steinhauer, C., and Tinnefeld, P. (2009) Controlling the fluorescence of ordinary oxazine dyes for single-molecule switching and superresolution microscopy. *Proceedings of the National Academy of Sciences of the United States of America 106*, 8107-12.

21. Martinez-Manez, R., and Sancenon, F. (2003) Fluorogenic and chromogenic chemosensors and reagents for anions. *Chemical reviews 103*, 4419-76.

22. Suksai, C., and Tuntulani, T. (2003) Chromogenic anion sensors. *Chemical Society reviews 32*, 192-202.

23. Taki, M., Iyoshi, S., Ojida, A., Hamachi, I., and Yamamoto, Y. (2010) Development of highly sensitive fluorescent probes for detection of intracellular copper(I) in living systems. *Journal of the American Chemical Society 132*, 5938-9.

24. Taki, M., Desaki, M., Ojida, A., Iyoshi, S., Hirayama, T., Hamachi, I., and Yamamoto, Y. (2008) Fluorescence imaging of intracellular cadmium using a dual-excitation ratiometric chemosensor. *Journal of the American Chemical Society 130*, 12564-5.

25. Gabe, Y., Urano, Y., Kikuchi, K., Kojima, H., and Nagano, T. (2004) Highly sensitive fluorescence probes for nitric oxide based on boron dipyrromethene chromophore-rational design of potentially useful bioimaging fluorescence probe. *Journal of the American Chemical Society 126*, 3357-67.

26. Dickinson, B. C., and Chang, C. J. (2008) A targetable fluorescent probe for imaging hydrogen peroxide in the mitochondria of living cells. *Journal of the American Chemical Society 130*, 9638-9.

27. Ueno, T., Urano, Y., Kojima, H., and Nagano, T. (2006) Mechanism-based molecular design of highly selective fluorescence probes for nitrative stress. *Journal of the American Chemical Society 128*, 10640-1.

28. Setsukinai, K., Urano, Y., Kakinuma, K., Majima, H. J., and Nagano, T. (2003) Development of novel fluorescence probes that can reliably detect reactive oxygen species and distinguish specific species. *The Journal of biological chemistry 278*, 3170-5.

29. Tanaka, K., Miura, T., Umezawa, N., Urano, Y., Kikuchi, K., Higuchi, T., and Nagano, T. (2001) Rational design of fluorescein-based fluorescence probes. Mechanism-based design of a maximum fluorescence probe for singlet oxygen. *Journal of the American Chemical Society 123*, 2530-6.

30. Rurack, K., and Resch-Genger, U. (2002) Rigidization, preorientation and electronic decoupling--the 'magic triangle' for the design of highly efficient fluorescent sensors and switches. *Chemical Society reviews 31*, 116-27.

31. Mello, J. V., and Finney, N. S. (2005) Reversing the discovery paradigm: a new approach to the combinatorial discovery of fluorescent chemosensors. *Journal of the American Chemical Society 127*, 10124-5.

32. Finney, N. S. (2006) Combinatorial discovery of fluorophores and fluorescent probes. *Current opinion in chemical biology 10*, 238-45.

33. Schiedel, M. S., Briehn, C. A., and Bauerle, P. (2001) Single-Compound Libraries of Organic Materials: Parallel Synthesis and Screening of Fluorescent Dyes. *Angew Chem Int Ed Engl 40*, 4677-4680.

34. Peng, T., and Yang, D. (2010) Construction of a library of rhodol fluorophores for developing new fluorescent probes. *Organic letters 12*, 496-9.

35. Lee, J. S., Kang, N. Y., Kim, Y. K., Samanta, A., Feng, S., Kim, H. K., Vendrell, M., Park, J. H., and Chang, Y. T. (2009) Synthesis of a BODIPY library and its application to the development of live cell glucagon imaging probe. *Journal of the American Chemical Society 131*, 10077-82.

36. Lee, J. W., Jung, M., Rosania, G. R., and Chang, Y. T. (2003) Development of novel cell-permeable DNA sensitive dyes using combinatorial synthesis and cell-based screening. *Chem Commun (Camb)*, 1852-3.

37. Li, Q., and Chang, Y. T. (2006) A protocol for preparing, characterizing and using three RNA-specific, live cell imaging probes: E36, E144 and F22. *Nature protocols 1*, 2922-32.

38. Li, Q., Lee, J. S., Ha, C., Park, C. B., Yang, G., Gan, W. B. and Chang, Y. T. (2004) Solid phase synthesis of styryl dye library and its application to amyloid sensors, *Angew Chem Int Ed Engl 43*, 6331–35.

39. Wang, S. and Chang Y.T. (2008) Discovery of heparin chemosensors through diversity oriented fuorescence library approach. *Chem. Commun.* 1173-1175

40. Ahn, Y. H., Lee, J. S., and Chang, Y. T. (2007) Combinatorial rosamine library and application to in vivo glutathione probe. *Journal of the American Chemical Society 129*, 4510-1.

41. Ahn, Y. H., Lee, J. S., and Chang, Y. T. (2008) Selective human serum albumin sensor from the screening of a fluorescent rosamine library. *Journal of combinatorial chemistry 10*, 376-80.

42. Im, C. N., Kang, N. Y., Ha, H. H., Bi, X., Lee, J. J., Park, S. J., Lee, S. Y., Vendrell, M., Kim, Y. K., Lee, J. S., Li, J., Ahn, Y. H., Feng, B., Ng, H. H., Yun, S. W., and

Chang, Y. T. (2010) A fluorescent rosamine compound selectively stains pluripotent stem cells. *Angew Chem Int Ed Engl 49*, 7497-500.

43. Gordon, K. and Balasubramanian, S. (1999) Solid phase synthesis – designer linkers for combinatorial chemistry: a review. *Journal of Chemical Technology and Biotechnology 74*, 835-51

44. Merrifield RB, (1963) Solid phase synthesis I. The synthesis of aTetrapeptide. *Journal of the American Chemical Society 85*, 2149-54

45.Caruthers, M. H. (1985) Gene synthesis machines: DNA chemistry and its uses. *Science 230*, 281-5.

46. Vendrell, M., Krishna, G. G., Ghosh, K. K., Zhai, D., Lee, J. S., Zhu, Q., Yau, Y. H., Shochat, S. G., Kim, H., Chung, J., and Chang, Y. T. (2011) Solid-phase synthesis of BODIPY dyes and development of an immunoglobulin fluorescent sensor. *Chem Commun 47*, 8424-6.

47. Min, J., Lee, J. W., Ahn, Y. H., and Chang, Y. T. (2007) Combinatorial dapoxyl dye library and its application to site selective probe for human serum albumin. *Journal of combinatorial chemistry 9*, 1079-83.

48. Kolb, H. C., Finn, M. G., and Sharpless, K. B. (2001) Click Chemistry: Diverse Chemical Function from a Few Good Reactions. *Angew Chem Int Ed Engl 40*, 2004-2021.

49. Kolb, H. C., and Sharpless, K. B. (2003) The growing impact of click chemistry on drug discovery. *Drug discovery today 8*, 1128-37.

50. Bock, V. D., Perciaccante, R., Jansen, T. P., Hiemstra, H., and van Maarseveen, J. H. (2006) Click chemistry as a route to cyclic tetrapeptide analogues: synthesis of cyclo-[Pro-Val-psi(triazole)-Pro-Tyr]. *Organic letters 8*, 919-22.

51. R. Huisgen. (1963) 1,3-Dipolar cycloadditions. *Angew Chem Int Ed Engl*. *75*, 604–637

52. Meldal, M., and Tornoe, C. W. (2008) Cu-catalyzed azide-alkyne cycloaddition. *Chemical reviews 108*, 2952-3015.

53. M. G. Finn, H. C. Kolb, V. V. Fokin and K. B. Sharpless, Prog. Chem., 2008, 20, 1–4

54.Tron, G. C., Pirali, T., Billington, R. A., Canonico, P. L., Sorba, G., and Genazzani, A. A. (2008) Click chemistry reactions in medicinal chemistry: applications of the 1,3-dipolar cycloaddition between azides and alkynes. *Medicinal research reviews 28*, 278-308.

55. Lecomte, P., Riva, R., Schmeits, S., Rieger, J., Van Butsele, K., Jérôme, C., andJérôme, R. (2006) New prospects for the grafting of functional groups onto aliphatic polyesters. Ring-opening polymerization of α- or γ-substituted ε-caprolactone followed by chemical derivatization of the substituents. Macromol. Symp. *240*, 157 –65.

56. Hawker, C. J., and Wooley, K. L. (2005) The convergence of synthetic organic and polymer chemistries. *Science 309*, 1200-5.

57. Read, E. S., and Armes, S. P. (2007) Recent advances in shell cross-linked micelles. *Chem Commun* , 3021-35.

58. Goodall, G. W., and Hayes, W. (2006) Advances in cycloaddition polymerizations. *Chemical Society reviews 35*, 280-312.

59, Evans, R. A. (2007) The Rise of Azide-Alkyne 1,3-Dipolar "Click" Cycloaddition and Its Application to Polymer Science and Surface Modification *Aust. J. Chem. 60*, 384 – 95.

60.Yeo, D. S., Srinivasan, R., Chen, G. Y., and Yao, S. Q. (2004) Expanded utility of the native chemical ligation reaction. *Chemistry 10*, 4664-72.

61. Kohn, M., and Breinbauer, R. (2004) The Staudinger ligation-a gift to chemical biology. *Angew Chem Int Ed Engl 43*, 3106-16.

62. Kaiser, J., Kinderman, S. S., van Esseveldt, B. C., van Delft, F. L., Schoemaker, H. E., Blaauw, R. H., and Rutjes, F. P. (2005) Synthetic applications of aliphatic unsaturated alpha-H-alpha-amino acids. *Organic & biomolecular chemistry 3*, 3435-67.

63. *Angell*; *Y. L., and Burgess*, *K.* (*2007*) Peptidomimetics via copper-catalyzed azide—alkyne cycloadditions, *Chemical Society reviews 36*,1674–89.

64. Breinbauer, R., and Kçhn, M. (2003) Azide-alkyne Coupling - A Powerful Reaction for Bioconjugate Chemistry *ChemBioChem 4*, 1147 –1149.

65. Dong, W. L.; Zhao, W. G.; Li, Y. X.; Liu, Z. X.; Li, Z. M. (2006) Click Chemistry and Its Applications. *Chin. J. Org. Chem. 26*, 271–77.

66. Durek, T., and Becker, C. F. (2005) Protein semi-synthesis: new proteins for functional and structural studies. *Biomolecular engineering 22*, 153-72.

67. Devaraj, N. K., and Collman, J. P.(2007), Copper Catalyzed Azide-Alkyne Cycloadditions on Solid Surfaces: Applications and Future Directions. *QSAR Comb. Sci. 26*, 1253 –60.

68. Struthers, H., Mindt, T. L., and Schibli, R. (2010) Metal chelating systems synthesized using the copper(I) catalyzed azide-alkyne cycloaddition. *Dalton Trans 39*, 675-96.

69.Zhou, Z., and Fahrni, C. J. (2004) A fluorogenic probe for the copper(I)-catalyzed azide-alkyne ligation reaction: modulation of the fluorescence emission via 3(n,pi)-1(pi,pi) inversion. *Journal of the American Chemical Society 126*, 8862-3.

70. Xie, F., Sivakumar, K., Zeng, Q., Bruckman, M. A., Hodges, B., and Wang, Q. (2008) A fluorogenic ‘click’ reaction of azidoanthracene derivatives. *Tetrahedron 64*, 2906–14.

71. Sawa, M., Hsu, T. L., Itoh, T., Sugiyama, M., Hanson, S. R., Vogt, P. K., and Wong, C. H. (2006) Glycoproteomic probes for fluorescent imaging of fucosylated glycans in vivo. *Proceedings of the National Academy of Sciences of the United States of America 103*, 12371-6.

72. Tong, A. J., Yamauchi, A., Hayashita, T., Zhang, Z. Y., Smith, B. D., and Teramae, N. (2001) Boronic acid fluorophore/beta-cyclodextrin complex sensors for selective sugar recognition in water. *Analytical chemistry 73*, 1530-6.

73. Schiller, A., Wessling, R. A., and Singaram, B. (2007) A fluorescent sensor array for saccharides based on boronic Acid appended bipyridinium salts. *Angew Chem Int Ed Engl 46*, 6457-9.

74. Gamsey, S., Miller, A., Olmstead, M. M., Beavers, C. M., Hirayama, L. C., Pradhan, S., Wessling, R. A., and Singaram, B. (2007) Boronic acid-based bipyridinium salts as tunable receptors for monosaccharides and alpha-hydroxycarboxylates. *Journal of the American Chemical Society 129*, 1278-86.

75. Kim, Y., Hilderbrand, S. A., Weissleder, R., and Tung, C. H. (2007) Sugar sensing based on induced pH changes. *Chem Commun* 2299-301.

76. Musto, C. J., Lim, S. H., and Suslick, K. S. (2009) Colorimetric detection and identification of natural and artificial sweeteners. *Analytical chemistry 81*, 6526-33.

77. Zhang, C., and Suslick, K. S. (2005) A colorimetric sensor array for organics in water. *Journal of the American Chemical Society 127*, 11548-9.

78. Rakow, N. A., Sen, A., Janzen, M. C., Ponder, J. B., and Suslick, K. S. (2005) Molecular recognition and discrimination of amines with a colorimetric array. *Angew Chem Int Ed Engl 44*, 4528-32.

79. Miyaji, H., and Sessler, J. L. (2001) Off-the-Shelf Colorimetric Anion Sensors This research was supported by the National Institutes of Health (grant GM 58907) and the Texas Advanced Research Program. *Angew Chem Int Ed Engl 40*, 154-157

Chapter 2

Diversity Oriented Solid Phase Synthesis of Fluorescent Xanthone Libraries and Their Applications in Bio imaging

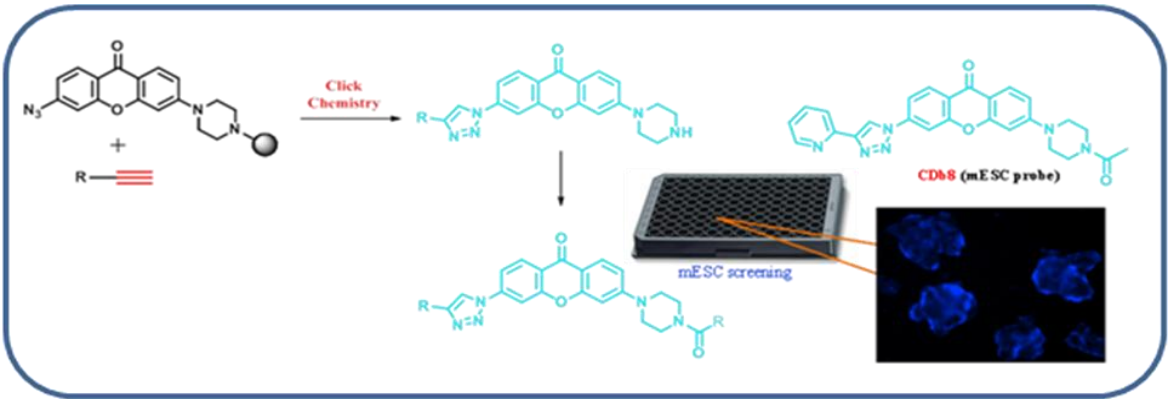

2.1 Introduction

Fluorescent small molecules have received considerable attention due to their huge potential for chemosensing and bio imaging. These fluorescent sensor molecules undergo a change in their fluorescent properties, intensity or wavelength, upon interaction with target molecules or under an environmental change[1-3]. As discussed in the earlier section, the most commonly used fluorescent scaffolds in chemical biology and medicinal applications are coumarin, dapoxyl, styryl, hemicyanine, fluorescein, rosamine and BODIPY[4-10]. Although, several medicinal uses of xanthones are well known, their fluorescent properties are yet to be explored for bio imaging purpose[11]. Few literatures have been published where xanthones are applied for fluorescent sensor development[12]. The xanthone scaffolds have superior photophysical properties such as high photostability, large stock shift and moderate quantum yield. In spite of these superior photophysical properties, the xanthone scaffold is still in its infancy for library synthesis and sensor application when compared to relatively well studied fluorescent scaffolds, such as BODIPY, rosamine, coumarin, cyanine and styryl.

There are several other fluorescents scaffolds reported such as coumarins,[13] carbostyrils,[14] anthracenes,[15] naphthalimides[16] and pyridyloxazoles[17] for which the click chemistry has been used as fluorogenic reaction or to generate analogs of the parental fluorophore. One of the serious problems of the reported "click" fluorophores is that they are UV-excited dyes, so it is difficult to apply them in bio imaging applications where live cells or tissues are used. Hence, it would be useful to extend the "click" chemistry mediated discovery of fluorescent dyes to the xanthone scaffolds, with an excitation wavelength in the visible range. We considered that the formation of a triazole ring via click chemistry may change the fluorescent property of xanthone core

through an extended π-conjugation, and this change could be tuned by the use of alkynes with different electronic properties.

2.2 Objectives

Here we report the solid phase diversity-synthesis of two fluorescent xanthone libraries, CX and AX. These CX and AX compounds were further diversified to their corresponding actyl (CXAC and ACAC) and chloroacetyl (CXCA and AXCA) derivatives using a simple but powerful solid phase activated ester chemistry. Next, we performed the full photophysical characterisation of these xanthone libraries. With the interest to develop a stem cell selective blue fluorescent probe CX, CXCA and CXAC libraries were screened against mouse embryonic stem cells and compound CXAC 59 was found to stain mESC selectively compared to MEF and other differentiated cells.

2.3 Results and discussion

2.3.1 Design and synthesis of CX library

In this particular section the synthesis, characterisation and applications of xanthone libraries are discussed. As shown in the Scheme 2.1, the general synthetic strategy of xanthone azide involves the reaction between 2-chloro-4-nitro benzoic acid and 3-fluorophenol followed by a cyclization in the presence of concentrated sulfuric acid to give 3-fluoro-6-nitro xanthone. The 3-fluoro group was then replaced by tertiary-butoxycarbonyl (Boc) protected piperazine and the nitro group was reduced to aniline with hydrazine and palladium on carbon in ethanol. Treatment of 1c with sodium nitrite in water–Acetic acid (1:1) at 0^{o}C followed by reaction with sodium azide afforded 6-azido-3-piperazine substituted xanthone. The reaction proceeded quantitatively, and subsequent deprotection of the Boc group with trifluoroacetic acid in DCM afforded the desired azide.

Scheme 2.1. Synthesis of xanthone azide.

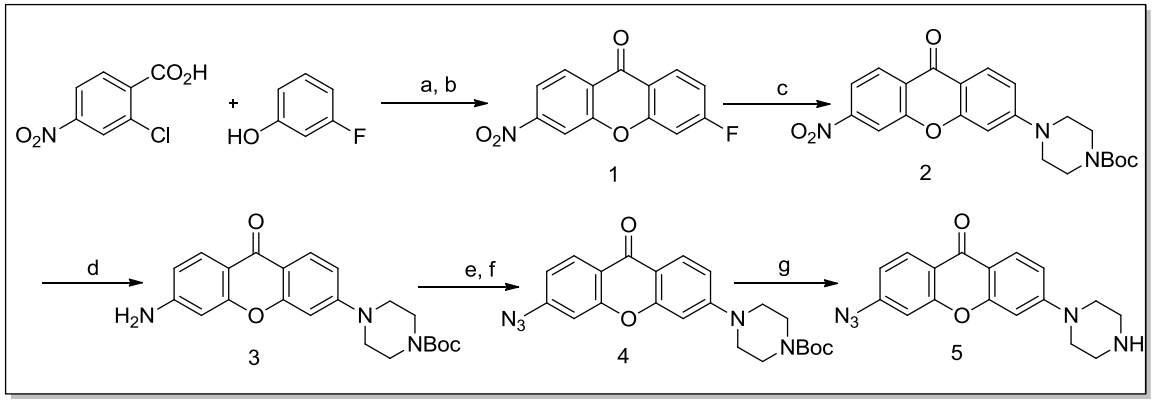

Reagents and conditions: (a) K_2CO_3, Cu, DMF, 130 ^oC, 12 h; (b) H_2SO_4, 90 ^oC, 1 h; (c) 1-Boc Piperazine, DMSO, 90 ^oC, 12 h; (d) NH_2-NH_2.H_2O, Pd/C, EtOH, 90 ^oC, 4 h; (e) H_2O/AcOH (1:1), $NaNO_2$, 0^oC, 1 h; (f) NaN_3, 0 ^oC to r.t., 1 h; (g) 10% TFA in DCM, r.t., 2 h.

After synthesizing the desired xanthone azide intermediate, the compound was loaded to the solid support and a broad chemical diversity was obtained when the azide reacted with aliphatic and aromatic terminal alkynes (Chart 2.1) in the presence of CuI (Scheme 2.2). The formation of the heterocyclic triazole moiety following Huisgen 1, 3-dipolar cycloaddition of azides and alkynes are very efficient and regioselective. For most of the cases the reaction was completed within 12 to 16 h. All the compounds in the library were characterized by HPLC-MS and 80 relatively pure compounds (average purity is 90%, measured at 254 nm (Table 2.1) were collected for further study.

Scheme 2.2. Synthesis of CX derivatives

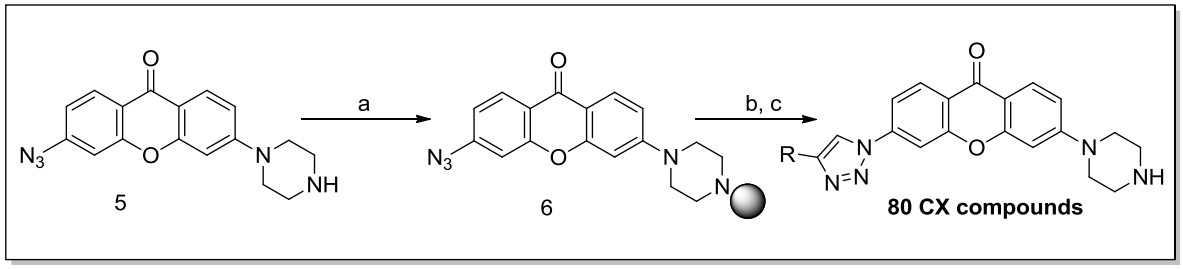

Reagents and conditions: (a) DMF/DCM, DIEA, Trityl-Cl, r.t., 12 h; (b) DMF/Piperidine (4:1), CuI, Ascorbic acid, RCCH, r.t., 16 h, (c) 2% TFA in DCM, r.t., 10 min.

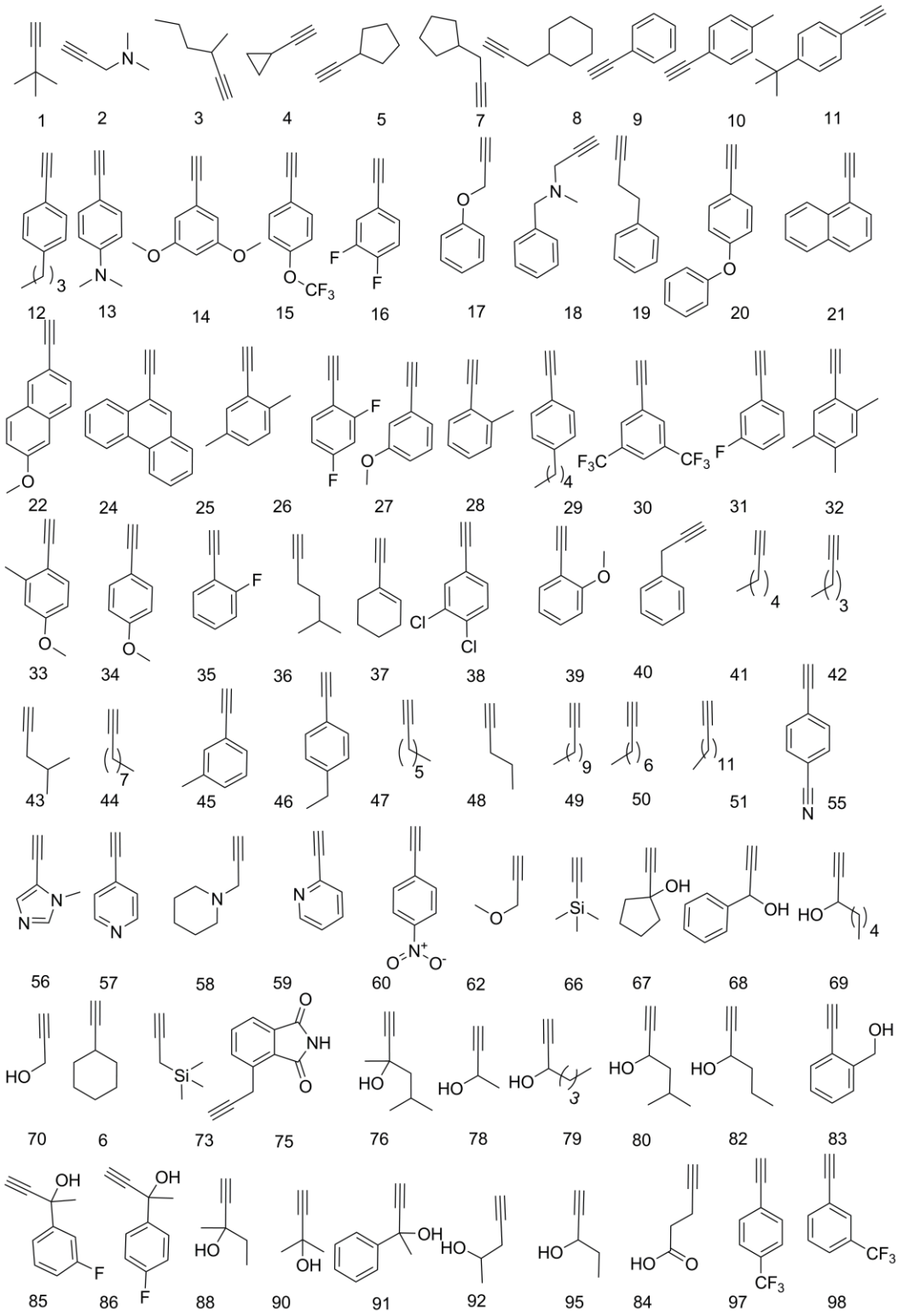

Chart 2.1. Alkyne building blocks for CX library

2.3.2 Synthesis of CXCA and CXAC libraries

After successfully synthesizing the CX library, we incorporated the affinity matrixes to the CX compounds for developing another set of bio imaging probes (CXCA compounds) that could facilitate the identification of the target proteins from the biological systems. Firstly, active ester resins were prepared by treating the nitrophenol resin with chloroacetyl chloride. The reaction of the resulting resin with the highly reactive piperazine moiety of CX compounds in presence of mild base $NaHCO_3$ afforded the corresponding CXCA compounds (Scheme 2.3)**.** The CX compounds were also derivatized to CXAC by introducing an acetyl moiety to the CX using the Scheme 2.3**.** The reaction completed within 2 hours and the products were obtained with an average purity above 90% for CXAC (Table 2.2), and for CXCA the purity was more than 85% (Table 2.3). This simple, but powerful chemistry can be applied to broad range of acyl group derivatization leaving the potential of further diversification of CX**.**

Scheme 2.3. Synthesis of CXCA and CXAC

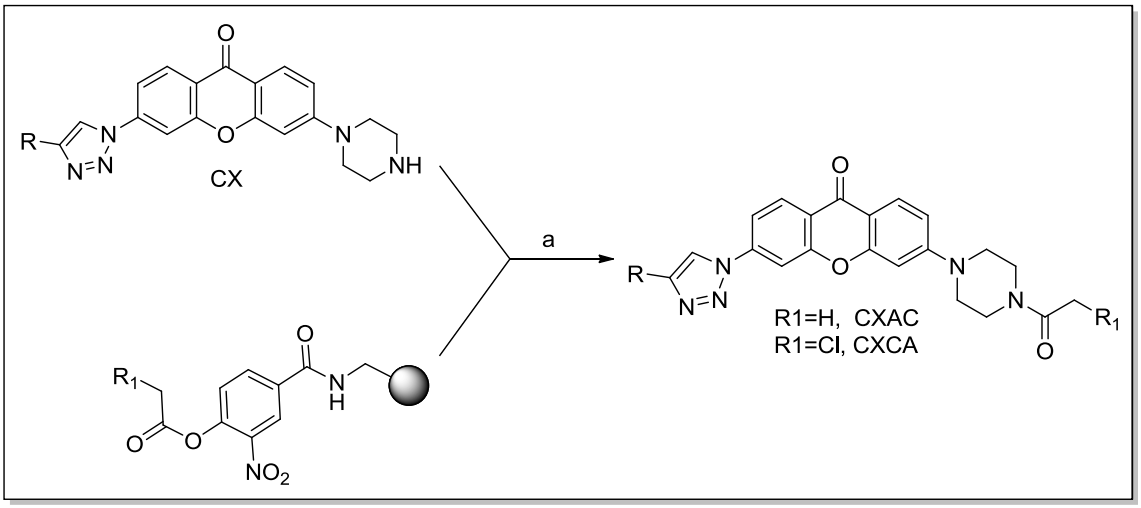

Reagent and conditions: (a) DCM/ACN (7:1), $NaHCO_3$, 2 h, r.t.

2.3.3. Spectral properties of CX, CXCA and CXAC libraries

The library compounds showed a range of spectral diversities (excitation ranges from 360 to 370 nm and emission ranges from 480 to 495 nm). The quantum yield of each molecule highly varies from 0.02 to 0.16 reflecting diverse structural and electronic characteristics.(Table 2.1, 2.2 and 2.3)

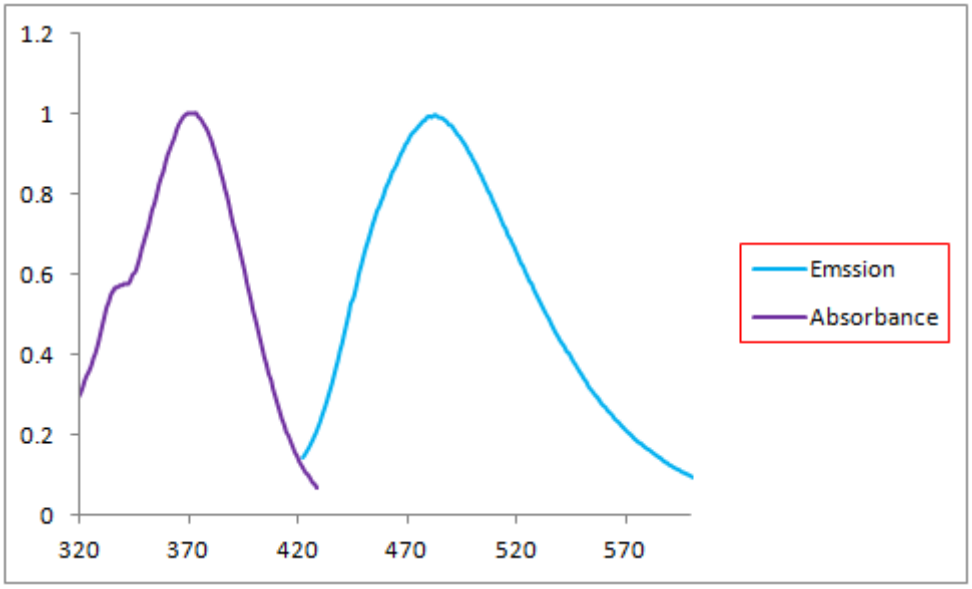

Figure 2.1. Representative (CX-1) and normalised absorbance and emission spectra of CX library

2.3.4 Design and synthesis of AX library

In order to make a more systematic investigation on bio imaging applications of xanthones we further developed a second xanthone library (named as AX) using acid chloride diversity. This time a small linker tag was incorporated which may enable to give some different responses towards the different biological targets. Propargyl amine was loaded to the chlorotrityl resin followed by the Cu(I)-catalysed click chemistry with the xanthene azide to give rise to the intermediate 2. The reaction between the intermediate 2 and commercially available aromatic or aliphatic acid chlorides (chart 2.2) and then subsequent cleavage of those compounds from the resin gave rise to the AX compounds (Scheme 2.4). This reaction was both fast and quantitative. 80 diverse compounds were obtained with an average purity above 90% at 254 nm wavelength (Table 2.4) .

Scheme 2.4. Synthesis of AX library

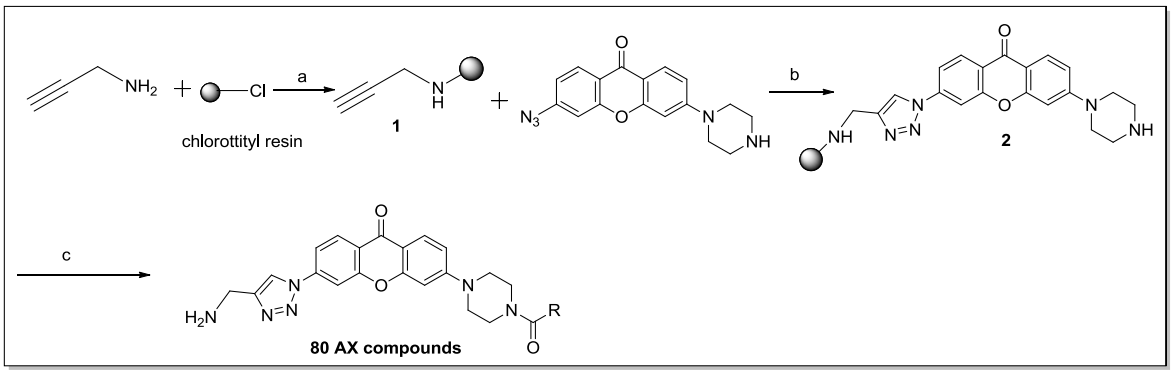

Reagents and Conditions: (a) DMF/DCM, DIEA, r.t, 12 h; (b) DMF/Piperidine (4:1) CuI, Ascorbic acid, r.t, 24 h; (c) DCM, DIEA, RCOCl , r.t, 4 h; (d) 2% TFA in DCM, r.t, 15min.

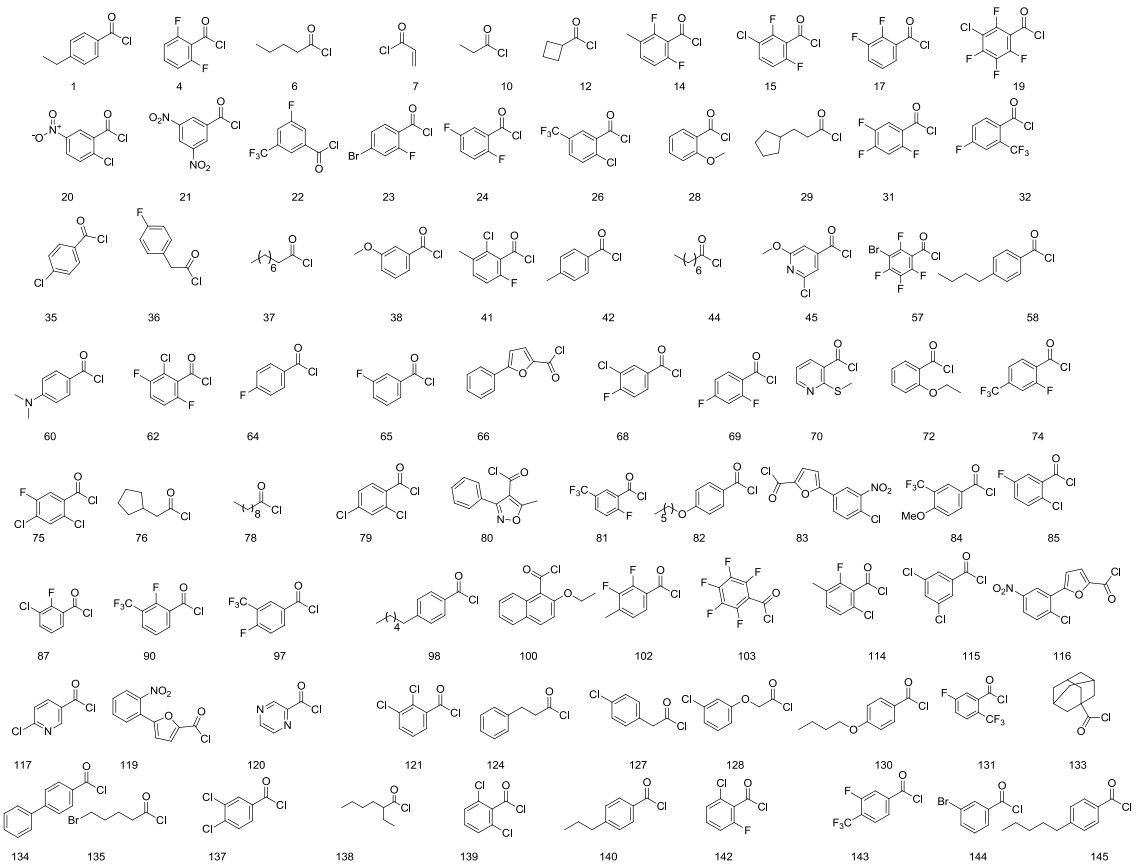

Chart 2.2. Structure of acid chloride building blocks used for the **AX** library

2.3.5 Synthesis of AXCA and AXAC library

To introduce the chemical affinity moiety, the AX compounds were further diversified to AXCA with the aid of the scheme 2.5. In order to evaluate the role of free primary amine linker in the biological system the AX compounds were acetylated and hence, the AXAC compounds were synthesized accordingly (scheme 2.5). All the compounds were characterised by HPLC-MS. The AXCA compounds have an average purity around 85% (Table 2.6) whereas AXAC compounds (Table 2.5) showed an average purity around 90% at 350 nm wavelength.

Scheme 2.5. Synthesis of AXCA and AXAC

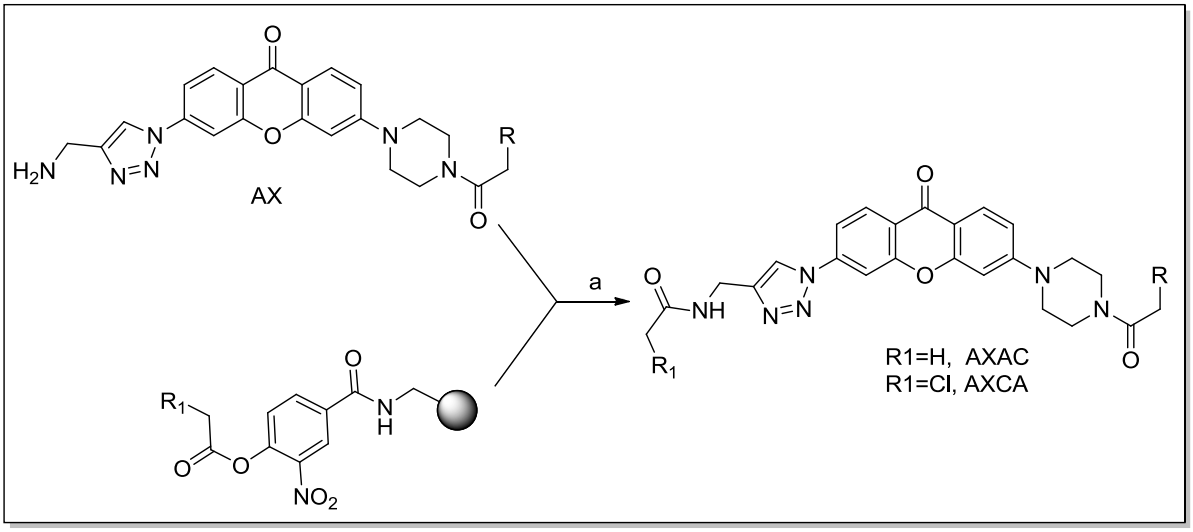

Reagent and conditions:

(a) DCM/ACN=7:1, $NaHCO_3$, 3 h, r.t

2.3.6 Spectral properties of AX, AXCA and AXAC libraries

These compounds showed an excitation wavelengths around 365 nm and emission around 495 nm with an average quantum yield 0.3 (Table 2.4, 2.5, 2.6).

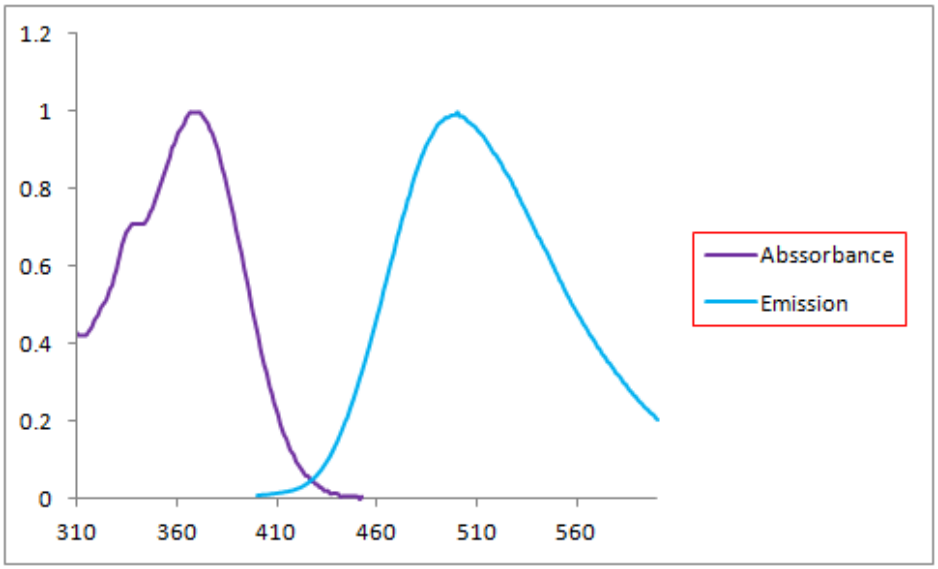

Figure 2.2. Representative (AX-1) and normalised absorbance and emission spectra of AX library

2.3.7 Identification of stem cell selective marker

The high throughput screening of a diversity oriented rosamine library, against Embryonic stem cell (ESC) and mouse embryonic fibroblast (MEF) identified CDy1 (Compound of Designation yellow 1, λex/λem = 535/570 nm) as the first embryonic stem cell (ESC) probe[19]. While powerful, the yellow region of the fluorescence by CDy1 has a significant colour overlapping when multi-colour staining was attempted together with standard YFP (yellow fluorescent protein). To overcome this colour limitation, we expanded our library to blue/green or red/near IR light emitting scaffolds. The xanthone scaffold was considered for the design of the blue library due to its superior photophysical properties and structural similarity with the rosamine library, which CDy1 belongs to.

For the discovery of a stem cell selective blue fluorescent probe, 240 library compounds from the CX, CXAC, and CXCA libraries were screened against mESC, MEF and a coculture of these two cell type via high throughput imaging. For the primary screening, the dye (1 μM) was incubated with cells and many of the compounds smoothly stained cells to different extent. The compounds were not toxic (Figure 2.4) over several days of incubation, demonstrating the purity of the compounds free from toxic copper catalyst**.** Dyes staining mESC stronger than MEF were selected as primary hits and further tested by flow cytometry to confirm the selective staining of mESC. CXAC 59 was selected as the best dye out of total 240 compounds in terms of selective staninging of mESC (Figure 2.3b) and separation of the two cell populations from flow cytometry (Figure 2.3d). This compound was named **CDb8** (Compound of Designation blue 8). We also investigated the selectivity of **CDb8** in differentiated mESC and observed the differentiated cells were not stained by **CDb8 (**Figure 2.5**).** This reflects its high selectivity for mESC.

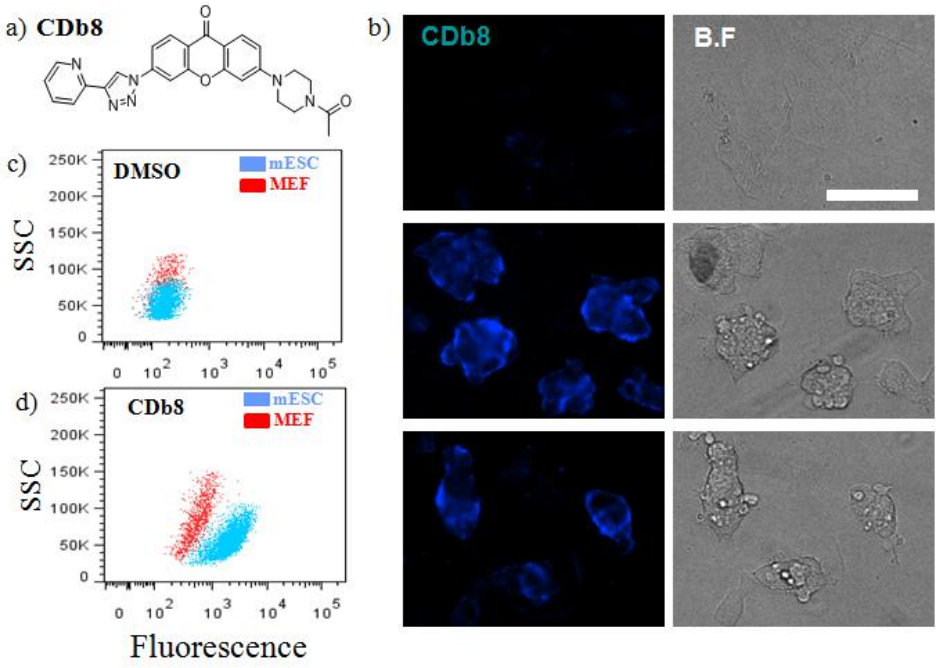

Fig. 2.3. Selective staining of mESC by **CDb8.** (a) Chemical structure of **CDb8** (b) mESC was selectively stained by **CDb8** at 1 µM for 1 h. Upper panel; Mouse embryonic fibroblasts (MEF), Middle; Mouse embryonic stem cells (mESC), Lower panel; mESC on MEF feeder (C) Flow Cytomerty analysis of DMSO control cells. (D) Flow Cytomerty analysis of **CDb8** stained cells. The cells are loaded after 1 h incubation at 1 µM. B.F: bright field, scale bar: 100 µm

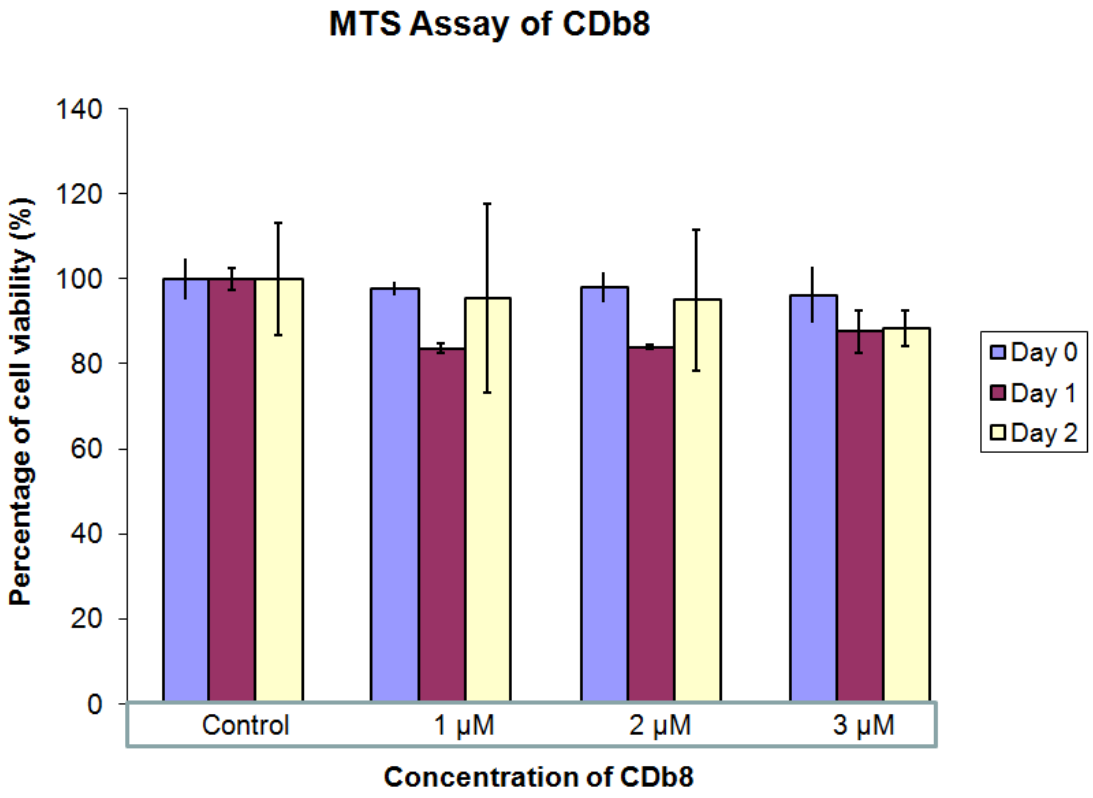

Figure 2.4. Cytotoxic effect of CDb8 (CXAC-F5) in mESC**.** The cytotoxic effect of **CDb8** was tested by the **MTS** (3-(4,5-dimethylthiazol-2-yl)-5-(3-carboxymethoxyphenyl)-2-(4-sulfophenyl)-2H-tetrazolium, inner salt) assay using the CellTiter 96 nonradioactive cell proliferation colorimetric assay kit (Promega) on mESC cells. First, the mESC cells (1 X 10^4 cells in 100 µl of media) were seeded onto 96 well plate and then different concentrations (0 µM, 1 µM, 2 µM and 3 µM) of **CDb8** was added to the cells on the following day and incubated them at 37^{o}C for 3days. After one day(Day 0), 20 µl of MTS solution was added to each well and incubated for another 2 hours before the absorbance was measured at 490 nm. The same experiments were done for Day 1 and Day 2. The control cells are 100% alive without compound condition. At least 80% of the **CDb8** treated cells are alive after 3 days of incubation at 3 µM concentration. This indicates that the **CDb8** is nontoxic to mESC.

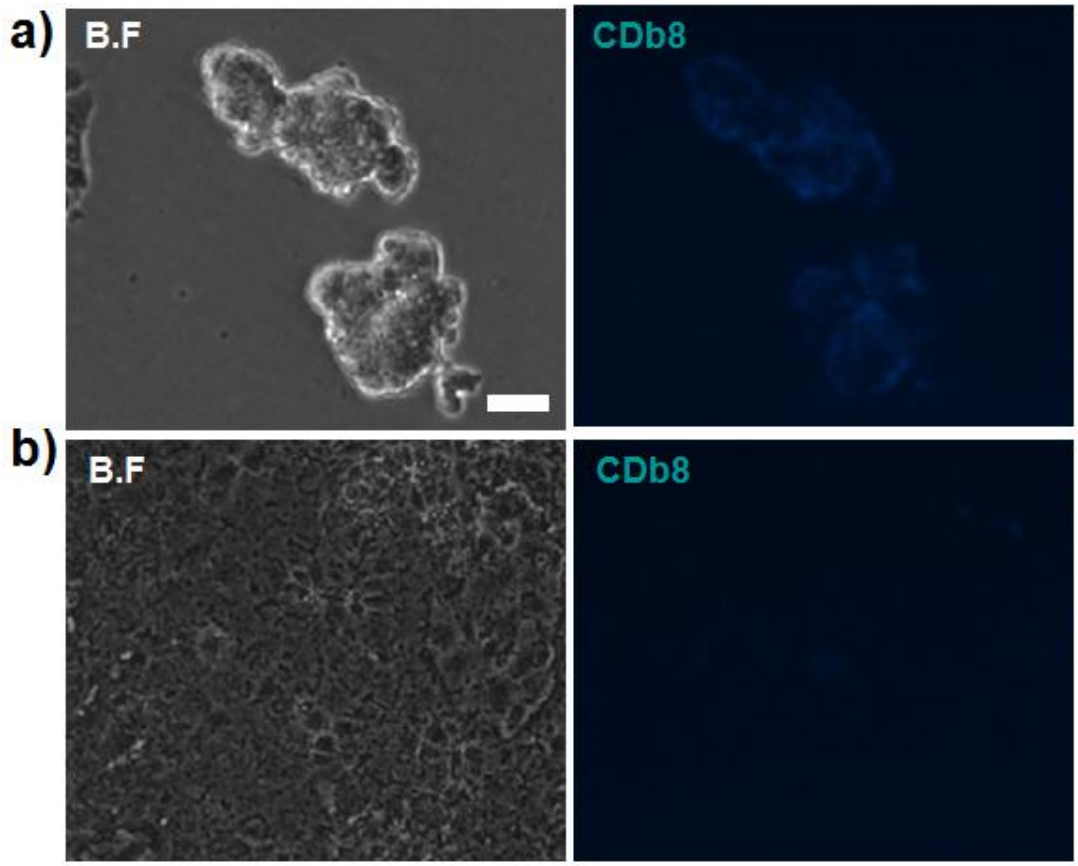

Figure 2.5. Differentiated mESC staining with CDb8. All of differentiated mESC were distinguished from mESC 14days after removing LIF culture. Almost all differentiated cells were **CDb8** negative. a) mESC selectively stained by **CDb8** b)The differentiated mESC were not stained by **CDb8.** B.F, bright field. Scale bar, 100 μm.

2.4 Conclusions

In conclusion, we have successfully synthesized two fluorescent xanthone libraries (CX and AX) and their corresponding acetyl (CXAC and AXAC) and chloroacetyl derivatives (CXCA and AXCA). Here, we also demonstrated the power of solid phase methodology for efficient synthesis of a library of fluorescent small molecules. These xanthone library compounds demonstrated biocompatibility in terms of easy cell penetration and low toxicity. One mESC selective compound **CDb8** was identified as a blue imaging and flow cytometry probe for embryonic stem cells.

Table 2.1. Characterization and photophysical properties of CX library

compound	M^+(calc.)	M^+ (exp.)	λ_{abs} (nm)	λ_{em} (nm)	ϕ^1	Purity[2]
CX 1	403.48	404	372	489	0.03	90
CX 2	404.46	405	372	491	0.04	89
CX 3	417.5	418	372	491	0.04	90
CX 4	387.43	388	371	485	0.08	89
CX 5	415.49	416	372	489	0.03	95
CX 7	429.51	430.1	371	487	0.11	88
CX 8	443.54	444	372	488	0.03	90
CX 9	423.47	424	374	494	0.06	92
CX 10	437.49	438	372	497	0.06	93
CX 11	479.57	480.1.0	371	494	0.07	96
CX 12	479.57	480	371	489	0.05	92
CX 13	466.53	467	374	492	0.01	85
CX 14	483.52	484	372	490	0.05	91
CX 15	507.46	507.9	371	496	0.06	91
CX 16	459.45	459.9	371	493	0.03	92
CX 17	453.49	454	372	493	0.06	91
CX 18	480.56	481	372	487	0.03	92
CX 19	451.52	552	371	490	0.02	93
CX 20	515.56	516	371	491	0.05	94
CX 21	473.53	474	371	484	0.35	91
CX 22	503.55	504	366	490	0.11	92
CX 24	523.58	523.9.0	372	490	0.05	91
CX 25	451.52	452	370	489	0.02	91
CX 26	459.45	459.9	366	490	0.06	90
CX 27	453.49	454	370	491	0.05	91
CX 28	437.49	438	371	488	0.06	90
CX 29	493.6	494	367	494	0.06	91
CX 30	559.46	595.9	366	496	0.06	90

CX 31	441.46	442	370	496	0.06	92
CX 32	465.55	466	366	489	0.06	90
CX 33	467.52	468	368	488	0.04	90
CX 34	453.49	453.9	366	486	0.05	88
CX 35	441.46	442	371	492	0.09	94
CX 36	417.5	418	371	489	0.02	93
CX 37	427.5	427.9	372	489	0.07	92
CX 38	492.36	491.8	371	488	0.07	90
CX 39	453.48	453.9	371	492	0.06	92
CX 40	437.49	438	372	488	0.07	95
CX 41	417.5	418	372	489	0.05	90
CX 42	403.48	404	372	489	0.07	95
CX 43	403.48	404.1	372	484	0.03	90
CX 44	459.58	460	371	487	0.11	87
CX 45	437.49	438	372	493	0.05	90
CX 46	451.52	452	372	490	0.07	90
CX 47	431.53	432.1	371	487	0.09	91
CX 48	389.45	390	371	482	0.04	94
CX 49	487.64	488	371	490	0.13	91
CX 50	445.56	446	370	489	0.11	90
CX 51	515.69	516	366	489	0.14	91
CX 55	448.48	448.9	371	495	0.1	95
CX 56	427.46	428	371	493	0.08	96
CX 57	424.45	425	366	498	0.08	95
CX 58	444.53	445.1	372	488	0.08	98
CX 59	424.45	425	372	494	0.08	94
CX 60	468.46	469	338	451	0.08	88
CX 62	391.42	392	372	495	0.08	91
CX 66	419.55	420	372	487	0.08	91
CX 67	431.49	432	366	489	0.08	87

CX 68	453.49	453.9	371	486	0.08	90
CX 69	447.53	448	371	493	0.08	91
CX 70	377.4	378	361	483	0.13	90
CX 6	429.51	430.1	361	478	0.17	92
CX 73	433.58	434	371	485	0.05	91
CX 75	506.51	592	369	493	0.1	88
CX 76	429.51	430.1	371	490	0.04	86
CX 78	391.42	392	372	486	0.05	88
CX 79	433.5	434.1	371	487	0.1	91
CX 80	433.5	434	369	485	0.03	91
CX 82	419.48	420	371	494	0.02	90
CX 83	453.49	454	371	494	0.07	91
CX 85	467.49	468	372	491	0.07	94
CX 86	467.49	468	372	485	0.07	89
CX 88	419.48	420.1	368	482	0.06	88
CX 90	405.45	406	371	484	0.06	91
CX 91	449.5	450	370	485	0.04	86
CX 92	405.45	406	371	483	0.06	90
CX 95	405.45	406	371	485	0.1	91
CX 84	485.51	486	372	488	0.02	90
CX 97	491.46	491.8	370	499	0.12	90
CX 98	491.46	491.9	369	495	0.11	92

Φ^{1} quantum yields are measured in DMSO solvent using Coumarin 1 as a standard (Φ=0.59)

purities[2] were determined according to UV absorbance at 254 nm

Table 2. 2 Characterization and photophysical properties of CXAC library

compound	M^+(calc.)	M^+ (exp.)	λ_{abs}(nm)	λ_{em}(nm)	ϕ^{*2}	purity*
CXAC 1	445.21	446.3	369	483	0.3	98
CXAC 2	446.21	447.3	369	485	0.27	90
CXAC 3	459.23	460.2	369	483	0.3	98
CXAC 4	429.18	430.2	368	486	0.19	96
CXAC 5	457.21	458.2	369	484	0.3	98
CXAC 7	471.23	472.3	372	484	0.19	94
CXAC 8	485.24	486.2	369	483	0.31	98
CXAC 9	465.18	466.2	370	488	0.28	98
CXAC 10	479.2	480.2	369	487	0.25	97
CXAC 11	521.24	522.3	369	487	0.29	98
CXAC 12	521.24	522.3	369	487	0.3	98
CXAC 13	508.22	509.3	372	483	0.06	90
CXAC 14	525.2	526.2	369	486	0.27	98
CXAC 15	549.16	550.2	369	492	0.28	98
CXAC 16	501.16	509.2	365	468	0.21	91
CXAC 17	495.19	496.2	369	487	0.32	89
CXAC 18	522.24	523	369	484	0.34	90
CXAC 19	493.21	494.2	369	484	0.35	99
CXAC 20	557.21	558.2	369	485	0.31	97
CXAC 21	515.2	516.2	369	487	0.32	94
CXAC 22	545.21	546.1	368	467	0.27	90
CXAC 24	565.21	566.2	368	487	0.29	98
CXAC 25	493.21	494.1	368	485	0.32	96
CXAC 26	501.16	502.1	368	483	0.27	98
CXAC 27	495.19	496.2	368	487	0.33	93
CXAC 28	479.2	480.2	369	485	0.33	97
CXAC 29	535.26	536.3	368	485	0.38	94
CXAC 30	601.15	602.2	372	503	0.3	95

CXAC 31	483.17	484.2	369	488	0.31	89
CXAC 32	507.23	508.3	368	471	0.31	90
CXAC 33	509.21	510.2	368	483	0.34	93
CXAC 34	495.19	496.2	366	485	0.31	89
CXAC 35	483.17	484.2	369	492	0.3	98
CXAC 36	459.23	460.3	368	482	0.4	98
CXAC 37	469.21	470.2	368	486	0.44	96
CXAC 38	533.1	533.9	368	488	0.4	90
CXAC 39	495.19	496.2	369	486	0.44	98
CXAC 40	479.2	480.2	369	486	0.43	98
CXAC 41	459.23	460.2	369	485	0.43	98
CXAC 42	445.21	446.3	369	482	0.47	97
CXAC 43	445.21	446.2	369	482	0.42	97
CXAC 44	501.27	502.3	369	489	0.4	98
CXAC 45	479.2	480.2	372	486	0.46	97
CXAC 46	493.21	494.2	368	485	0.4	97
CXAC 47	473.24	474.3	368	485	0.47	98
CXAC 48	431.2	432.2	369	483	0.41	96
CXAC 49	529.31	530.3	368	483	0.53	97
CXAC 50	487.59	488.3	369	482	0.43	98
CXAC 51	557.34	558.3	368	485	0.46	97
CXAC 55	490.18	491.2	369	496	0.61	92
CXAC 56	469.19	470.2	369	487	0.54	90
CXAC 57	466.18	467.2	368	494	0.47	89
CXAC 58	486.24	486.9	369	488	0.41	88
CXAC 59	466.18	467.2	369	487	0.39	94
CXAC 60	510.17	511.2	338	463	0.29	87
CXAC 62	433.18	434.2	369	488	0.43	94
CXAC 66	461.19	462.2	368	484	0.54	97
CXAC 67	473.21	474.2	372	479	0.08	85

CXAC 68	495.19	496.2	372	485	0.7	90
CXAC 69	489.24	490.3	369	483	0.48	88
CXAC 70	419.16	420.3	366	469	0.17	85
CXAC 6	471.23	472.1	369	484	0.44	85
CXAC 73	475.2	476.2	369	481	0.48	90
CXAC 75	448.18	449	368	480	0.35	87
CXAC 76	471.23	472.3	368	479	0.45	90
CXAC 78	433.18	434.2	369	483	0.58	96
CXAC 79	475.22	476.3	368	484	0.56	98
CXAC 80	475.22	476.2	369	482	0.54	91
CXAC 82	461.21	462.2	369	484	0.57	96
CXAC 83	495.19	496.2	369	487	0.34	84
CXAC 85	509.19	510.2	369	487	0.38	91
CXAC 86	509.19	510.2	369	485	0.32	93
CXAC 88	461.21	462.2	368	473	0.41	89
CXAC 90	447.19	448	368	483	0.47	87
CXAC 91	491.2	492.2	368	478	0.41	92
CXAC 92	447.19	448.2	368	485	0.41	96
CXAC 95	447.19	448.2	368	482	0.49	96
CXAC 84	527.2	528.2	365	473	0.3	86
CXAC 97	533.17	534.1	369	491	0.52	91
CXAC 98	533.17	534.1	372	493	0.44	93

Table 2. 3 Characterization and photophysical properties of CXCA library

compound	M^+ (exp.)	M^+ (exp.)	λ_{abs}(nm)	λ_{em}(nm)	Q	Purity
CXCA 1	479.96	480.2	367	482	0.40	98
CXCA 3	493.99	494.2	368	479	0.36	96
CXCA 4	463.92	464.2	367	484	0.24	92
CXCA 5	491.97	492.2	368	483	0.37	98
CXCA 7	506.00	506.2	367	481	0.23	91
CXCA 8	520.02	520.2	368	483	0.30	98
CXCA 9	499.95	500.1	367	486	0.34	96
CXCA 10	513.97	514.2	369	485	0.29	97
CXCA 11	556.05	556.2	369	485	0.35	98
CXCA 12	556.05	556.2	369	486	0.36	96
CXCA 13	543.02	543.2	373	489	0.06	85
CXCA 14	560.00	560.2	368	487	0.35	97
CXCA 15	583.95	584.2	369	488	0.37	96
CXCA 16	535.93	536.1	368	496	0.34	91
CXCA 17	529.97	530.2	368	484	0.39	87
CXCA 18	557.04	577.2	367	486	0.33	88
CXCA 20	592.04	592.2	367	485	0.37	90
CXCA 21	550.01	550.2	368	486	0.38	89
CXCA 22	580.03	580.2	365	493	0.40	87
CXCA 24	542.03	600.2	368	484	0.33	93
CXCA 25	528.00	528.2	368	484	0.37	88
CXCA 26	535.93	536.1	368	484	0.33	86
CXCA 27	529.97	530.2	368	485	0.37	89
CXCA 28	513.97	514.2	368	485	0.41	90
CXCA 29	570.08	570.2	368	484	0.38	87
CXCA 30	635.94	636.2	368	501	0.38	86
CXCA 31	517.94	518.2	368	486	0.35	89
CXCA 32	542.03	542.3	368	480	0.37	84

CXCA 33	544.00	544.2	368	484	0.37	88
CXCA 34	529.97	530.2	367	482	0.33	86
CXCA 35	517.94	518.2	368	487	0.49	96
CXCA 36	493.99	494.2	368	489	0.48	96
CXCA 37	503.98	504.2	368	484	0.48	93
CXCA 38	568.84	570.1	367	485	0.44	87
CXCA 39	529.97	530.2	349	484	0.40	98
CXCA 40	513.97	514.2	368	483	0.43	91
CXCA 41	493.99	494.2	368	482	0.51	97
CXCA 42	479.96	480.2	368	483	0.54	94
CXCA 43	479.96	480.2	368	482	0.64	99
CXCA 44	536.06	536.3	368	482	0.48	99
CXCA 45	513.97	514.2	368	485	0.57	97
CXCA 46	528.00	528.2	369	483	0.48	97
CXCA 47	508.01	508.2	368	483	0.55	97
CXCA 48	465.93	466.2	368	483	0.49	98
CXCA 49	564.12	564.3	368	479	0.54	98
CXCA 50	522.04	522.3	367	479	0.52	98
CXCA 51	592.17	592.2	367	481	0.49	98
CXCA 58	521.01	521	367	487	0.50	96
CXCA 59	500.94	501.2	368	486	0.54	93
CXCA 62	467.90	468.2	369	485	0.46	94
CXCA 66	496.03	496.2	367	485	0.76	95
CXCA 67	507.97	508.2	367	478	0.62	88
CXCA 69	524.01	524.2	368	483	0.67	96
CXCA 73	510.06	510.2	367	477	0.58	89
CXCA 76	506.00	506.2	367	481	0.57	90
CXCA 78	467.90	468.2	367	476	0.12	86
CXCA 79	509.98	510.2	368	478	0.58	80
CXCA 80	509.98	510.2	367	484	0.67	92

CXCA 82	495.96	496.2	368	484	0.49	92
CXCA 83	529.97	530.2	369	486	0.89	91
CXCA 85	543.98	544.1	369	485	0.47	94
CXCA 86	543.98	544.1	368	485	0.40	95
CXCA 88	495.96	496.2	365	474	0.49	88
CXCA 90	481.93	482.2	367	478	0.13	91
CXCA 92	481.93	482.1	368	485	0.50	89
CXCA 95	481.93	482.2	367	477	0.59	96
CXCA 84	561.99	562.2	367	483	0.08	87
CXCA 97	567.95	568.2	368	487	0.44	91
CXCA 98	567.95	568.2	369	487	0.49	97

For HPLC-MS characterisation of CXAC and CXCA Library following analytical method was used Eluents: A: H2O (0.1% HCOOH), B: ACN (0.1% HCOOH), gradient from 30 to 100% B in 2.5 min; C18(2) Luna column (4.6 x 50 mm^2, 5 µm particle size) purity check at 254 nm wavelength

Table 2.4 Characterization and photophysical properties of AX library

compound	M^+(calc.)	M^+ (exp.)	λ_{abs}(nm)	λ_{em}(nm)	ϕ[1]	Purity[2]
AX 1	508.57	509.0	369	500	0.34	91
AX 4	516.5	516.9	366	494	0.45	90
AX 6	460.53	461.2	370	502	0.30	92
AX 7	430.46	431.1	368	500	0.29	89
AX 10	432.48	433.0	369	503	0.29	92
AX 12	458.51	459.2	370	501	0.34	93
AX 14	530.53	531.0	366	494	0.54	90
AX 15	550.94	551.2	366	492	0.59	91
AX 17	516.5	517.1	368	495	0.42	92
AX 19	586.92	587.0	366	490	0.41	94
AX 20	559.96	560.1	368	491	0.01	95
AX 21	570.51	571.1	300	495	0.01	90
AX 22	566.51	567.1	368	499	0.15	94
AX 23	577.4	577.1	368	496	0.39	91
AX 24	516.5	517.2	367	494	0.37	96
AX 26	582.96	583.2	368	496	0.37	93
AX 28	510.54	511.2	369	498	0.34	92
AX 29	500.59	501.2	370	503	0.32	90
AX 31	534.49	535.2	367	491	0.34	95
AX 32	566.51	567.2	367	493	0.35	87
AX 35	514.96	515.2	368	500	0.29	89
AX 36	512.53	513.2	368	500	0.27	90
AX 37	516.63	517.3	369	505	0.30	93
AX 38	510.54	511.2	369	500	0.26	96
AX 41	546.98	547.2	367	493	0.39	85
AX 42	494.54	495.0	369	499	0.38	90
AX 44	502.61	503.2	369	503	0.31	90

AX 45	545.98	546.2	368	495	0.45	91
AX 57	631.38	632.3	366	493	0.29	92
AX 58	536.62	537.3	369	500	0.32	94
AX 60	523.59	524.3	300	504	0.04	91
AX 62	550.94	550.9	366	493	0.41	92
AX 64	498.51	498.9	369	500	0.30	91
AX 65	498.51	489.9	368	497	0.36	98
AX 66	546.58	547.2	300	500	0.37	98
AX 68	532.95	533.2	369	498	0.49	98
AX 69	516.5	517.2	368	496	0.38	98
AX 70	527.6	528.2	368	497	0.41	97
AX 72	524.57	525.0	369	500	0.47	96
AX 74	566.51	567.2	367	494	0.29	97
AX 75	567.4	567.1	367	496	0.32	95
AX 76	486.57	487.1	369	500	0.27	97
AX 78	530.66	531.4	369	503	0.29	97
AX 79	549.41	549.0	368	496	0.41	96
AX 80	561.59	562.2	367	496	0.41	91
AX 81	566.51	567.2	368	497	0.42	93
AX 82	580.68	581.4	369	501	0.37	92
AX 83	626	626.1	300	496	0.07	90
AX 84	578.54	579.0	369	499	0.30	91
AX 85	532.95	533.2	368	497	0.36	92
AX 87	532.95	533.2	368	495	0.32	92
AX 90	566.51	567.1	368	494	0.32	90
AX 97	566.51	567.2	369	500	0.34	98
AX 98	564.68	565.3	369	500	0.33	98
AX 100	574.63	575.3	368	497	0.42	95
AX 102	530.53	531.1	368	496	0.43	94
AX 103	570.47	571.1	365	492	0.51	96

AX 114	546.98	547.2	367	494	0.38	96
AX 115	549.41	549.0	369	496	0.31	93
AX 116	626.02	626.0	300	496	0.03	94
AX 117	515.95	515.9	369	498	0.34	96
AX 119	591.57	592.2	300	502	0.02	97
AX 120	482.49	483.1	368	497	0.26	97
AX 121	549.41	549.2	368	493	0.38	94
AX 124	508.57	509.2	370	500	0.31	97
AX 127	528.99	529.2	369	501	0.29	90
AX 128	544.99	545.2	370	499	0.29	91
AX 130	552.62	553.2	369	500	0.29	92
AX 131	566.51	567.1	368	494	0.33	93
AX 133	538.64	539.3	369	505	0.22	93
AX 134	556.61	557.3	368	499	0.29	92
AX 135	539.42	539.2	366	496	0.21	94
AX 137	549.41	549.1	369	499	0.38	93
AX 138	502.61	503.3	368	501	0.31	94
AX 139	549.41	548.8	366	490	0.41	95
AX 140	522.6	523.1	369	500	0.40	94
AX 142	532.95	533.0	367	494	0.40	98
AX 143	566.51	567.1	368	497	0.31	90
AX 144	559.41	560.4	369	498	0.31	93
AX 145	550.65	551.3	369	499	0.35	98

Table 2.5. Characterization and photophysical properties of AXAC library

compound	M^+ (exp.)	M^+ (exp.)	λ_{abs}(nm)	λ_{em}(nm)	Q	Purity
AXAC 1	550.61	551.2	369	486	0.43	98
AXAC 4	558.54	559.2	369	484	0.49	98
AXAC 6	502.56	503	372	494	0.35	97
AXAC 7	472.50	473.2	364	484	0.04	85
AXAC 10	474.51	475.2	368	490	0.35	98
AXAC 12	500.55	501.3	368	487	0.37	97
AXAC 14	572.56	573.3	368	483	0.50	98
AXAC 15	592.98	593.2	368	482	0.50	96
AXAC 17	558.54	559.2	368	486	0.50	98
AXAC 19	628.96	628.9	366	482	0.45	99
AXAC 20	602.00	602.1	369	487	0.03	93
AXAC 21	612.55	613.2	369	483	0.02	94
AXAC 22	608.54	609.2	369	486	0.45	90
AXAC 23	619.44	618.9	368	483	0.52	96
AXAC 24	558.54	559	368	483	0.50	93
AXAC 26	625.00	625	368	485	0.50	91
AXAC 28	552.58	553.1	368	487	0.41	87
AXAC 29	542.63	543.2	369	488	0.40	91
AXAC 31	576.53	577.1	368	485	0.42	94
AXAC 32	608.54	609.1	369	482	0.43	87
AXAC 35	557.00	557.2	369	487	0.54	97
AXAC 36	554.57	555.2	369	487	0.48	98
AXAC 37	558.67	559.2	375	490	0.46	98
AXAC 38	552.58	553.2	369	485	0.57	98
AXAC 41	589.02	589.2	368	484	0.61	98
AXAC 42	536.58	536.9	368	486	0.55	97
AXAC 44	544.64	545.4	368	488	0.15	89
AXAC 45	588.01	588	369	484	0.54	89

AXAC 57	673.41	574.9	368	483	0.72	91
AXAC 58	578.66	579	371	486	0.53	94
AXAC 60	565.62	566.1	369	490	0.08	86
AXAC 62	592.98	593.1	369	483	0.72	95
AXAC 64	540.55	541	369	486	0.66	91
AXAC 65	540.55	541.2	368	487	0.71	98
AXAC 66	588.61	589.3	369	485	0.61	98
AXAC 68	574.99	575.2	368	488	0.71	96
AXAC 69	558.54	559.2	368	483	0.75	97
AXAC 70	569.63	570.1	369	485	0.72	92
AXAC 72	566.61	567.2	369	486	0.72	93
AXAC 74	608.54	609.2	369	487	0.68	97
AXAC 75	609.44	609.1	369	483	0.85	98
AXAC 76	528.60	529.2	369	491	0.57	92
AXAC 78	572.70	573.1	369	487	0.61	92
AXAC 79	591.44	591.2	368	485	0.83	94
AXAC 80	603.63	604.2	368	483	0.81	95
AXAC 81	608.54	609.3	368	483	0.87	97
AXAC 82	622.71	623.4	368	486	0.70	92
AXAC 83	668.06	668.1	368	488	0.02	90
AXAC 84	620.58	621.2	369	489	0.84	91
AXAC 85	574.99	575.3	369	484	0.38	95
AXAC 87	574.99	575.1	369	484	0.54	94
AXAC 90	608.54	609.2	369	483	0.97	93
AXAC 97	608.54	609.2	369	484	0.71	97
AXAC 98	606.71	607.3	369	487	0.70	91
AXAC 100	616.67	617.3	368	486	0.76	96
AXAC 102	572.56	573.1	368	484	0.28	92
AXAC 103	612.51	613.1	368	482	0.34	92
AXAC 114	589.02	589.1	368	485	0.40	97

AXAC 115	591.44	591	369	487	0.49	96
AXAC 116	668.06	668.1	371	491	0.58	99
AXAC 117	557.99	558.1	369	485	0.28	96
AXAC 119	633.61	634.3	369	485	0.19	98
AXAC 120	524.53	525	369	483	0.40	91
AXAC 121	591.44	591.2	368	483	0.86	96
AXAC 124	550.61	551.3	372	487	0.72	92
AXAC 127	571.03	571.1	368	488	0.81	95
AXAC 128	587.03	587.2	368	488	0.19	93
AXAC 130	594.66	594.9	369	487	0.69	98
AXAC 131	608.54	609.2	368	483	0.76	98
AXAC 133	580.68	581.3	371	487	0.68	93
AXAC 134	598.65	599.3	371	487	0.38	89
AXAC 135	581.46	X	369	485	0.06	X
AXAC 137	591.44	591.2	369	484	0.78	96
AXAC 138	544.64	545.1	369	490	0.83	97
AXAC 139	591.44	590	368	484	0.52	96
AXAC 140	564.63	565.3	368	485	0.83	98
AXAC 142	574.99	575.2	368	483	0.53	97
AXAC 143	608.54	609.2	369	485	0.53	98
AXAC 144	601.45	603.1	368	486	0.37	96
AXAC 145	592.69	593.3	369	487	0.71	95

Table 2.6. Characterization and photophysical properties of AXCA library

compound	M^+ (exp.)	M^+ (exp.)	λ_{abs}(nm)	λ_{em}(nm)	Q	Purity
AXCA 1	585.05	585.2	369	488	0.42	92
AXCA 4	592.98	593.2	369	485	0.85	93
AXCA 6	537.01	537	371	487	0.36	92
AXCA 7	506.94	506.9	371	487	0.22	90
AXCA 10	508.96	509.1	374	487	0.36	92
AXCA 12	534.99	535.1	368	489	0.35	90
AXCA 14	607.01	607.1	368	483	0.52	97
AXCA 15	627.43	626.8	368	483	0.54	96
AXCA 17	592.98	593	368	485	0.46	94
AXCA 19	663.41	663	368	483	0.44	94
AXCA 20	636.44	636	369	487	0.03	92
AXCA 21	646.99	647	369	485	0.01	90
AXCA 22	642.99	643.2	369	485	0.44	89
AXCA 23	653.89	654.6	371	484	0.58	93
AXCA 24	592.98	593.2	369	486	0.53	93
AXCA 26	659.44	659.1	368	483	0.53	88
AXCA 28	587.03	587.2	368	487	0.47	90
AXCA 29	577.07	577.2	373	488	0.41	93
AXCA 31	610.97	611	368	485	0.53	90
AXCA 32	642.99	643.2	368	485	0.50	89
AXCA 35	591.44	591	368	487	0.52	89
AXCA 36	589.02	589.3	369	492	0.48	90
AXCA 37	593.12	593	369	496	0.46	94
AXCA 38	587.03	587.2	369	484	0.51	94
AXCA 41	623.46	623.2	369	481	0.57	96
AXCA 42	571.03	571.2	369	487	0.54	97
AXCA 44	579.09	579.1	371	491	0.50	89
AXCA 45	622.46	623.2	368	486	0.61	85

AXCA 57	707.86	709	368	487	0.74	94
AXCA 58	613.11	613.2	368	489	0.58	96
AXCA 60	600.07	600.2	376	486	0.16	86
AXCA 62	627.43	627.1	369	483	0.75	92
AXCA 64	574.99	575.1	369	487	0.75	87
AXCA 65	574.99	575	370	487	0.67	96
AXCA 66	623.06	623.1	371	486	0.75	85
AXCA 68	609.44	608.8	369	487	0.73	91
AXCA 69	592.98	592.8	369	486	0.78	94
AXCA 70	604.08	604	368	487	0.84	96
AXCA 72	601.05	601.2	368	486	0.73	96
AXCA 74	642.99	643.2	368	483	0.70	97
AXCA 75	643.88	643.1	369	483	0.75	90
AXCA 76	563.05	563	369	491	0.54	95
AXCA 78	607.14	607.2	369	494	0.60	90
AXCA 79	625.89	627.1	369	488	0.73	92
AXCA 80	638.07	638.2	369	484	0.75	97
AXCA 81	642.99	643.1	369	483	0.80	94
AXCA 82	657.16	657.2	371	486	0.63	95
AXCA 83	702.50	701.1	368	490	0.15	60
AXCA 84	655.02	655.1	368	492	0.82	90
AXCA 85	609.44	609.2	368	484	1.00	89
AXCA 87	609.44	609.2	369	486	0.88	91
AXCA 90	642.99	643.1	369	483	0.75	96
AXCA 97	642.99	643.1	369	487	0.73	97
AXCA 98	641.16	641.3	371	487	0.74	92
AXCA 100	651.11	651.2	369	486	0.84	98
AXCA 102	607.01	607.1	368	485	2.44	93
AXCA 103	646.95	647.1	368	482	0.46	93
AXCA 114	623.46	623.2	368	485	0.37	96

AXCA 115	625.89	626.9	368	487	0.42	94
AXCA 116	702.50	702.1	368	488	0.32	X
AXCA 117	592.43	591.8	369	498	0.96	94
AXCA 119	668.06	668.3	369	487	0.05	91
AXCA 120	558.98	559	369	488	0.11	89
AXCA 121	625.89	626.9	369	491	0.47	96
AXCA 124	585.05	585.2	371	487	0.85	91
AXCA 127	605.47	605.2	371	492	0.51	92
AXCA 128	621.47	621.2	376	493	0.16	84
AXCA 130	629.11	628.9	368	488	0.73	91
AXCA 131	642.99	642.9	368	485	0.79	94
AXCA 133	615.12	615.2	371	490	0.80	92
AXCA 134	633.10	633.3	370	489	0.67	85
AXCA 135	615.91	X	368	487	0.03	X
AXCA 137	625.89	625.2	369	487	0.19	82
AXCA 138	579.09	579.3	371	487	0.71	92
AXCA 139	625.89	625.1	369	484	0.95	92
AXCA 140	599.08	599.2	371	487	0.59	92
AXCA 142	609.44	609.2	368	481	0.56	96
AXCA 143	642.99	642.7	368	487	0.81	93
AXCA 144	635.90	637.2	368	485	0.92	96
AXCA 145	627.13	627.3	371	488	0.68	93

2.5 Experimental section

2.5.1 Synthetic materials and methods

All the chemicals including the entire alkyne building blocks and solvents were purchased from Sigma Aldrich, Alfa Aesar, Fluka, MERCK or Across, and used without further purification. 2-Chlorotrityl alcohol resin (1.37 mmol/g) was purchased from BeadTech Inc., Korea. All library compounds were characterised by HPLC-MS (Agilent-1200 series) with a DAD detector and a single quadrupole mass spectrometer (6130 series) with an ESI probe. Unless indicated, the analytical method: eluents: A: H_2O (0.1% HCOOH), B: ACN (0.1% HCOOH), gradient from 5 to 95%B in 7 min; C18(2) Luna column (4.6 x 50 mm^2, 5 µm particle size). ^1H NMR spectra was recorded on a Bruker Avance 300 NMR spectrometer. Spectroscopic measurements were done in BioTek microplate reader or SpectraMax M2 spectrophotometer (Molecular Devices). All the spectroscopic measurements were done in DMSO solutions and coumarin1 (quantum yield = 0.59) was used as a reference for quantum yield calculations.

2.5.2 Synthetic procedure of CX library intermediates and characterisation

Synthesis of 3-fluoro-6-nitro-9H-xanthen-9-one (1)

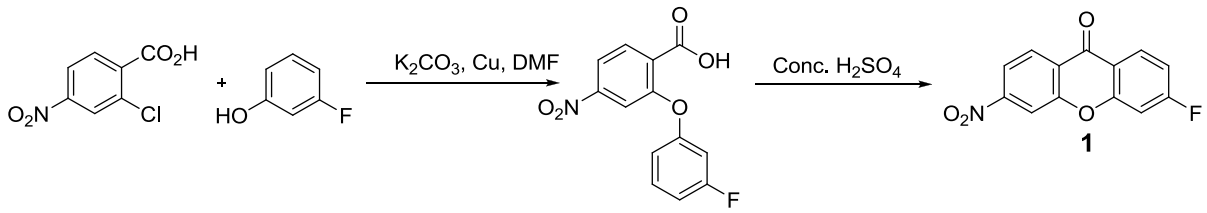

To a solution of 2-chloro-4-nitrobenzoic acid (3.0 g, 14.88 mmol) in DMF (40 mL) was added 3- fluorophenol (2.47 g, 16.38 mmol), potassium carbonate (3.08 g, 16.38 mmol) and copper Powder (102 mg, 1.61 mmol). After heating at 130 ^oC overnight the reaction mixture was then filtered through celite and washed with DMF. Once evaporating the

DMF, 1 N HCl at 0 ^{o}C was added to it. The solution was stirred until the brown solid was formed. The solid was filtered off and washed with cold water to yield a brown solid (3.1 g). A crude solid was dissolved in concentrated sulfuric acid (20 mL) and heated at 90 ^{o}C for 1 hour. After cooling to room temperature, the reaction mixture was poured to ice (350 mL volume) and stirred for one hour. ^{1}H-NMR (300 MHz, $CDCl_3$): δ 8.50 (d, 1H, *J*=8.7 Hz), 8.37 (m, 2H), 8.20 (dd, 1H, *J*=8.7 Hz, 2.1 Hz), 7.21 (m, 2H) ESI *m/z* ($C_{13}H_6FNO_4$) calc: 259.03; found: 260.0

Synthesis of tert-butyl 4-(6-nitro-9-oxo-9H-xanthen-3-yl)piperazine-1 carboxylate (2)

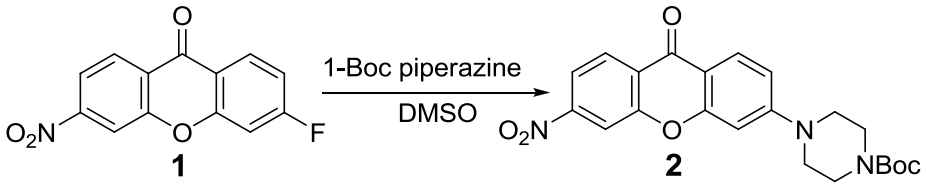

To a solution of 6-fluoro-3-Nitro-9H-Xanthone (**1**) in (2 g, 7.72 mmol) in DMSO (23 mL) 1-Boc piperazine (3.59 g, 19.3 mmol) was added. After heated at 90 ^{o}C for overnight the solution was diluted with EtOAc and washed with water and brine. The organic layer was collected and solvents were removed under reduced pressure and the residue was purified by flash column chromatography (30 to 40% EtOAc/Hexane). Yield=1.2 g (36%). ^{1}H-NMR (300 MHz, $CDCl_3$) δ 8.46 (d, 1H, *J*=8.7 Hz), 8.29 (d, 1H, *J*=2.0 Hz), 8.18 (d, 1H, *J*=9.0 Hz), 8.13 (dd, 1H, *J*=8.7 Hz, 2.1 Hz), 6.94 (dd, 1H, *J*=9.0, 2.1 Hz), 6.73 (d, 1H, *J*=2.1 Hz), 3.64 (t, 4H, *J*=4.8 Hz), 3.48 (t, 4H, *J*=4.8 Hz), 1.50 (s, 9H).^{13}C-NMR (300MHz, $CDCl_3$) δ174.1, 158.5, 155.7, 155.5, 154.5, 150.7, 128.3, 126.1, 117.8, 113.7, 113.2, 112.3, 99.5, 80.4, 46.8, 28.3. ESI *m/z* ($C_{13}H_6FNO_4$) calc: 425.16; found: 426.0

Synthesis of tert-butyl 4-(6-amino-9-oxo-9H-xanthen-3-yl)piperazine-1-carboxylate (3)

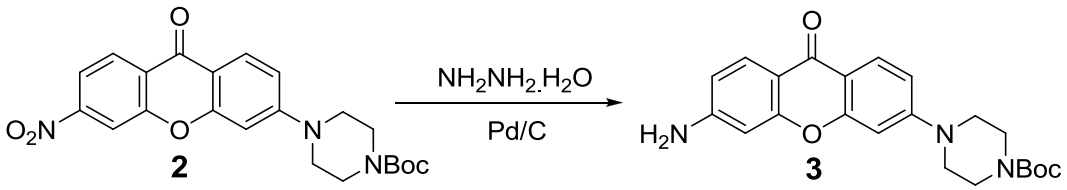

To a solution of **2** was added $NH_2NH_2.H_2O$ (1.76 g, 32.5 mmol) and Pd/C (300 mg, 20% of the compound) and heated at 90 ^oC for 4 hour .The hot solution was filtered through celite and the solvents were removed under reduced pressure. ^{1}H-NMR (300 MHz, $CDCl_3$): δ 8.12 (d, 1H, *J*=9.0 Hz), 8.07 (d, 1H, *J*=9.0 Hz), 6.83 (dd, 1H, *J*=9.0, 2.4 Hz), 6.64 (d, 1H, *J*=2.4 Hz), 6.60 (dd, 1H, *J*=9.0, 2.1 Hz), 6.51(d, 1H, *J*= 2.1 Hz), 3.59 (t, 4H, *J*=4.8 Hz), 3.35 (t, 4H, *J*=4.8 Hz), 1.48 (s, 9H). ^{13}C NMR (300 MHz, $CDCl_3$): δ 175.0, 158.2, 157.9, 154.8, 154.6, 152.3, 128.2, 127.7, 113.9, 112.0, 111.5, 100.3, 99.9, 80.2, 47.3, 28.4. ESI *m/z* ($C_{13}H_6FNO_4$) calc: 395.18; found: 396.0

Synthesis of tert-butyl 4-(6-azido-9-oxo-9H-xanthen-3-yl) piperazine-1-carboxylate (4)

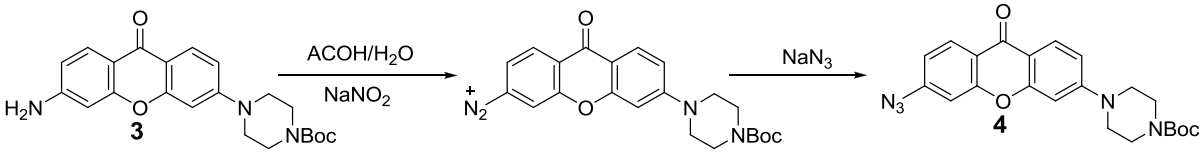

To a solution of tert-butyl 4-(6-amino-9-oxo-9H-xanthen-3-yl) piperazine-1-carboxylate (1 g, 2.53 mmol) in AcOH/H_2O (1:1) $NaNO_2$ (209.6 mg, 3.03 mmol) at 0 ^oC was added and stir it for 1 hour. The diazonium salt obtained was filtered and to the filtrate at 0 ^oC NaN_3 (246.7 mg, 3.8 mmol) was added and stirred it for one and half hour. The solution was then neutralised with saturated $NaHCO_3$ and extracted with DCM. After evaporating solvents the residue was subjected to flash column chromatography (30 to

40% EtOAc in Hexane). Yield=980 mg (92%). ^{1}H-NMR (300 MHz, $CDCl_3$): δ 8.24 (d, 1H, *J*=9.0 Hz), 8.12 (d, 1H, *J*=9.0 Hz), 8.96 (m, 2H), 8.87 (dd, 1H, *J*=9, 2.4), 6.65 (d, 1H, *J*=2.4 Hz), 3.60 (t, 4H, *J*=4.5 Hz), 3.40 (t, 4H, *J*=4.5 Hz), 1.48 (s, 9H). ^{13}C-NMR (300MHz, $CDCl_3$): δ 175.5, 158.7, 157.7, 156.0, 155.3, 146.5, 129.2, 128.7, 119.9, 115.7, 114.1, 112.5, 107.6, 100.56, 81.0, 47.7, 29.1 ESI *m/z* ($C_{13}H_6FNO_4$) calc: 421.18; found: 422.0

Synthesis of 3-azido-6-(piperazin-1-yl)-9H-xanthen-9-one (5)

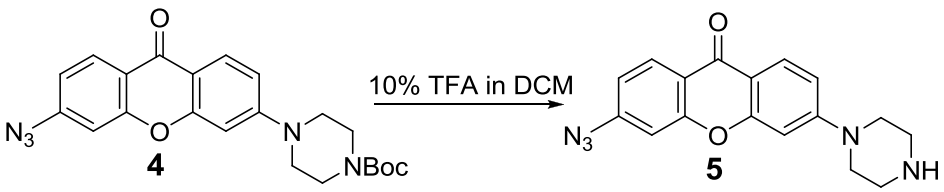

500 mg (1.2 mmol) of compound **4** was added to 25 mL of 10% TFA in DCM and stir it at room temperature for one hour. The solution was then evaporated several times with DCM. The compound used in the next step without further purifications. ESI *m/z* ($C_{13}H_6FNO_4$) calc: 321.12; found: 322.0

Preparation of 2-chlorotrityl chloride from 2-chlorotrityl alcohol resin

2-Chlorotrityl alcohol resin (2 g 1.37 mmol/g) was suspended in dichloromethane (20 mL) for 10 min. Thionyl chloride (600 μL, 8.24 mmol) was added and the resin solution was shaken for 5 hour at room temperature. The resin was filtered and washed with DMF and DCM then dried in high vacuum.

General procedure for loading 3-azido-6-(piperazin-1-yl)-9H-xanthen-9-one to solid resin (6)

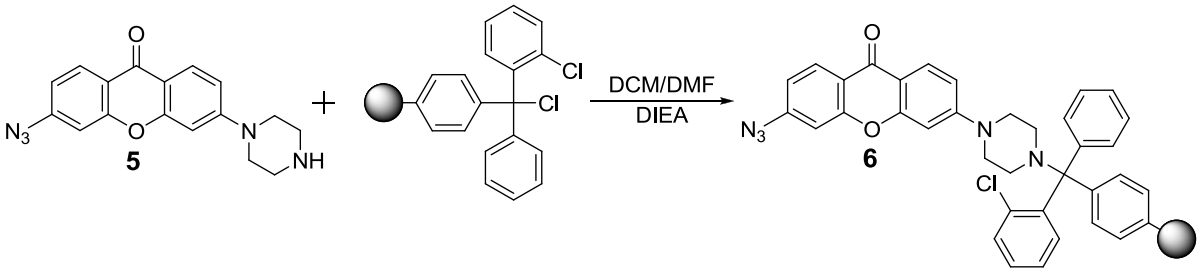

1.2 mmol of **5** was dissolved in 10 mL DMF/DCM (9:1) and DIEA was added to it. The solution was then added to 2-chlorotrityl chloride resin (0.6 mmol) suspended in dichloromethane (2 mL). After stirring for 12 h, the resin was filtered through a 10 mL cartridge and washed with DMF (x 5), MeOH (x 10), and DCM (x 10). The resin was then shaken with 20% MeOH in DMF for 2 hours. The resin again washed with DMF (x 5), methanol (x 5), and dichloromethane (x 5) and dried using high vacuum for 2 hours. The loading was 80%.

2.5.3 General Procedure for CX Library Synthesis on Solid Support

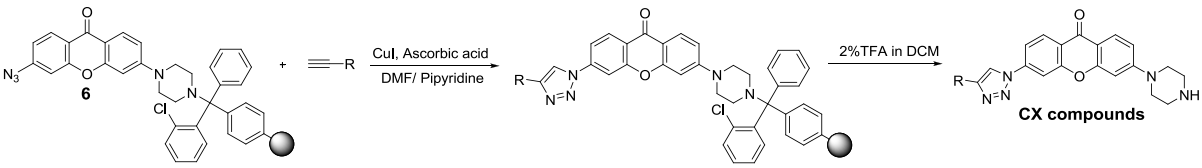

For each reaction, a resin (60 mg, 0.048 mmol) was suspended in 2 mL of DMF/ Pipyridine (4:1) in a 10 mL of syringe. 5 eq of CuI (0.24 mmol) and 5 eq (0.24 mmol) of ascorbic acid was then dissolve in 2 mL of the same solvent and added to the resin along with the 5 eq (0.24 mmol) of alkynes. The reaction mixture was shaken for overnight at room temperature and the resin was filtered through 10 mL cartridge and washed with DMF, 1% Sodium diethylthiocarbamate in DMF, 1% DIEA in DMF, 10% H_20 in DMF. Finally the resin washed with DMF (x 5), MeOH (x 5), and DCM (x 5).

The resin was dried and treated with 2% TFA in DCM (5 mL) for 10 min. The solution was drained to the 20 mL vial, and dried using Speed Vacuum.

Synthesis of active ester p-nitrophenol resin

In a 50 mL polystyrene cartridge, to an amino polystyrene resin (1 g, 1.2 mmol) in DMF (15 mL) were added 4-hydroxy-3-nitrobenzoic acid (1 g, 5.5 mmol), HOBt (1 g, 7.4 mmol), and DIC (1 mL, 6.4 mmol). After overnight shaking, the reaction mixture was washed with DMF (20 mL, 5 times), DCM, and methanol (20 mL, 5 times alternatively). To remove any undesirable side product, DMF (5 mL) and piperidine (0.5 mL) were added to the cartridge and allowed to shake for 1.5 h. The resin was filtered and washed with DMF (20 mL, 5 times). The resulting piperidine salt was removed via the addition of a 10% HCl solution (in DMF, 20 mL) and was allowed to shake for 1.5 hour. The resin was then filtered; washed with DMF, methanol, and DCM (20 mL, 5 times each); and dried by nitrogen gas flow. This nitrophenol resin is subsequently treated with acetyl chloride at room temperature for 2 hours and then washed with DCM (5 times) to obtain the active ester resin.

2.5.4 General procedure for synthesis of CXAC and CXCA

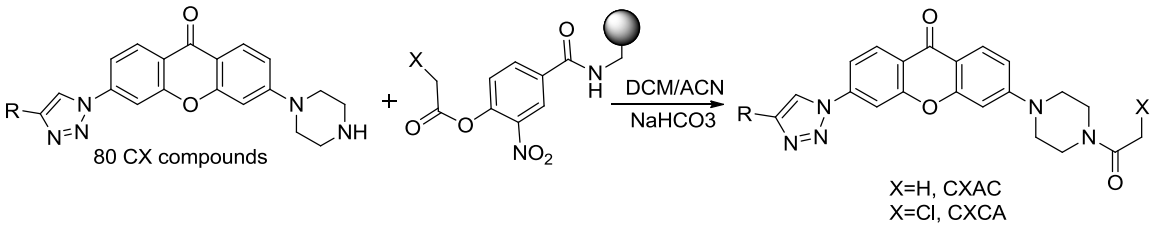

20 mg of active ester resin was suspended in 400 µl of DCM/ACN (7:1). 1 µmol of each CX compound was also dissolved in 200 µl of same solvent and added to the resin shake it at room temperature. After 3 hours the solution was filtered and dried it

2.5.5 General protocol for spectral measurement of CX , CXAC and CXCA compounds

CX and CXAC compounds spectral properties were measured in DMSO solvents. The CX compounds are excited at 360 nm wavelength and their emission spectrum are recorded from 390 nm to 600 nm. The CXAC compounds are excited at 365nm and their corresponding emission spectra are recorded from 410 nm to 540 nm. For quantum yield calculation we integrated emission area of the fluorescent spectra and compared the value to the same area measured for **Coumarin 1** (φ=0.58) in DMSO. The quantum yield is calculated using the equation **1**, where *F* stands for area of fluorescent emission, η is reflective index of the solvent, and *Abs* is absorbance at excitation wavelength selected for standards and samples. Emission was integrated 390 nm to 600 nm for CX and for CXAC the integrated area was 410 nm to 540 nm.

$$\varphi_{flu}^{sample} = \varphi_{flu}^{reference}\left(\frac{F^{sample}}{F^{reference}}\right)\left(\frac{\eta^{sample}}{\eta^{reference}}\right)\left(\frac{Abs^{reference}}{Abs^{sample}}\right) \quad \text{.....(1)}$$

2.5.6 Characterisation of CDb8

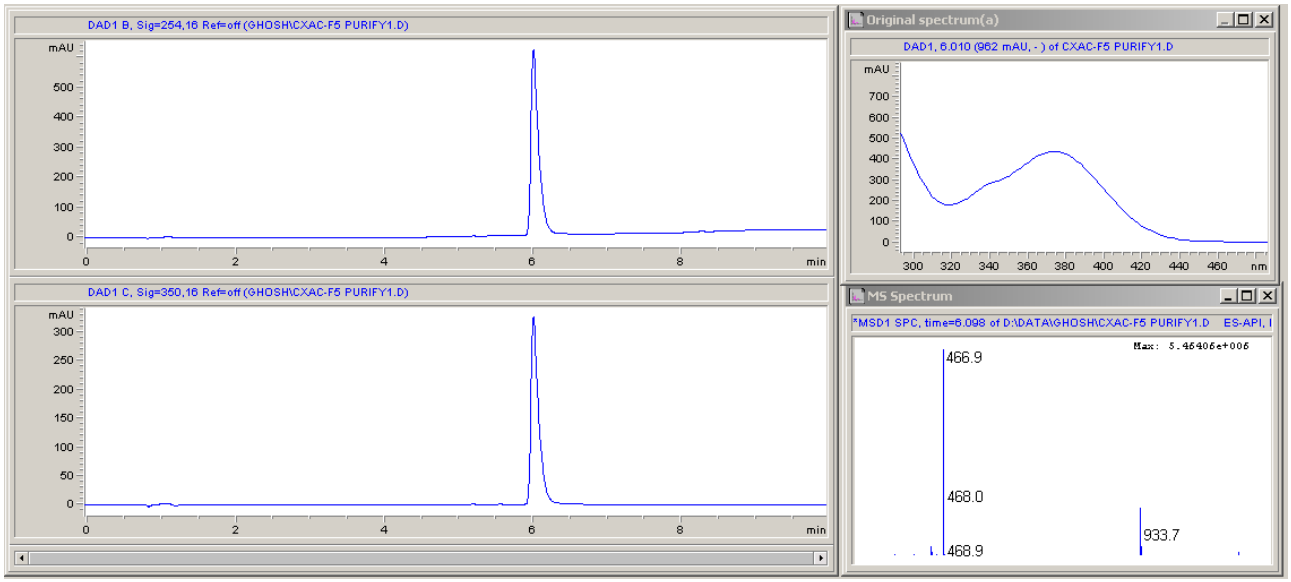

HPLC-MS characterization of CDb8**.** Chromatograms (*descending order*) at 254 nm, 350 nm. Spectra profile (300-500 nm). ESI-MS positive spectra. HPLC conditions: A: H_2O-HCOOH: 99.9:0.1. B: ACN-HCOOH: 99.9:0.1; gradient 5% B to 95% B (7 min), isocratic 95% B (1.5 min). Reverse-phase Phenomenex C_{18} Luna column (4.6 x 50 mm^2) 3.5 µm, flow rate: 0.8 mL/min.

^{1}H-NMR (300 MHz, $CDCl_3$): δ 8.76 (1H, *s*), 8.64 (1H, dd, *J*= 2.7 Hz, 1.8 Hz), 8.47 (1H, dd, *J*= 8.7, 1.8 Hz), 8.28 (1H, d, *J*= 8.1 Hz), 8.20 (1H, dd, *J*= 9, 2.7 Hz), 7.98 (1H, dd, *J* = 2.7, 2.1 Hz), 7.85 (1H, td, *J*= 8.7, 1.8 Hz), 7.78 (1H, dd, *J*= 8.7 Hz, 2.4 Hz), 7.30 (1H, m), 6.94 (1H, dd, *J* = 9, 2.4 Hz), 6.77 (1H, d, *J*= 2.4 Hz), 3.83 (1H, m), 3.70 (1H, m), 3.50 (1H, m) & 2.17 (3H, s). ESI *m/z* ($C_{26}H_{22}N_6O_3$) calc: 466.18; found: 466.9

Structure of **CDb8**:

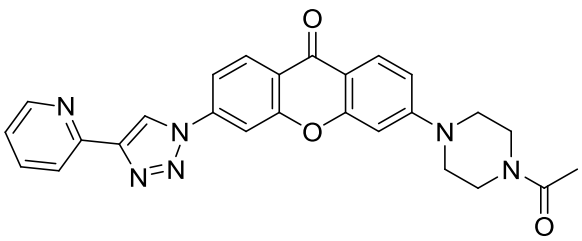

2.5.7 Synthetic procedure for AX library and intermediates

Loading of proparzylamine to solid support (1)

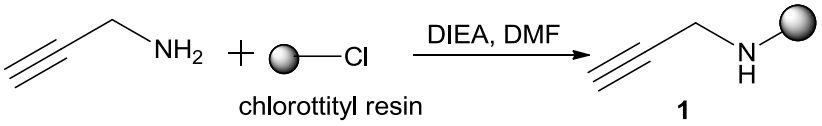

To a solution of proparzylamine hydrochloride (910mg, 10mmol) in DMF , DIEA(6.45g, 50mmol) was added to it. To this solution the chloro trityl resin (1g, 1mol/g) was added and was shaken it for 24 hours. The resin was then washed with DMF, MeOH and DCM (5 times each). The washed resin was then quenched with 40% MeOH in DMF for 1 hour. Finally, the resin was washed with DMF, MeOH and DCM and dried under high vacuum.

Synthesis of intermediate (2)

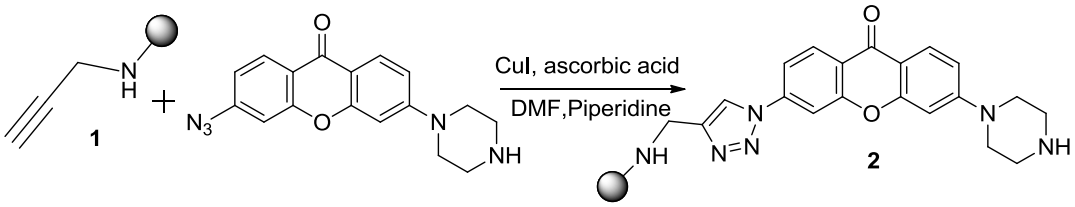

The resin (778 mg, 0.788 mmol, 1 eq) was added to a solution of (750 mg, 2.33 mmol, 3 eq) xanthone azide in DMF/piperidine (4:1). Then copper iodide (741 mg , 3.89 mmol, 5 eq) and ascorbic acid (684 mg, 3.89 mmol, 5 eq) were dissolved in the same solution and added to the resin. The reaction mixture was then shaken for 24 hours. After the reaction, the resin was washed with, 1% Diethylthiocarbamate and 1% DIEA in DMF, 10 % water in DMF, MeOH and DCM. Finally the resin was dried under vacuum.

Synthesis of AX compounds

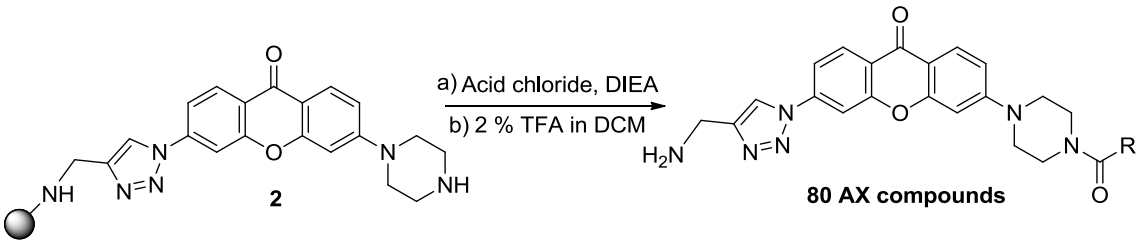

80 mg (0.056 mmol, 1 eq) of resin B, was suspended in DCM. To it, DIEA (72.24 mg, 0.56 mmol, 10 eq) was added. Then, 10 equivalents of acid chloride were added and shake it for 4 hours at rt. After 4 hours the resin was washed with DMF, MeOH and DCM. Finally the resin was cleaved with 2 % DCM in MeOH. The solution was then evaporated and the excess TFA was fully removed by a work up , using 2 N NaOH and DCM . The excess unreacted proparzyl amine was removed from the DCM layer using a short a short silica gel filtrations.

2.5.8 Procedure for AXCA and AXAC synthesis

30 mg of chloroacetyl or acetyl loaded nitrophenol resin was suspended in 7:1 DCM/ACN solution in an eppendrof tube. To this 1 µmol quantity of AX dissolved in the same solvent mixture was added and shake it for three hours. After the reaction the solution was filtered out from the resin and the corresponding AXCA and AXAC was collected.

2.6 General protocol for cell imaging and flow cytometry

The 384 well plates were coated with gelatin for at least 1 hour. Then MEF (2.5 X 10^4/mL) and mESC (1 X 10^5/mL) were seeded into the wells. After one day, 1 uM concentration of compound was added to the cells and incubated for 1 hour. The image were then acquired using the Meta Xpress software using the DAPI filter. Transmitted light images were also taken.

2.7 General protocol for flow cytometry measurement

1 μM concentration of compound was added to the cells and incubated for 1 hour. After which the staining pattern of the cells were checked before and after washing (3 times with PBS) using the fluorescent microscopy. The cells were trypsinized using Trypsin, 0.25% (1 x) with EDTA and transferred to 5 mL polystyrene round bottom tube (Falcon®). The pellet obtained was then resuspended and washed with cold PBS (3 times).

2.8 References

1. Valeur, B. (2002) Molecular fluorescence: Principles and applications; Wiley: Weinheim, New York
2. Lakowicz, J. R. (1999) Principles of fluorescence spectroscopy; 2nd ed.; Kluwer/Plenum: New York
3. Czarnik, A. W. (1993) Fluorescent chemosensors for ion and molecule recognition; American Chemical Society: Washington, DC
4. Schiedel, M. S., Briehn, C. A., and Bauerle, P. (2001) Single-Compound Libraries of Organic Materials: Parallel Synthesis and Screening of Fluorescent Dyes. *Angew Chem Int Ed Engl 40*, 4677-4680
5. Sivakumar, K., Xie, F., Cash, B. M., Long, S., Barnhill, H. N., and Wang, Q. (2004) A fluorogenic 1,3-dipolar cycloaddition reaction of 3-azidocoumarins and acetylenes. *Organic letters 6*, 4603-6.
6. Zhu, Q., Yoon, H.S., Parikh, P.B., Chang, Y.T., Yao, S.Q.(2002) "Combinatorial discovery of novel fluorescent dyes based on Dapoxyl TM", Tetrahedron Lett. 43, 5083-5086.
7. Li, Q., Lee, J. S., Ha, C., Park, C. B., Yang, G., Gan, W. B. and Chang, Y. T. (2004) Solid phase synthesis of styryl dye library and its application to amyloid sensors, *Angew Chem Int Ed Engl 43*, 6331–35.
8. Wang, S., and Chang, Y. T. (2006**)** Combinatorial synthesis of benzimidazolium dyes and its diversity directed application toward GTP-selective fluorescent chemosensors, *Journal of the American Chemical Society 128*, 10380-81
9. Ahn, Y. H., Lee, J. S., and Chang, Y. T. (2007) Combinatorial rosamine library and application to in vivo glutathione probe. *Journal of the American Chemical Society 129*, 4510-1.

10. Lee, J. S., Kang, N. Y., Kim, Y. K., Samanta, A., Feng, S., Kim, H. K., Vendrell, M., Park, J. H., and Chang, Y. T. (2009) Synthesis of a BODIPY library and its application to the development of live cell glucagon imaging probe. *Journal of the American Chemical Society 131*, 10077-82.
11. Akao, Y., Nakagawa, Y., Iinuma, M., and Nozawa, Y. (2008) Anti-cancer effects of xanthones from pericarps of mangosteen. *International journal of molecular sciences 9*, 355-70.
12. Li, J., Hu, M., and Yao, S. Q. (2009) Rapid synthesis, screening, and identification of xanthone- and xanthene-based fluorophores using click chemistry. *Organic letters 11*, 3008-11.
13. Zhou, Z., and Fahrni, C. J. (2004) A fluorogenic probe for the copper(I)-catalyzed azide-alkyne ligation reaction: modulation of the fluorescence emission via 3(n,pi)-1(pi,pi) inversion. *Journal of the American Chemical Society 126*, 8862-3.
14. Devaraj, N. K., and Collman, J. P.(2007), Copper Catalyzed Azide-Alkyne Cycloadditions on Solid Surfaces: Applications and Future Directions *QSAR Comb. Sci. 26*, 1253 –60.
15. Xie, F.; Sivakumar, K.; Zeng, Q.; Bruckman, M. A.; Hodges, B.; Wang, Q.; (2008) "A Fluorogenic Cu(I) Catalyzed Azide-Alkyne Cycloaddition Reaction of Azidoanthracene Derivatives", Tetrahedron 64, 2906-14.
16. Sawa, M., Hsu, T. L., Itoh, T., Sugiyama, M., Hanson, S. R., Vogt, P. K., and Wong, C. H. (2006) Glycoproteomic probes for fluorescent imaging of fucosylated glycans in vivo. *Proceedings of the National Academy of Sciences of the United States of America 103*, 12371-6.

17. Shi, J.; Liu, L.; He, J.; Meng, X.; Guo, Q. (2007**)** Facile Derivatization of Pyridyloxazole-type Fluorophore via Click Chemistry**.** *Chem. Lett.*, *36*, 1142
18. Im, C. N., Kang, N. Y., Ha, H. H., Bi, X., Lee, J. J., Park, S. J., Lee, S. Y., Vendrell, M., Kim, Y. K., Lee, J. S., Li, J., Ahn, Y. H., Feng, B., Ng, H. H., Yun, S. W., and Chang, Y. T. (2010) A fluorescent rosamine compound selectively stains pluripotent stem cells. *Angew Chem Int Ed Engl 49*, 7497-500.

Combinatorial Synthesis of FRET Based Fluorescent Libraries for Optical Sensor Development

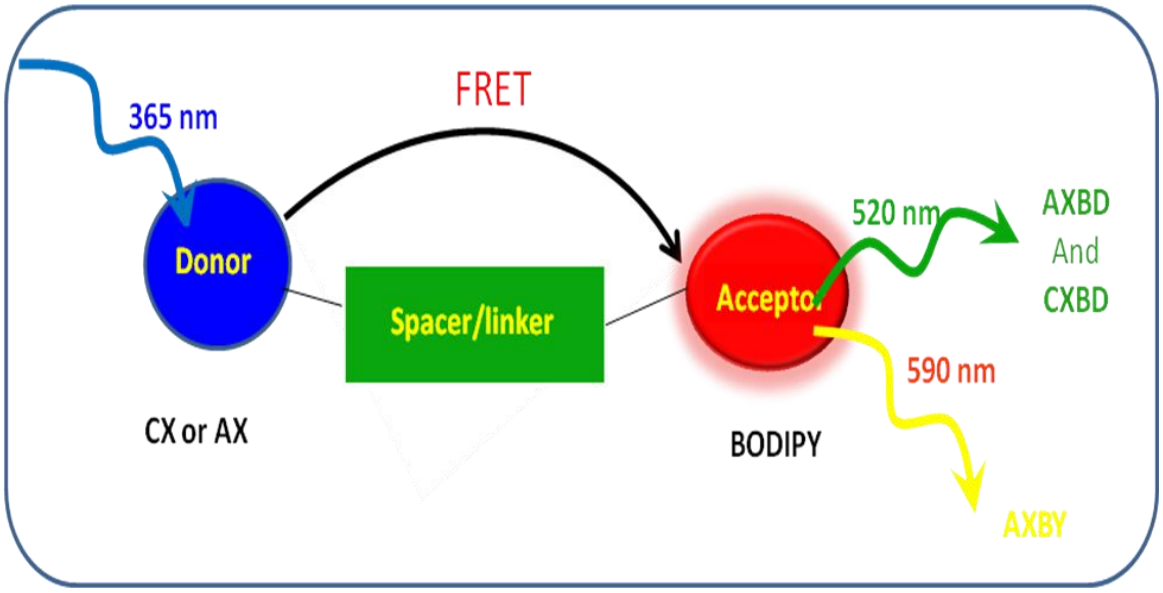

3.1 Introduction

Fluorescent sensor molecules have widely been used in cellular imaging and became one of the most attractive topics in the field of chemical biology research during the last few decades [1–3]. In this period, numerous sensor molecules have been reported for biological applications and also commercialized[4–7]. These fluorescent sensors are beneficial because of their high sensitivity and specificity. However, fluorescence measurement by measuring the change of fluorescence intensity without a substantial shift of excitation or emission wavelength can be influenced by many factors. The localization of the sensor, changes of environment around the sensor (e.g., pH, polarity and temperature), emission collection efficiency, effective cell thickness in the optical beam, and changes in excitation intensity could change the fluorescent intensity dramatically. Therefore, it is difficult to measure the exact analyte concentration by measuring only the intensity changes of the fluorescent sensor molecule. Ratiometric measurement, the simultaneous measurement of the fluorescence intensities at two different wavelengths and calculation of their ratio[8] could be utilized to reduce the influence of such factors. Ratiometric measurements involve observation of changes in the ratio of the fluorescence intensities of the excitation or the emission at two wavelengths. This technique helps to determine the target analytes more precisely and quantitatively. In order to carry out a ratiometric measurement, it is required that the sensor molecule should exhibit a large shift in its emission or excitation wavelength upon interaction with target analytes. Fluorescence resonance energy transfer (FRET) is one mechanism used to obtain a large spectral shift. Recently, several fluorescent sensor molecules based on FRET have been developed and extensively used, such as the calcium sensor cameleon[9] and the *â*-lactamase sensor CCF2[10].

Fluorescence resonance energy transfer (FRET) is generally a non-radiative energy transfer process to measure the interaction between two molecules labelled with two different chromophores, named donor (D) and acceptor (A). This non-radiative transfer of energy occurs from a donor molecule to an acceptor molecule when they are in close proximity. The physical phenomenon of FRET was first described by the German scientist Theodor Förster[11] in 1948. Although FRET is termed as fluorescence resonance energy transfer, there are no photons or fluorescence light transfer to the acceptor from the donor molecule. Besides, the acceptor fluorescence is not necessarily required for resonance energy transfer to occur. To avoid this controversy, some scientists prefer to use the term FRET as an abbreviation for Forster resonance energy transfer, instead of fluorescence resonance energy transfer. In this chapter, we will use the term FRET as an abbreviation for fluorescent resonance energy transfer.

The most commonly used Donor–Acceptor pairs for biological study are synthetic organic dyes and Fluorescent Proteins [12]. In recent years, several FRET based sensors have also been developed where semiconductor nanoparticles (quantum dots)[13] or non-natural auto fluorescent amino acids [14], were combined with synthetic organic dyes as a FRET pair [15]. Although several kinds of FRET pairs are reported, in most of the cases the use of synthetic organic FRET molecules is advantageous over others for biological studies. The major advantages of synthetic organic fluorophores over fluorescent proteins include their small size (<1 kDa) and favourable spectral and photochemical properties. Moreover, these organic fluorophores have better solubility and lower cytotoxicity when compared to quantum dots. A series of organic dyes including Cy3, Cy5, Cy3.5, Alexa dyes and BODIPY have been reported in FRET studies because of their superior photostability and high quantum yield[16]. Considering

all these advantages of the organic FRET pairs, we have synthesised the FRET libraries by coupling two organic fluorophores, namely xanthone and BODIPY.

3.2 Objectives

Herein, we report the synthesis of first diversity-oriented FRET libraries. To utilize the superior properties of FRET molecule over single fluorescent molecules, we have synthesized three FRET based fluorescent libraries (AXBD, CXBD, AXBY) and applied them for optical sensor development. We have adopted a solid phase methodology for the simple and efficient synthesis of these FRET libraries. This chapter mainly covers the synthesis and evolutions of the photophysical properties of these synthetic FRET libraries.

3.3 Selection of the dyes for FRET

BODIPY dyes are generally bright fluorophores with relatively high quantum yields (almost trends to 1) and large extinction coefficients. Structural modifications of these BODIPY compounds can be done very easily and their emission spectra can be turned over a large range of visible region, from green to red [17]. Hence, several FRET sensors were reported based on the modified BODIPY dyes.[18] However, xanthone's applications in FRET as a donor have not been well illustrated even though these dyes are highly photostable and their rigid structure helps them to serve as a very good donor. The xanthones can be excited around 350 nm and usually emits blue light around 490 nm. As the emission wavelength of xanthone's overlaps with the excitation wavelength of BODIPY (around 500 nm), the combination of these two dyes can serve as an effective FRET pair. This study will help to evaluate the usefulness of xanthone as a FRET donor.

3.4 Results and discussion

3.4.1 Synthesis of tetramethylbodipy acid

The synthesis of BODIPY acid involves the reaction between 2,4- Dimethyl-pyrrole and Methyl 4-chloro-4-oxobutyrate followed by the addition of triethyl amine and borontrifluoride to provide the BODIPY ester. The hydrolysis of the BODIPY ester in presence of potassium hydroxide provides the desired BODIPY acid (Scheme 3.1).

Scheme 3.1. Synthesis of tetramethylbodipy acid

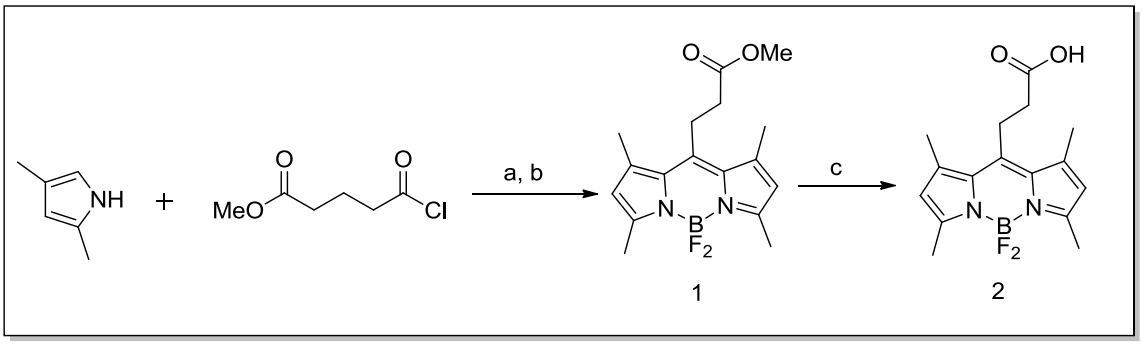

Reagents and conditions: (a) DCM, rt, 6 h; (b) TEA, $BF_3.OEt_2$ 12 h; (c) 0.2 M KOH , DCM, MeOH , rt, 6 h.

3.4.2 Synthesis of AXBD and CXBD libraries

The tetramethyl BODIPY acid was reacted with the nitrophenol resin in the presence of DIC and a catalyst DMAP to provide an activated ester resin (Scheme 3.2). The synthetic procedure of CXBD involves a reaction between the BODIPY activated ester resin (3) with the CX library compounds BODIPY acid to in a mixture of dichloromethane and acetonitrile. The solutions were filtered out and collected as CXBD and 70 relatively pure compounds were isolated for further study. The CXBD compounds have an average purity over 90 percent at 254 nm wavelength (Table 3.1).

Scheme 3.2. Synthesis of CXBD library

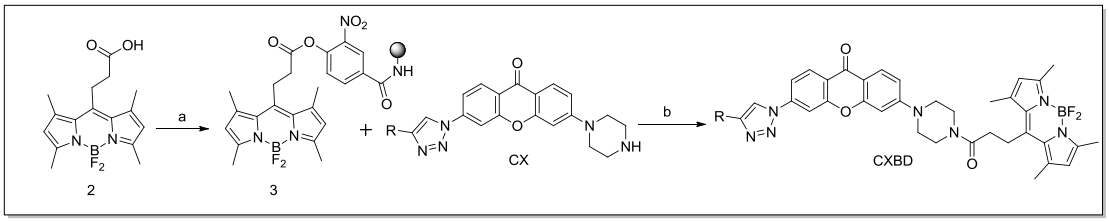

Reagents and conditions: (a) DIC, DMAP, DMF, rt, 24 h; (b) DCM/ACN (7/1), rt, 3 h

The AXBD library was also synthesized using the same approach as CXBD. The bodipy activated ester resin was reacted with 80 AX compounds in dichloromethane and acetonitrile mixture and the solution was collected as the pure AXBD compounds (Scheme 3.3). 78 compounds with an average purity over 90 percent at 254 nm wavelength were selected for the further study (Table 3.2).

Scheme 3.3. Synthesis of AXBD library

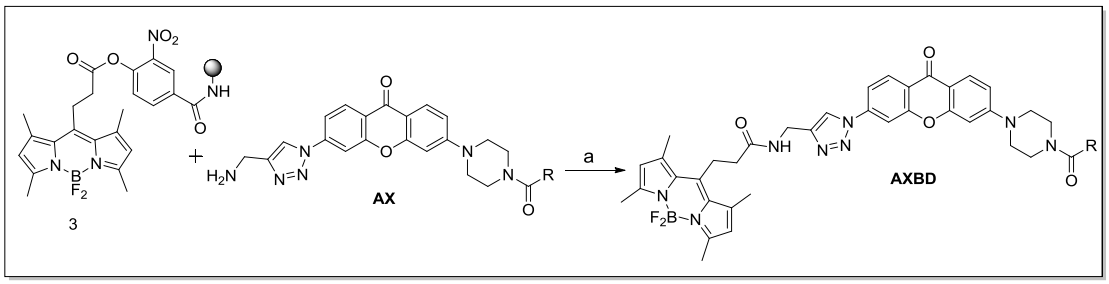

Reagents and Conditions: (a) DCM/ACN (7/1), rt, 3 h.

3.4.3. Spectroscopic properties of AXBD and CXBD libraries

These AXBD and CXBD compounds show similar photo physical properties. These compounds have an average excitation at around 370 nm and emission around 520 nm (Table 3.1 and Table 3.2). These green fluorescent AXBD and CXBD compounds show large stock shift around 150 nm and the donor to acceptor energy transfer efficiency is more than 95 percent.

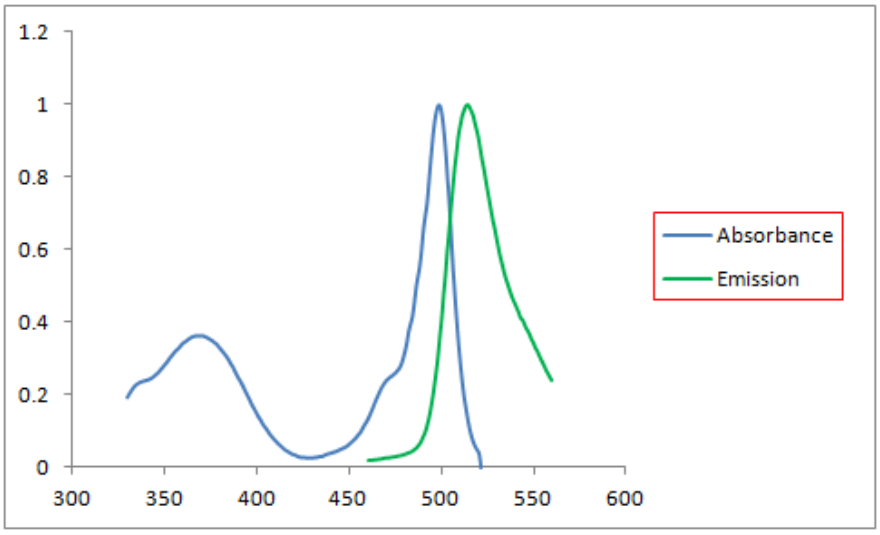

Figure 3.1. Representative(AXBD 1) and normalised absorbance and emission spectra for AXBD library. Absorbance (2.5 µM) and emission (2.5 µM) are taken in DMSO solvent.

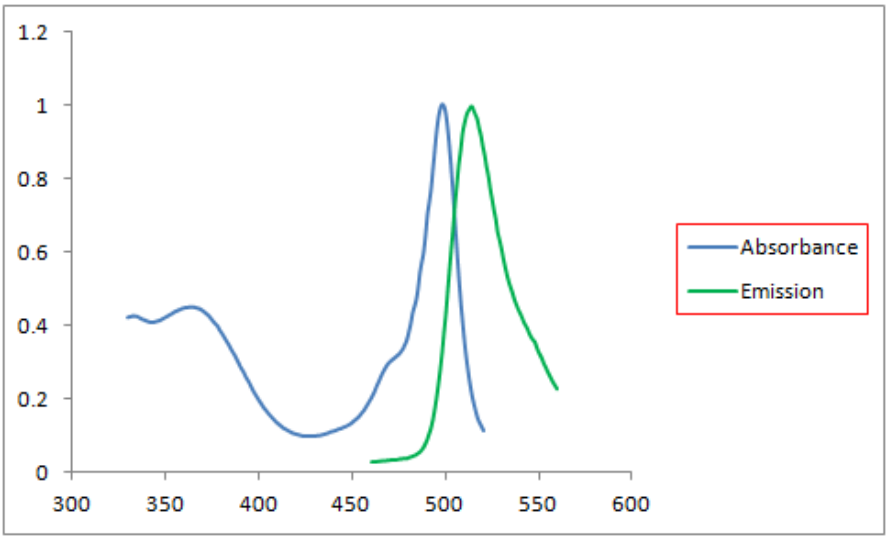

Figure 3.2. Representative (CXBD 1) and normalised absorbance and emission spectra for CXBD library. Absorbance (2.5 µM) and emission (2.5 µM) are taken in DMSO solvent.

3.4.4 Synthesis of AXBY Library

To monitor several biochemical experiments, it is required to label a few particular biomolecules with different colours of fluorescent dyes. Usually, different coloured fluorescent molecules have different wavelength of excitation. Hence, it is difficult to excite them simultaneously by using a common light. The use of fluorescent resonance energy transfer molecules could be a partial solution in this problem. In order to achieve this goal this, a common donor molecule can be attached to different acceptor molecules which are significantly different in terms of their emission wavelength. The FRET molecules which have very high energy transfer efficiency from donor to acceptor would be used successfully in this purpose. Keeping these practical problems in mind, we want to develop the FRET libraries using a common donor molecule with several acceptor molecules having different wavelengths of emission. In order to fulfil this strategy, we want to introduce a new FRET library which will have the same excitation as AXBD or CXBD but it should show much higher wavelength of emission either yellow or red region . For this reason, AX compounds are coupled with a BODIPY derivative (scheme 6, Intermediate 5) to generate the new FRET library (AXBY) which shows yellow fluorescence.

3.4.5 Synthesis of 4-methyoxy benzaldehyde conjugated bodily acid (5)

As shown in the scheme 3.4, the synthesis of intermediate 5 involves five successive steps. First, Pyrrole-2 carboxaldehyde was heated with hydrogen ethyl malonate in pyridine and piperidine mixture to generate the intermediate 1. The intermediate 1, was then reduce to intermediate 2. The reaction of intermediate 2 with 3, 5-dimethylpyrrole-2-carboxaldehyde in presence of phosphorosoxychloride and followed by the addition of DIEA and $BF_3.Et_2O$ provides the BODIPY ester (3). This

ester was then hydrolysed and condensed with 4-methoxy benzaldehyde to provide the desired BODIPY acid.

Scheme 3.4. Synthesis of 4-methoxybenzaldehyde conjugated bodipy acid (5)

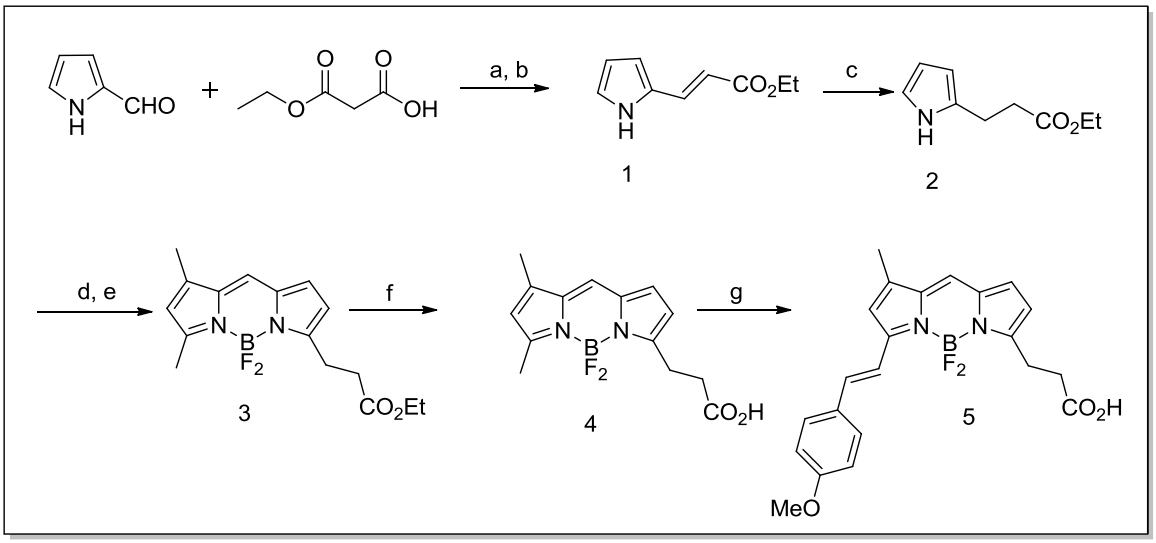

Reagents and conditions: (a)Pyridine/ piperidine , 50 ^{o}C, 2 day,(b) then 80 ^{o}C, 1 day. (c) Pd/C , MeOH, 6 h. (d) 3,5-dimethyl-1H-pyrrole-2-carbaldehyde, $POCl_3$, DCM, 0^{o}C to r.t , 6 h, (e) DIEA, BF_3.OEt, 0^{o}C to r.t , 12 h. (f) HCl, THF/ H_2O (3:2), Reflux, 12 h. (g) p-OMe C_6H_4CHO, Pyrrolidine/acetic acid(1:1), ACN, 80 ^{o}C

3.4.6 Synthesis of AXBY library compounds

Scheme 3.5. Synthesis of AXBY library

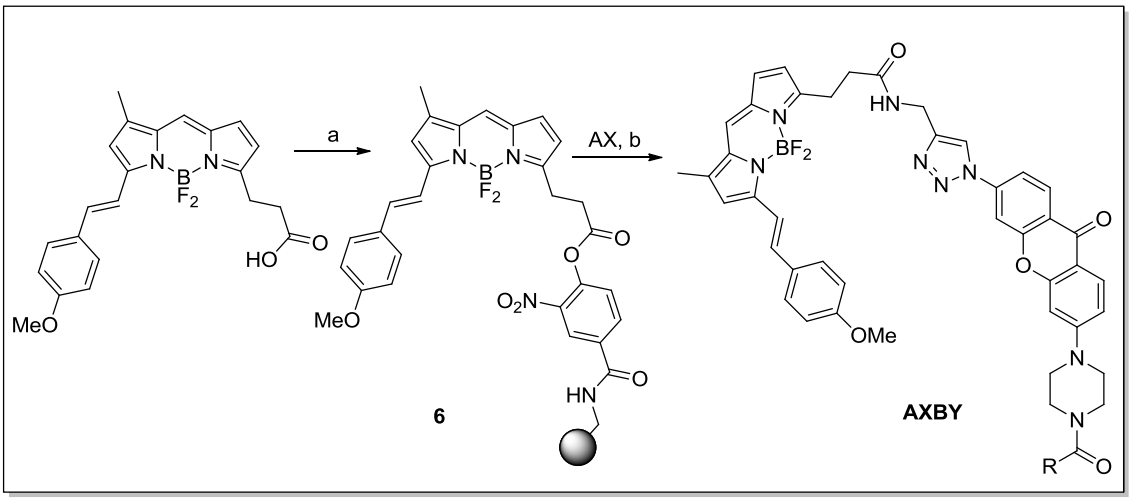

Reagents and conditions: (a) DMF, DIC, DMAP, 24 h, rt, (b)DCM, CAN(9:1) , overnight

After successfully synthesizing 4-methoxybenzaldehyde conjugated BODIPY acid, the intermediate 5 was loaded to the nitrophenol resin to provide the activated ester resin . The reaction of AX compounds with active ester resin (6) generate AXBY library (scheme 3.5).

3.4.7. Photophysical properties of AXBY library

The AXBY compounds show similar excitation like AXBD and CXBD compounds (λ_{ex} = 370 nm) but emit much higher wavelength (λ_{em} = 590 nm) in the yellow region (Table 3.3). Surprisingly, without any significant overlap between the excitation wavelength of AX (donor) with the 4-methoxybenzaldehyde conjugated BODIPY acid (Acceptor) these compound show the energy transfer efficiency from xanthone to BODIPY over 95%.

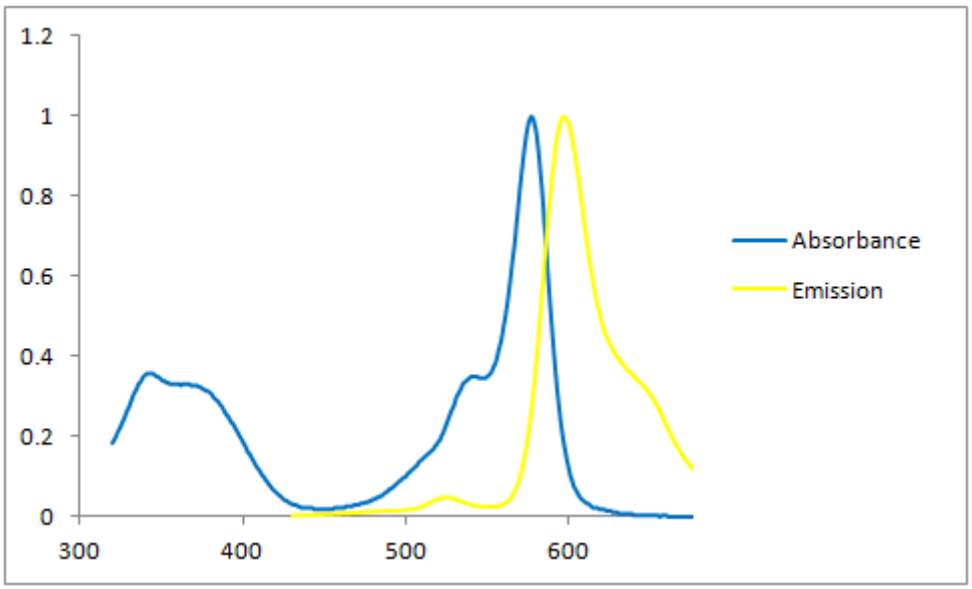

Figure 3.3. Representative (AXBY 37) and normalised absorbance and emission spectra for AXBY library. Absorbance (2.5 µM) and emission (2.5 µM) are taken in DMSO solvent.

3.5 Conclusion

In conclusion, we have successfully synthesized three FRET based fluorescent libraries using a solid phase activated ester methodology. We also evaluated their interesting photophysical properties. Surprisingly, these mega stock shift dyes have almost 90 percent energy transfer efficiency from xanthone to BODIPY. In addition to this, the AXBY compounds showed the perfect energy transfer ability from xanthone to BODIPY without having any spectral overlap between donor emission and acceptor absorbance.

Table 3.1. Characterization and photophysical properties of CXBD library

compound	M^+ (exp.)	M^+ (exp.)	λ_{abs}(nm)	λ_{em}(nm)	purity
CXBD 1	705.60	686.1	498	514	97
CXBD 2	706.59	687.3	498	512	90
CXBD 3	719.63	700.3	498	514	94
CXBD 4	689.56	670.3	498	513	87
CXBD 5	717.61	698.3	498	514	95
CXBD 7	731.64	711.1	498	512	84
CXBD 8	745.67	726.4	498	514	96
CXBD 9	725.59	706.3	498	513	93
CXBD 10	739.62	720	498	514	92
CXBD 11	781.70	762.3	498	513	91
CXBD 12	781.70	762.3	498	514	94
CXBD 13	768.66	749.3	499	513	82
CXBD 14	785.65	766.3	498	513	93
CXBD 15	809.59	790.2	498	513	94
CXBD 16	761.57	742.3	498	513	95
CXBD 17	755.62	736.3	498	514	95
CXBD 18	782.69	783.3	498	513	96
CXBD 19	753.65	734.3	498	514	96
CXBD 20	817.69	798.3	498	514	94
CXBD 21	775.65	773.9(MSD2)	498	513	91
CXBD 22	805.68	786.3	498	513	92
CXBD 24	767.67	806.3	498	514	93
CXBD 25	753.65	734.3	498	513	92
CXBD 26	761.57	742.3	498	512	89
CXBD 27	755.62	736.3	498	514	91
CXBD 28	739.62	720.3	498	514	94
CXBD 29	795.73	776.3	498	514	92
CXBD 30	861.59	842.2	498	513	90

CXBD 31	743.58	724	498	514	91
CXBD 32	767.67	746.1	498	513	89
CXBD 33	769.65	767.8(MSD2)	498	514	92
CXBD 34	755.62	736.2	498	514	89
CXBD 35	743.58	724.3	498	513	92
CXBD 36	719.63	700.3	498	514	95
CXBD 37	729.63	710.3	498	514	92
CXBD 38	794.48	774.2	498	514	87
CXBD 39	755.62	736.3	498	514	95
CXBD 40	739.62	720.3	498	513	90
CXBD 41	719.63	700.3	498	514	96
CXBD 42	705.60	686.3	498	513	96
CXBD 43	705.60	686.3	498	514	89
CXBD 44	761.71	742.4	498	513	92
CXBD 45	739.62	720.3	498	513	88
CXBD 46	753.65	734.3	498	513	95
CXBD 47	733.66	714.4	498	514	96
CXBD 48	691.58	672.3	498	514	96
CXBD 49	789.76	768.4	498	514	91
CXBD 50	747.68	728.4	499	514	93
CXBD 85	769.62	750.3	498	514	91
CXBD 86	769.62	750.3	498	514	89
CXBD 88	721.60	702.1	498	512	88
CXBD 57	726.58	727.3	498	514	86
CXBD 58	746.66	747.4	498	514	88
CXBD 59	726.58	707.3	498	513	82
CXBD 90	707.58	688.1	498	513	92
CXBD 62	693.55	674.3	498	514	89
CXBD 66	721.68	702.2	498	513	90
CXBD 91	751.63	732.1	498	513	84

CXBD 68	755.62	736.3	498	513	90
CXBD 92	707.58	688.3	498	513	93
CXBD 95	707.58	688.1	498	513	92
CXBD 84	787.64	768	498	512	85
CXBD 73	735.71	716.4	498	513	88
CXBD 97	793.59	774	498	513	91
CXBD 76	731.64	712.1	498	513	88
CXBD 98	793.59	774.2	498	512	94
CXBD 79	735.63	716.1	498	513	89
CXBD 80	735.63	716.1	498	513	84
CXBD 82	721.60	702.3	498	513	87
CXBD 83	755.62	736.1	498	513	88

HPLC-MS characterization of AXBD, CXBD and AXBY library compounds. Chromatograms (descending order) at 254 nm, 350 nm, 500nm, 560 nm spectra profile (300-650 nm); ESI-MS positive spectra. HPLC conditions: A: H_2O-HCOOH: 99.9:0.1. B: ACN-HCOOH: 99.9:0.1; gradient 5% B to 95% B (10 min), isocratic 95% B (2.5 min). Reverse-phase Phenomenex C_{18} Luna column (4.6 x 50 mm^2) 3.5 um, flow rate: 0.8 mL/min.

The spectral measurement done using DMSO solvent

The purity is calculated at 254 nm wavelength.

Table 3.2. Characterization and photophysical properties of AXBD library

compound	M^+ (exp.)	M^+ (exp.)	λ_{abs}(nm)	λ_{em}(nm)	Purity
AXBD 1	810.7	810.36	498	514	94
AXBD 4	818.63	818.31	498	514	90
AXBD 6	762.66	762.36	498	514	88
AXBD 7	732.59	732.32	498	513	80
AXBD 10	734.6	734.33	498	514	92
AXBD 12	760.64	760.35	498	513	90
AXBD 14	832.65	832.33	498	514	95
AXBD 15	853.07	852.27	498	514	91
AXBD 17	818.63	818.31	498	515	93
AXBD 19	889.05	888.25	498	514	88
AXBD 20	862.09	861.28	498	513	86
AXBD 21	862.09	861.28	499	513	85
AXBD 22	868.63	868.31	498	514	87
AXBD 23	879.53	878.23	498	514	85
AXBD 24	818.63	818.31	498	514	88
AXBD 26	885.09	884.28	498	513	89
AXBD 28	812.67	812.34	498	514	84
AXBD 29	802.72	802.39	498	515	83
AXBD 31	836.62	836.3	498	514	88
AXBD 32	868.63	868.31	498	514	85
AXBD 35	817.09	816.29	498	514	90
AXBD 36	814.66	814.34	498	514	83
AXBD 37	818.76	818.43	498	514	91
AXBD 38	812.67	812.34	498	514	94
AXBD 41	849.11	848.3	498	514	97
AXBD 42	796.67	796.35	498	514	94
AXBD 44	804.73	804.41	498	514	88
AXBD 45	848.1	847.3	498	513	85

AXBD 57	933.5	932.2	498	513	89
AXBD 58	838.75	838.39	498	514	95
AXBD 60	825.71	825.37	498	513	81
AXBD 62	853.07	852.27	498	514	89
AXBD 64	800.64	800.32	498	514	90
AXBD 65	800.64	800.32	498	514	93
AXBD 66	848.7	848.34	498	514	92
AXBD 68	835.08	834.28	498	513	94
AXBD 69	818.63	818.31	498	514	95
AXBD 70	829.72	829.31	498	514	90
AXBD 72	826.7	826.36	498	514	92
AXBD 74	868.63	868.31	498	514	96
AXBD 75	869.53	868.24	498	514	92
AXBD 76	788.69	788.38	498	513	94
AXBD 78	832.79	832.44	498	514	90
AXBD 79	851.53	850.25	498	514	96
AXBD 80	863.72	863.35	498	514	96
AXBD 81	868.63	868.31	498	513	96
AXBD 82	882.8	882.42	498	515	95
AXBD 83	928.15	927.29	499	515	91
AXBD 84	880.67	880.33	498	514	95
AXBD 85	835.08	834.28	498	513	91
AXBD 87	835.08	834.28	498	514	90
AXBD 90	868.63	868.31	498	514	88
AXBD 97	868.63	868.31	498	514	93
AXBD 98	866.8	866.43	498	514	92
AXBD 100	876.76	876.37	498	521	95
AXBD 102	832.65	832.33	498	514	95
AXBD 103	872.6	872.28	498	514	88
AXBD 114	849.11	848.3	498	514	91

AXBD 115	851.53	850.25	498	514	93
AXBD 116	928.15	927.29	498	513	89
AXBD 117	818.08	817.29	498	514	93
AXBD 119	893.7	893.33	498	514	85
AXBD 120	784.62	784.32	498	514	98
AXBD 121	851.53	850.25	498	514	97
AXBD 124	810.7	810.36	498	514	93
AXBD 127	831.12	830.31	498	514	90
AXBD 128	847.12	846.3	498	513	89
AXBD 130	854.75	854.39	498	514	90
AXBD 131	868.63	868.31	498	514	94
AXBD 133	840.77	840.41	498	513	95
AXBD 134	858.74	858.36	498	514	86
AXBD 135	841.55	840.27	499	513	blank
AXBD 137	851.53	850.25	498	513	90
AXBD 138	804.73	804.41	498	514	91
AXBD 139	851.53	850.25	498	513	92
AXBD 140	824.72	824.38	498	514	96
AXBD 142	835.08	834.28	498	514	92
AXBD 143	868.63	868.31	498	514	90
AXBD 144	861.54	860.24	498	513	91
AXBD 145	852.78	852.41	498	514	92

Table 3.3. Characterization and photophysical properties of AXBY library

compound	M^+ (exp.)	M^+ (exp.)	λ_{abs}(nm)	λ_{em}(nm)	purity
AXBY 1	900.78	881.3	577	598	91
AXBY 4	908.71	889.3	576	595	98
AXBY 6	852.73	833.4	577	596	94
AXBY 12	850.72	831.4	577	595	93
AXBY 14	922.73	903.3	577	596	99
AXBY 15	943.15	923.3	578	595	98
AXBY 17	908.71	889.2	577	595	97
AXBY 19	979.13	959.2	577	594	96
AXBY 29	892.8	873.3	577	595	96
AXBY 36	904.74	885.3	577	595	91
AXBY 37	908.84	889.4	577	596	98
AXBY 38	902.75	883.3	577	594	97
AXBY 41	939.19	919.2	577	595	98
AXBY 42	886.75	867.3	577	595	98
AXBY 57	1023.58	1004.5	577	595	93
AXBY 58	928.83	909.3	577	596	92
AXBY 65	890.72	871.3	576	594	99
AXBY 66	938.78	919.3	577	596	95
AXBY 68	925.16	906.2	577	595	98
AXBY 69	908.71	889.3	577	597	91
AXBY 70	919.8	900.2	577	595	93
AXBY 72	916.78	897.3	577	595	98
AXBY 74	958.71	939.3	577	594	98
AXBY 75	959.61	939.1	576	594	98
AXBY 76	878.77	859.4	577	596	99
AXBY 78	922.87	903.3	577	594	99
AXBY 79	941.61	921.2	577	598	98
AXBY 80	953.8	934.3	577	597	96

AXBY 81	958.71	939.2	577	597	92
AXBY 82	972.88	953.4	577	596	94
AXBY 83	1018.23	998.2	578	594	96
AXBY 84	970.75	951.3	577	596	98
AXBY 85	925.16	905.3	577	595	98
AXBY 90	958.71	939.3	577	594	99
AXBY 97	958.71	939.2	577	595	95
AXBY 98	956.88	937.4	577	595	96
AXBY 100	966.84	947.3	577	595	96
AXBY 103	962.68	943.2	577	596	98
AXBY 115	941.61	921.2	578	594	98
AXBY 116	1018.23	998.2	577	595	97
AXBY 117	908.16	888.2	577	597	99
AXBY 119	983.78	964.3	577	597	99
AXBY 120	874.7	855.3	577	596	99
AXBY 121	941.61	921.3	577	597	99
AXBY 124	900.78	881.3	577	595	97
AXBY 127	921.2	901.3	577	595	96
AXBY 128	937.2	919.1	577	595	92
AXBY 130	944.83	925.3	577	596	95
AXBY 131	958.71	939.3	577	595	98
AXBY 133	930.85	911.4	577	596	98
AXBY 137	941.61	921.2	577	595	94
AXBY 138	894.81	875.3	577	595	98
AXBY 139	941.61	921.3	577	596	92
AXBY 142	925.16	906.2	577	596	90
AXBY 143	958.71	939.3	577	602	97
AXBY 144	951.62	931.2	577	595	98
AXBY 145	942.86	923.3	577	596	96
AXBY 114	939.19	919.3	577	596	93

AXBY 45	938.18	918.2	577	596	92
AXBY 35	907.17	887.2	577	595	92

3.6. Experimental Procedure

3.6.1 Synthesis and characterization of AXBD and CXBD library intermediates.

Synthesis Of 5,5-difluoro-10-(3-methoxy-3-oxopropyl)-1,3,7,9-tetramethyl-5H-dipyrrolo[1,2-c:2',1'-f][1,3,2]diazaborinin-4-ium-5-uide (1)

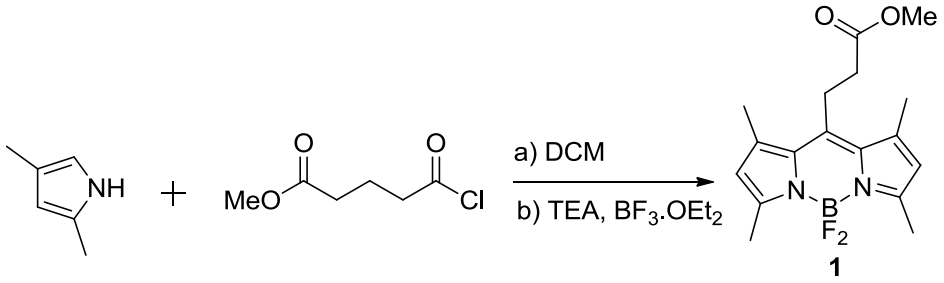

1

To a solution of 2,4-dimethyl-1H-pyrrole (2.16 ml, 20.94 mmol, 2.05 eq) in DCM , methyl 5-chloro-5-oxopentanoate (1.28 ml, 10.47 mmol, 1eq) was added and the resulting mixture was stirred at room temperature for 6 hours. Then triethyl amine (7 ml, 52.35 mmol, 5 eq) and $BF_3.OEt_2$ (13.89 ml, 109.17 mmol, 7eq) were added to the solution sequentially. The mixture was then stirred for 12 hours at room temperature. Then the reaction was quenched with water and work up with DCM and brine. The organic layer was dried over Na_2SO_4. After filtration and evaporation of the organic layer, the compound was purified using by silica gel column. Yield=1.75 g (50 %) ^{1}H-NMR (300 MHz, $CDCl_3$) δ 6.06 (s, 2H), 3.73 (s, 3H), 3.30 (t, 2H, *J*=8.5 Hz), 2.60 (t, 2H, *J*=8.5), 2.51 (s, 6H), 2.43 (s, 6H).^{13}C-NMR (500MHz, DMSO-d6) δ171.6, 153.6, 143.9, 140.9, 130.6, 121.8, 51.7, 34.3, 23.1, 15.7, 14.0. ESI *m/z* ($C_{17}H_{21}BF_2N_2O_2$) calc: 334.17; found: 335.1

Synthesis Of 10-(2-carboxyethyl)-5,5-difluoro-1,3,7,9-tetramethyl-5H dipyrrolo[1,2-c:2',1'-f][1,3,2]diazaborinin-4-ium-5-uide (2)

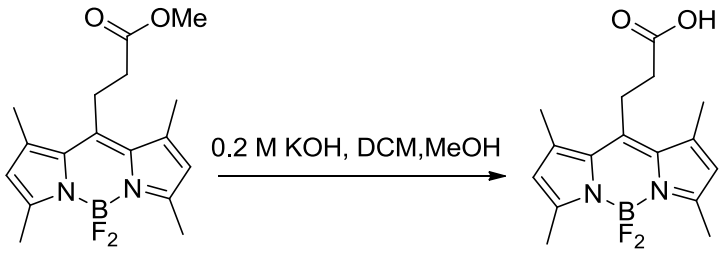

1 **2**

Intermediate **1**, (1 g, 2.99 mmol, 1eq) was dissolve in minimum amount of DCM. To it, 150 ml 0.2 M KOH was added. The aqueous and organic layer was then homogenised by adding excess amount of methanol. The reaction mixture was stirred for 6 hour and then quenched with 100 ml acetic acid –water mixture (1:1). The solvent was then evaporated and the residue was extracted with DCM. The organic layer was dried over Na_2SO_4 and then filtered out. After evaporation of DCM the compound was purified by silica gel column chromatography. Yield=574 mg (60%) ^{1}H-NMR (500 MHz, DMSO-d6) δ 6.24 (s, 2H), 3.22 (t, 2H, *J*=8.5 Hz), 2.51 (t, 2H, *J*=8.5), 2.42 (s, 6H), 2.41 (s, 6H).^{13}C-NMR (500MHz, DMSO-d6) δ172.8, 153.5, 144.6, 140.9, 130.6, 121.8, 35.1, 23.5, 15.7, 14.0. ESI *m/z* ($C_{16}H_{19}BF_2N_2O_2$) calc: 320.14; found: 321.1

Loading Of 10-(2-carboxyethyl)-5,5-difluoro-1,3,7,9-tetramethyl-5H dipyrrolo[1,2-c:2',1'-f][1,3,2]diazaborinin-4-ium-5-uide (2) to Nitrophenol Resin

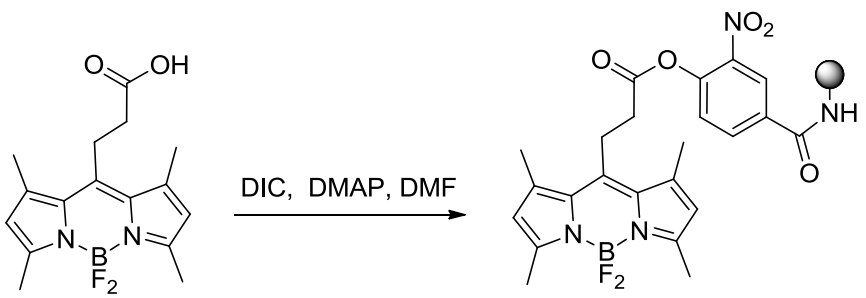

2 **3**

To a solution of intermediate **2** (200 mg, 0.62 mmol, 2 eq) in DMF , DIC (236 mg, 1.87 mmol, 6 eq) and catalytic amount of DMAP were added. To this solution nitro-phenol resin (312 mg, 0.312 mmol, 1 eq) was added. The resin was then shaken for 16 hr at room temperature. After this, the resin was washed with DMF, THF and DCM and then dried under high vacuum.

3.6.2 General Procedure for Synthesis of AXBD and CXBD libraries

20 mg of the resin was suspended in 500 µL of DCM/ACN mixture (7:1) in an eppendrof tube. Then 1 µmol of CX or AX was dissolved in 200 µL of the same solvent mixture and added to the resin. The resin in the solution was then shaken for 3 hours at room temperature. The solution was then filtered out, evaporated and corresponding CXBD or AXBD was collected as a pure compound without any purification.

3.6.3 Synthesis and characterization of AXBY library intermediates

Synthesis of (E)-ethyl 3-(1H-pyrrol-2-yl)acrylate (1)

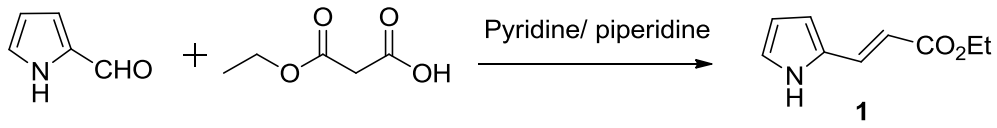

Pyrrole-2 carboxaldehyde (5 g, 52.6 mmol, 1eq) was mixed with hydrogen ethyl malonate (13.89 g, 1 eq) in pyridine (50 ml) and piperidine (2.5 ml). The mixture was warmed to 50 ^{O}C with stirring for 48 hours and then the temperature increased to 80 ^{O}C and heated for another 24 hours. Then pyridine was evaporated and the reaction mixture was diluted with 300 mL ether. This was then washed with 10 percent HCl (3x 100 mL), Na_2CO_3(3x 100 mL) and dried over Na_2SO_4. The solvent was removed in vacuum and the product was purified by silica gel column chromatography. Yield=7.4 g (85%)

Synthesis Of ethyl 3-(1H-pyrrol-2-yl)propanoate (2)

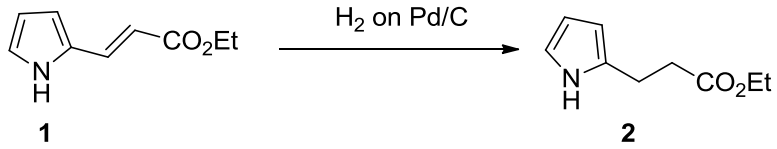

Intermediate **1** (2.5 g, 15 mmol) was dissolve in anhydrous methanol (150 mL) and hydrogenated over 10 percent Pd/C for 6 hours. Then the catalyst was removed by celite filtration and the solvent was evaporated. The residue was purified by silica gel column chromatography. Yield=1.25 g (60%)

Synthesis Of 7-(3-ethoxy-3-oxopropyl)-5,5-difluoro-1,3-dimethyl-5H-dipyrrolo[1,2-c:2',1'-f][1,3,2]diazaborinin-4-ium-5-uide (3)

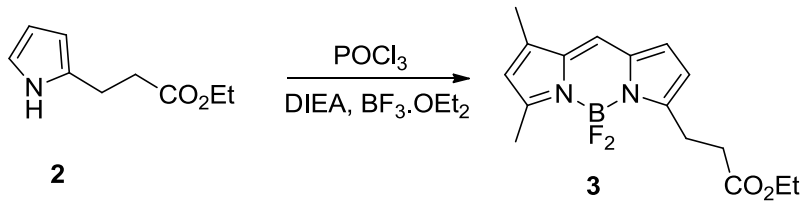

Intermediate **2** (0.65 g, 1 eq) was dissolved in DCM (40 mL). The solution was then cooled to 0 ^{O}C and $POCl_3$ in DCM was added drop wise and stirred at 0 ^{O}C for half an hour. Then the solution was stirred 6 hours at room temperature. After six hours the solution was cooled to 0 ^{O}C again and DIEA (2.57 mL) was added followed by $BF_3.OEt_2$ (2.04 mL). The reaction mixture was stirred for overnight at room temperature. Product is purified by silica gel column chronmatography**.** Yield=436 mg (35%). ^{1}H-NMR (500 MHz, DMSO-d6) δ 7.70 (s, 1H), 7.09 (d, 1H, *J*=4 Hz), 6.38 (d, 1H, *J*=4 Hz), 6.31 (s, 1H), 4.09 (q, 2H, *J*=7 Hz), 3.12 (t, 2H, *J*=7.5 Hz), 2.72 (t, 2H, *J*=7.5 Hz), 2.48 (s, 3H), 2.26 (s, 3H), 1.19 (t, 3H, *J*=7 Hz).^{13}C-NMR (500MHz, DMSO-d6) δ171.8, 159.6, 156.3, 144.4, 134.6, 132.9, 128.7, 125.4, 120.4, 116.4, 60.0, 32.2, 23.4, 14.5, 14.0, 10.9. ESI *m/z* ($C_{16}H_{19}BF_2N_2O_2$) calc: 320.14; found: 301.2(M-F)

Synthesis Of 7-(2-carboxyethyl)-5,5-difluoro-1,3-dimethyl-5H-dipyrrolo[1,2-c:2',1'-f][1,3,2]diazaborinin-4-ium-5-uide (4)

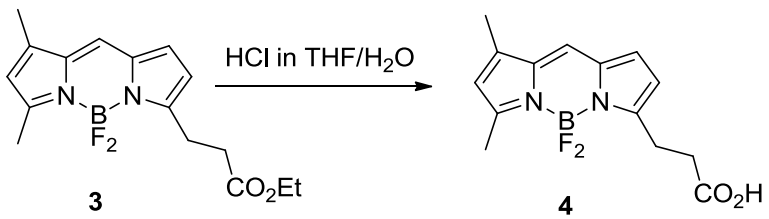

To a solution of **3** (1.5 g, 4.88 mmol) was dissolved in 200 mL THF/H2O (3:2) solvent mixture. To this 37 % concentrated HCl (8 mL) was added and reflux for 6 hours. The

reaction mixture was then cooled to room temperature and water was added to it to make the pH over 1. The THF was evaporated and DCM was added to the residue and extracted with brine. The organic layer was collected and dried over Na_2SO_4. The filtrate was then evaporated and the residue was purified with silica gel column chromatography using ethyl acetate and hexane as a solvent system. Yield=570 mg (40%). ^{1}H-NMR (500 MHz, DMSO-d6) δ 7.69 (s, 1H), 7.08 (d, 1H, *J*=4 Hz), 6.37 (d, 1H, *J*=4 Hz), 6.30 (s, 1H), 3.08 (t, 2H, *J*=8 Hz), 2.64 (t, 2H, *J*=8 Hz), 2.47 (s, 3H), 2.25 (s, 3H).^{13}C-NMR (500MHz, DMSO-d6) δ173.4, 159.4, 156.9, 144.3, 134.5, 132.9, 128.7, 125.4, 120.3, 116.5, 32.3, 23.5, 14.5, 10.9. ESI *m/z* ($C_{14}H_{15}BF_2N_2O_2$) calc: 292.09; found: 273.2

Synthesis Of (E)-7-(2-carboxyethyl)-5,5-difluoro-3-(4-methoxystyryl)-1-methyl-5H-dipyrrolo[1,2-c:2',1'-f][1,3,2]diazaborinin-4-ium-5-uide (5)

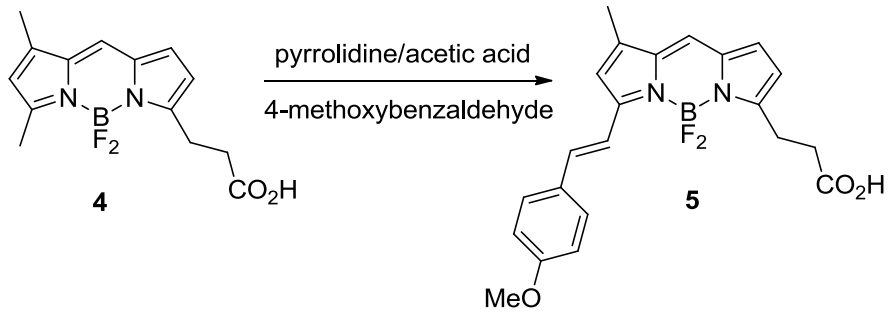

To a solution of intermediate **4** (500 mg, 1.88 mmol, 1eq) in 10 ml ACN, 4- methoxy benzaldehyde (1.03 g, 7.53 mmol, 4 eq) and pyrrolidine (541 mg, 7.53 mmol, 4 eq) - acetic acid (452 mg, 7.53 mmol, 4 eq) mixture were added. Then the reaction mixture was heated at 80 ^{o}C for 15 minutes. The reaction mixture was then cooled to room temperature and ACN was evaporated. The residue was then purified with silica gel column chromatography using DCM-MeOH solvent system. Yield=231 mg (30%). ^{1}H-NMR (500 MHz, DMSO-d6) δ 7.65 (d, 1H, 16.5 Hz), 7.60 (t, 2H, *J*=8.5 Hz), 7.31 (d, 1H, *J*=16.5 Hz), 7.04 (t, 2H, *J*=8.5 Hz), 6.39 (d, 1H, J=3.5 Hz), 3.8 (s, 3H_), 3.12 (t,

2H, *J*=7.5 Hz), 2.66 (t, 2H, *J*=7.5 Hz), 2.30 (s, 3H).^{13}C-NMR (500MHz, DMSO-d6) δ173.5, 160.7, 156.6, 155.9, 143.5, 139.1, 136.1, 133.2, 129.2, 128.4, 127.6, 123.1, 116.9, 116.2,115.3, 114.7, 55.3, 32.3, 23.6, 11.0. ESI *m/z* ($C_{22}H_{21}BF_2N_2O_3$) calc: 410.22; found: 391.1

Loading of intermetdiate 5 to nitrophenol resin

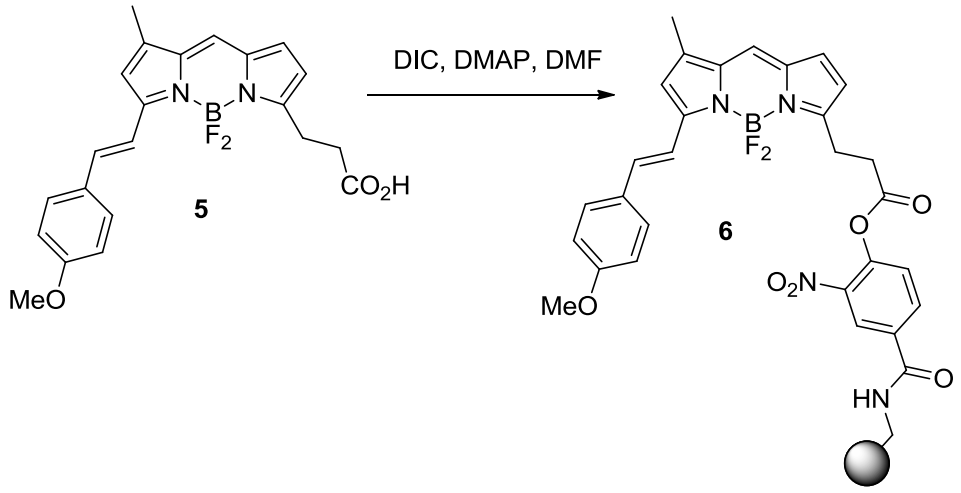

To a solution of **5** (10 mg, 0.024 mmol, 1 eq) in 2 ml DMF, DIC (19 mg, 0.15 mmol, 6 eq) and catalytic amount of DMAP were added to it. The mixture was then shaken for 10 minutes at room temperature. Nitro phenol resin (72 mg, 0.72 mmol, 3 eq) was added to this solution and was shaken for 24 hour at room temperature. Then the resin was washed with DMF (10x) and DCM (10x) before drying in high vacuum.

3.6.4 General procedure for synthesis of AXBY library

400 µL of DCM was added to 50 mg of the BODIPY acid loaded resin in an eppendrof tube. 1 µmol of AX was dissolved in 300 µL of DCM and was added to the resin and shaken for 16 hours. The resin was then filtered out and the solution was collected and evaporated. The residue was purified by TLC.

3.7 References

1. Tsien, R.Y. (1994) Fluorescence Imaging Creates A Window On The Cell. *Chem. Eng. News 72* 34-44.
2. Czarnik, A. W. (1995) Desperately seeking sensors. *Chemistry & biology 2*, 423-8.
3. Rurack, K., and Resch-Genger, U. (2002) Rigidization, preorientation and electronic decoupling--the 'magic triangle' for the design of highly efficient fluorescent sensors and switches. *Chemical Society reviews 31*, 116-27.
4. Grynkiewicz, G., Poenie, M., and Tsien, R. Y. (1985) A new generation of Ca2+ indicators with greatly improved fluorescence properties. *The Journal of biological chemistry 260*, 3440-50.
5. Miyawaki, A., Llopis, J., Heim, R., McCaffery, J. M., Adams, J. A., Ikura, M., and Tsien, R. Y. (1997) Fluorescent indicators for Ca2+ based on green fluorescent proteins and calmodulin. *Nature 388*, 882-7.
6. Kojima, H., Nakatsubo, N., Kikuchi, K., Kawahara, S., Kirino, Y., Nagoshi, H., Hirata, Y., and Nagano, T. (1998) Detection and imaging of nitric oxide with novel fluorescent indicators: diaminofluoresceins. *Analytical chemistry 70*, 2446-53.
7. Hirano, T.; Kikuchi, K.; Urano, Y.; Higuchi, T.; Nagano, T. (2000) Highly Zinc-Selective Fluroescent Sensor Molecules Suitable for Biological Applications. *Journal of the American Chemical Society, 122*, 12399–12400.
8. Tsien, R. Y., and Harootunian, A. T. (1990) Practical design criteria for a dynamic ratio imaging system. *Cell calcium 11*, 93-109.

9. Kikuchi, K., Takakusa, H., and Nagano, T. (2004) Recent advances in the design of small molecule-based FRET sensors for cell biology. Trends in Analytical Chemistry
10. Zlokarnik, G., Negulescu, P. A., Knapp, T. E., Mere, L., Burres, N., Feng, L., Whitney, M., Roemer, K., and Tsien, R. Y. (1998) Quantitation of transcription and clonal selection of single living cells with beta-lactamase as reporter. *Science 279*, 84-8.
11. Förster, T.(1948) Zwischenmolekulare Energiewanderung und Fluoreszenz *Ann. Physik 437*, 55–75
12. Truong, K., and Ikura, M. (2001) The use of FRET imaging microscopy to detect protein-protein interactions and protein conformational changes in vivo. *Current opinion in structural biology 11*, 573-8.
13. Clapp, A. R., Medintz, I. L., Mauro, J. M., Fisher, B. R., Bawendi, M. G., and Mattoussi, H. (2004) Fluorescence resonance energy transfer between quantum dot donors and dye-labeled protein acceptors. *Journal of the American Chemical Society 126*, 301-10.
14. Chino, S., Sakaguchi , A., Yamoto, R., Ferri, S., and Sode, K. (2007) Branched-chain Amino Acid Biosensing Using Fluorescent Modified Engineered Leucine/Isoleucine/Valine Binding Protein. *International Journal of Molecular Sciences 8*, 513-25.
15. Sapsford, K. E., Berti, L., and Medintz, I. L. (2006) Materials for fluorescence resonance energy transfer analysis: beyond traditional donor-acceptor combinations. *Angew Chem Int Ed Engl 45*, 4562-89.

16. Tsourkas, A., Behlke, M. A., Xu, Y., and Bao, G. (2003) Spectroscopic features of dual fluorescence/luminescence resonance energy-transfer molecular beacons. *Analytical chemistry 75*, 3697-703.
17. Loudet, A., and Burgess, K. (2007) BODIPY dyes and their derivatives: syntheses and spectroscopic properties. *Chemical reviews 107*, 4891-932.
18. Pochorovski, I., Breiten, B., Schweizer, W. B., and Diederich, F. (2010) FRET studies on a series of BODIPY-dye-labeled switchable resorcin[4]arene cavitands. *Chemistry 16*, 12590-602.
19. Jiao, G. S., Thoresen, L. H., and Burgess, K. (2003) Fluorescent, through-bond energy transfer cassettes for labeling multiple biological molecules in one experiment. *Journal of the American Chemical Society 125*, 14668-9.

Developement of an Artificial Tongue by Using Colorimetric pH indicator and boronic acid ensemble array for quantitative sugar analysis

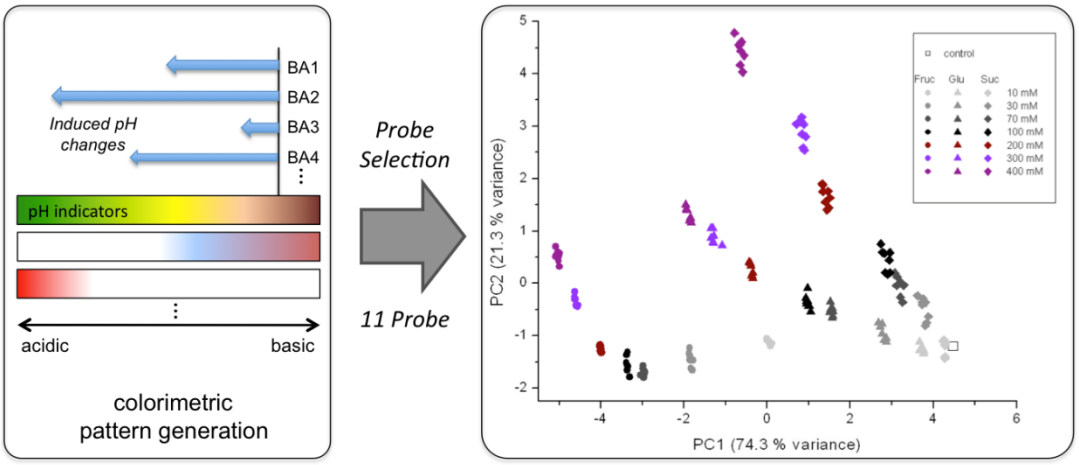

4.1 Introduction

Human tongue has a number of receptors that respond differently to bitter, salty, sour , and sweet tastes. The combined fingerprint from the tongue receptors produce the distinct pattern for each gourmet taste. As a mimic of the mammalian tongue, researchers developed the concept of sensor array. In this sensor architecture individual probes need not to be selective for a particular anayte however series of collection of sensors complement each other and collaborative effect yield significant improved performance. Inspired by this combinatorial sensing strategy many artificial sensor system has been developed. This chapter mainly focus on the development of an artificial tongue for the discrimination of highly cross reactive sugars using the ensembles of boronic acids as host molecules and the pH responsive dyes as the indicator molecules.

Sugars are essential molecules that play important roles in biological processes[1-2]. Since they serve as critical nutritional ingredients as well as metabolic markers to diagnose diseases such as diabetics[3-4], development of carbohydrate sensors are of great interest for a broad range of applications. The challenge of carbohydrate recognition has presented several detection strategies utilizing fluorescent photoinduced electron transfer (PeT), indicator displacement assay (IDA), or pH alteration induced by boronic ester formation. The most popular conventional method employed is thes design of fluorescent turn-on or quenching sensor based on sugar recognition motif[5-7]. Alternatively, the IDA system has a merit in that its receptor can utilize multiple recognition moieties maximizing interactions depending on the structure of a target carbohydrate[8-13].

Instead of designing a specific carbohydrate sensor or a recognition receptor, our group utilized the pH change profile induced by boronic ester formation and

demonstrated the successful discrimination of 23 carbohydrates[14]. While the following studies proved this principle can be generally applied for sugar detection[15] and the identification of artificial and natural sweetners[16-17], it has limited utilityin fingerprint analysis for carbohydrate classification at the given concentrations. Since the color change signals are not always linearly correlated to the amount of sugars, quantitation is one of the major challenges faced. Here, we report the first dose dependent quantitative sugar analysis using boronic acid derivative and pH indicator ensemble array.

The performance of the carbohydrate sensor based on pH alteration relies on three components; diversity of boronic acids, pH indicators, and proper buffer conditions. Boronic acids form reversible cyclic ester complexes with diols in carbohydrates[18]. Both boronic acid/ester undergo Lewis acid–base reaction with water as a conjugate acid (Figure 4.1), but boronic ester tends to be more acidic than its corresponding boronic acid form[14-19]. Therefore, a series of boronic acid derivatives can generate a distinct pH change pattern depending on the binding affinity to target sugars together with buffer capacity, and the pH profile can be distinguished by color change pattern of pH indicators.

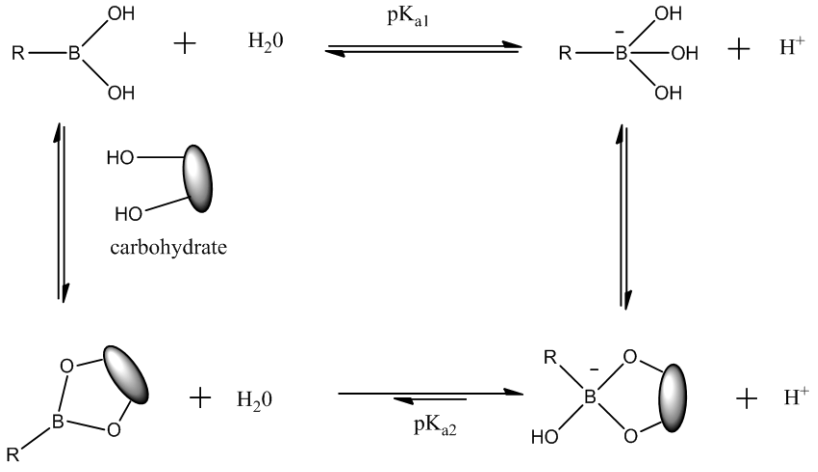

Figure 4.1. Interaction of boronic acids with diols in carbohydrates

boronic acid derivatives can generate distinct pH change pattern depending on the binding affinity to target sugars together with buffer capacity, and the pH profile can be distinguished by color change pattern of pH indicators. For instance, fructose induces substantial color changes due to its favored stereo chemistry of cis-diol moiety and boronic acids interaction. However many other carbohydrates, including glucose or sucrose exhibited very weak signals which could hardly be used for quantitative analysis[14].

4.2 Objectives

In this study, we have constructed an artificial tongue by using pH indicators and a boronic acid ensemble array for the quantitative discrimination of three different sugars- glucose, fructose and sucrose. Furthermore, this ensemble array was successfully applied to quantify the sugar content in clinically used saline solutions.

4.3 Results and discussions

Three abundant mono-, disaccharides (glucose, fructose, and sucrose) from soft drinks were selected as target sugars, and the monosaccharides were tested from 10 mM to 1M ranges whereas the disaccharide's (sucrose) working concentration range was determined from 10 mM to 700 mM. Prior to investigating dose responses, we first optimized the assay buffer conditions. Buffer capacity of sodium phosphate and the amount of boronic acid should be well balanced to maximize the pH change, and we finalized the condition as 50 mM phosphate buffer with 2.5 mM boronic acids (pH 7.5). Then, we tested 7 serial concentrations of sugar solutions on 273 ensemble array (7 boronic acid derivative x 39 pH indicator pairs). The absorbance spectra was collected from 350 nm to 750 nm using a microtiter plate reader, and the changes in absorbance was calculated for further analysis following the previously reported procedure.[20] Eight independent measurements were performed for the statistical data process.

4.3.1 Selection of probes

11 pairs of probes were selected (Figure 4.2) based on the color change data. Each probe pair was examined in terms of the consistent dose response. Probe pairs that exhibit unique signals with linear dose tendency were chosen for probe development. For example, aniline blue black/2-(hydroxymethyl) phenylboronic acid ensemble did not exhibit consistent dose dependent signal (Figure 4.3-a), and such probe pairs were discarded. On the other hand, probes like alizarin red S/2-(hydroxymethyl) phenylboronic acid, which showed coherent response within given concentration range of sugars (Figure 4.3-b), were chosen. The response pattern of most probes corresponds to the order of "Fruc > Glu > Suc" as previous report[14], however, we found one probe (methyl orange/ 4-methylphenyl boronic acid ensemble) which exhibited a unique opposite response pattern (Figure 4.4). It is noteworthy that this probe showed stronger color change signal in glucose than fructose.

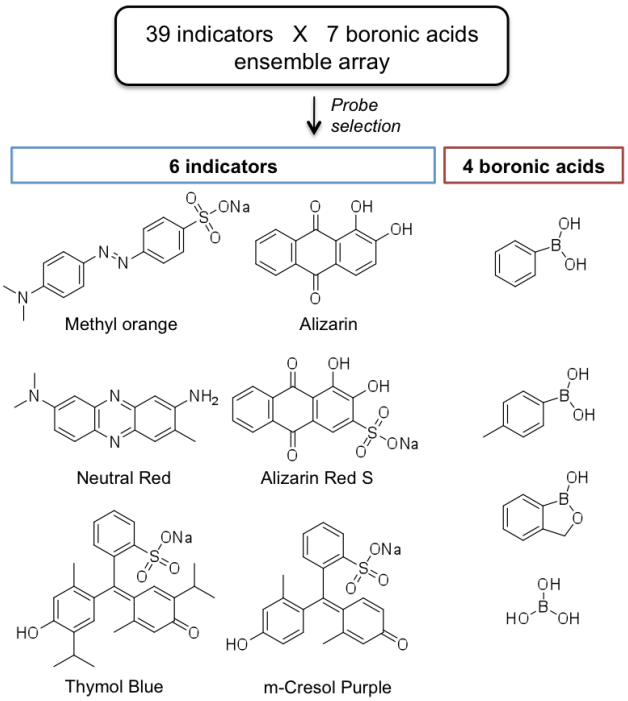

Fig. 4.2. Structures of selected colorimetric pH indicator/ boronic acid ensemble probes

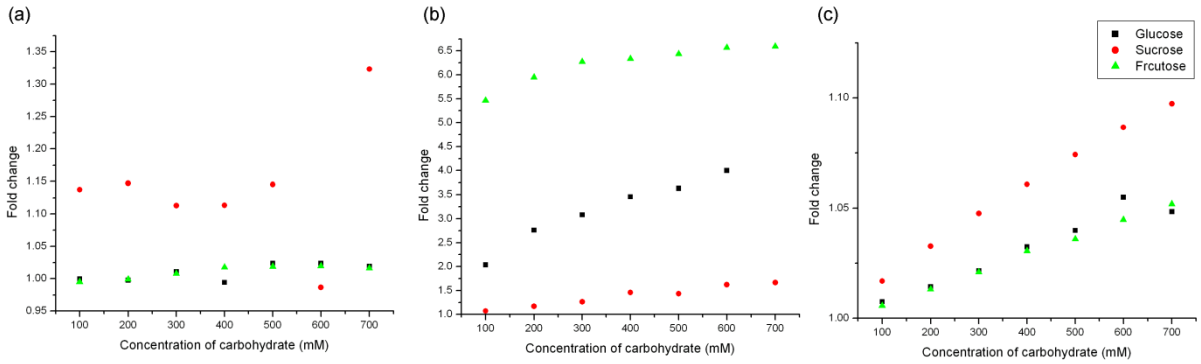

Figure 4.3. Representative dose response evaluation for probe selection. 2-(hydroxymethyl)phenylboronic acid was mixed with (a) aniline blue black (b) alizarin red S (c) Ethyl orange.

(a)

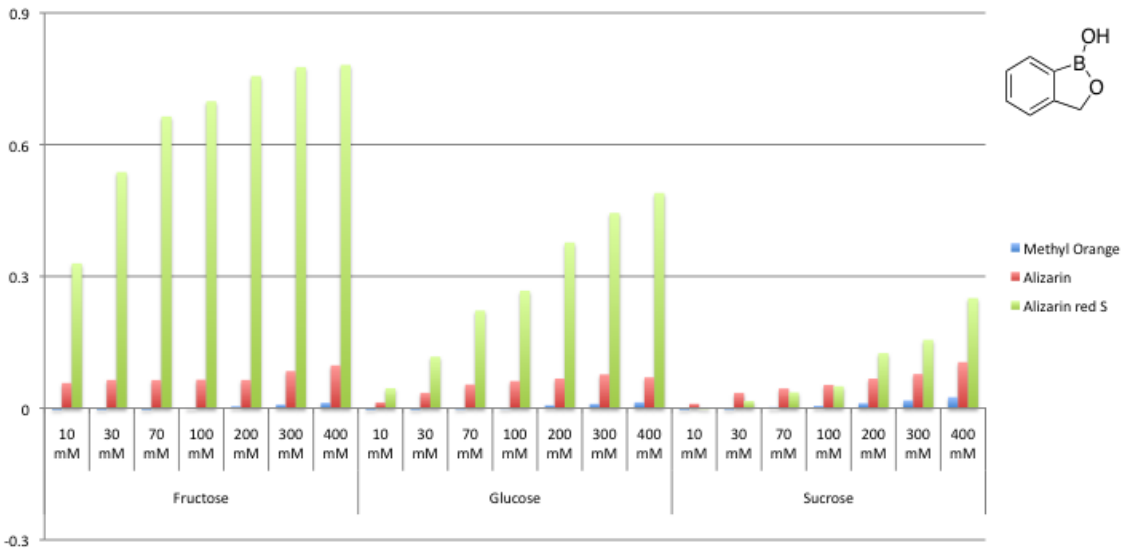
0.9
0.6
0.3
0
-0.3
10 mM
30 mM
70 mM
100 mM
200 mM
300 mM
400 mM
Fructose
Glucose
Sucrose
OH
B
O
Methyl Orange
Alizarin
Alizarin red S

(b)

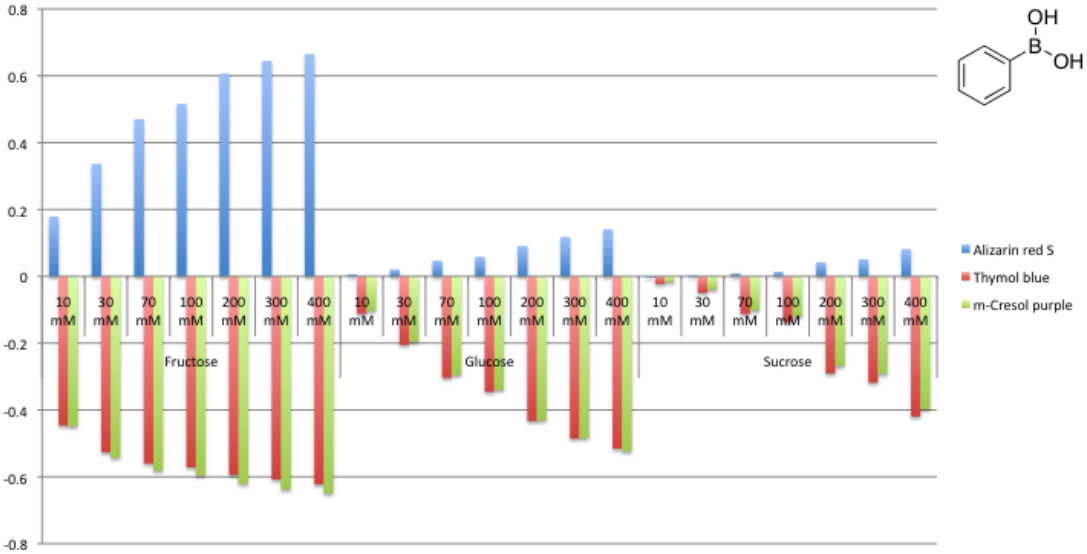
0.8
0.6
0.4
0.2
0
-0.2
-0.4
-0.6
-0.8
10 mM
30 mM
70 mM
100 mM
200 mM
300 mM
400 mM
Fructose
Glucose
Sucrose
OH
B
OH
Alizarin red S
Thymol blue
m-Cresol purple

(c)

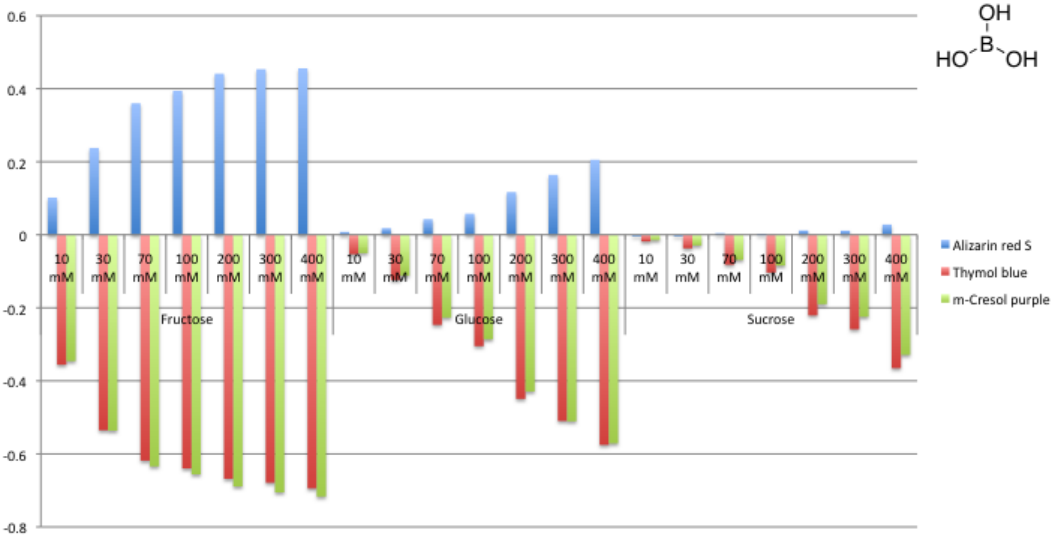
0.6
0.4
0.2
0
-0.2
-0.4
-0.6
-0.8
10 mM
30 mM
70 mM
100 mM
200 mM
300 mM
400 mM
Fructose
Glucose
Sucrose
OH
HO
B
OH
Alizarin red S
Thymol blue
m-Cresol purple

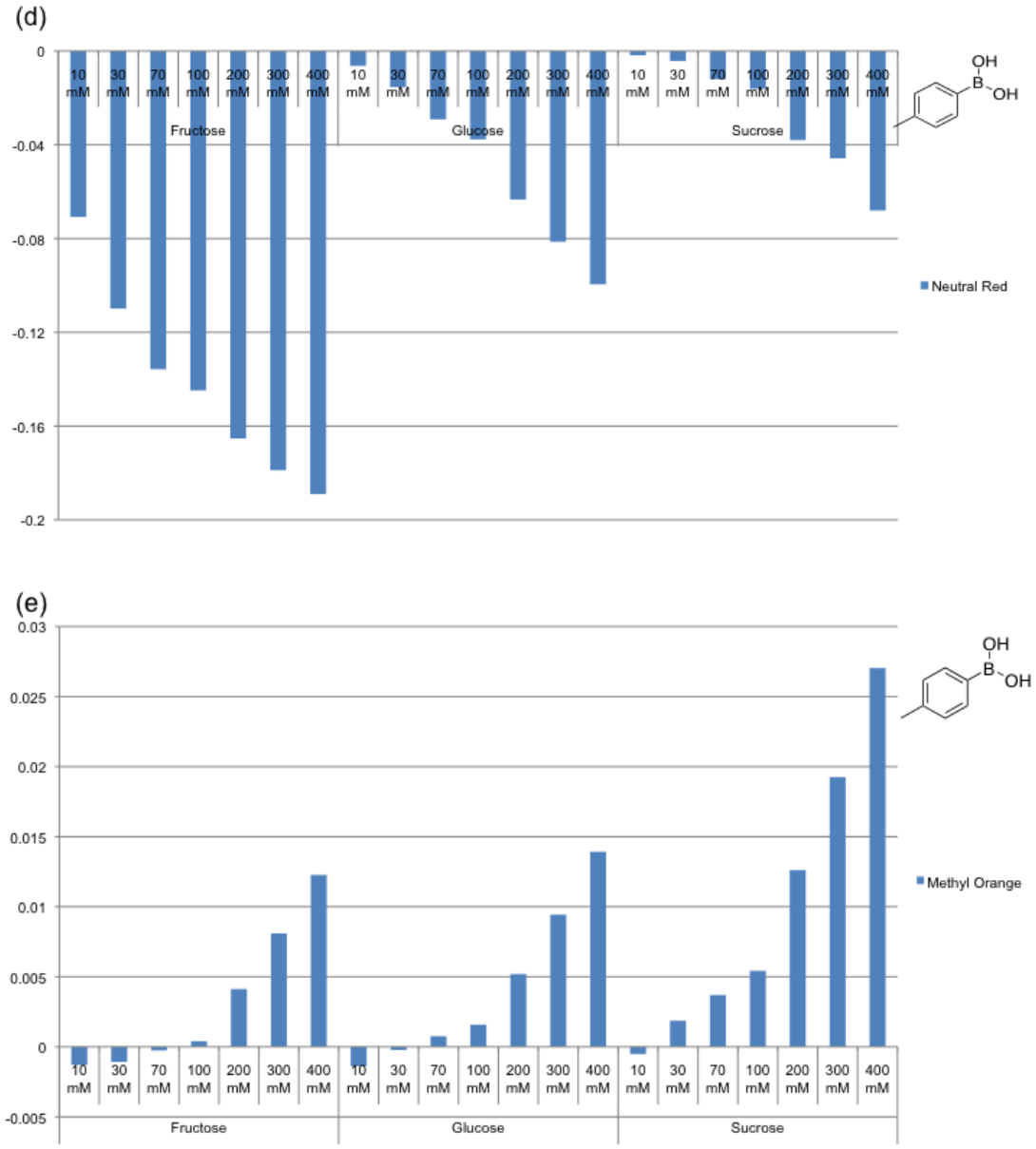

Figure 4.4. Bar graph of ensemble array's Log(fold) values for three cabohydrates (glucose, fructose, sucrose). Ensemble probes with (a) 2-(hydroxymethyl)phenylboronic acid, (b) phenyl boronic acid, (c) boric acid, (d) 4-methylphenyl boronic acid.

4.3.2 Discrimination of the sugars

After the probe selection process, 11 final ensemble pairs were selected for further analysis (Table 4.2). To compress and visualize high demensional disciminant information, we applied principal component analysis (PCA). Within the two

principal components, over 94% of all discriminatory information is contained. In figure 4.5, nine serial dose response patterns were visualized in PCA plot (eight serial dose for sucrose). Three sugars clearly draw independent dose trajectory from control point to higher concentration of corresponding sugar. Based on these results, all three sugars exhibit good dose dependent profile and visually distinguishable in the PCA space.

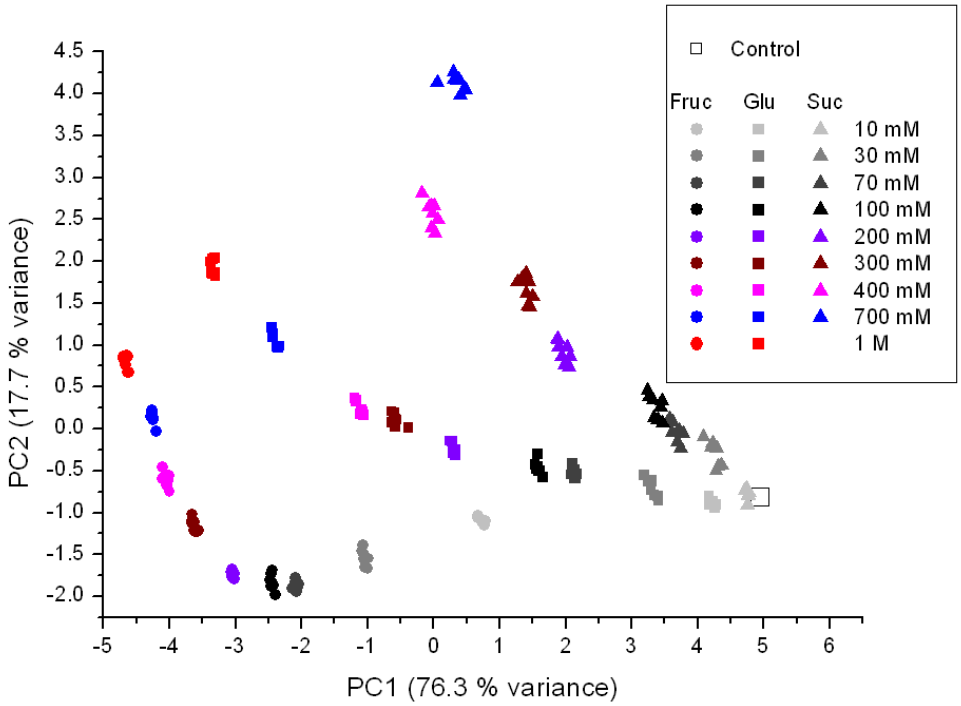

Figure. 4.5 Principal component analysis (PCA) plot for dose dependent quantitative carbohydrate analysis. 11 selected ensemble probes were used to generate PCA plot (Table 4.2). Fruc: fructose, Glu: glucose, Suc: sucrose

4.3.3 Quantification of sugar content in saline

Encouraged by this successful quantitative discrimination results, we further evaluated our system for complex mixture analysis. Saline solution is a salted mixture solution commonly used as an intravenous infusion agent in the clinic. In order to quantify glucose content in saline, we tested two distinct concentrations of

saline as a real matrix in our system. In figure 4.6, two saline samples containing 13.9 mM and 34.7 mM glucose appear in an expected position in PCA space.

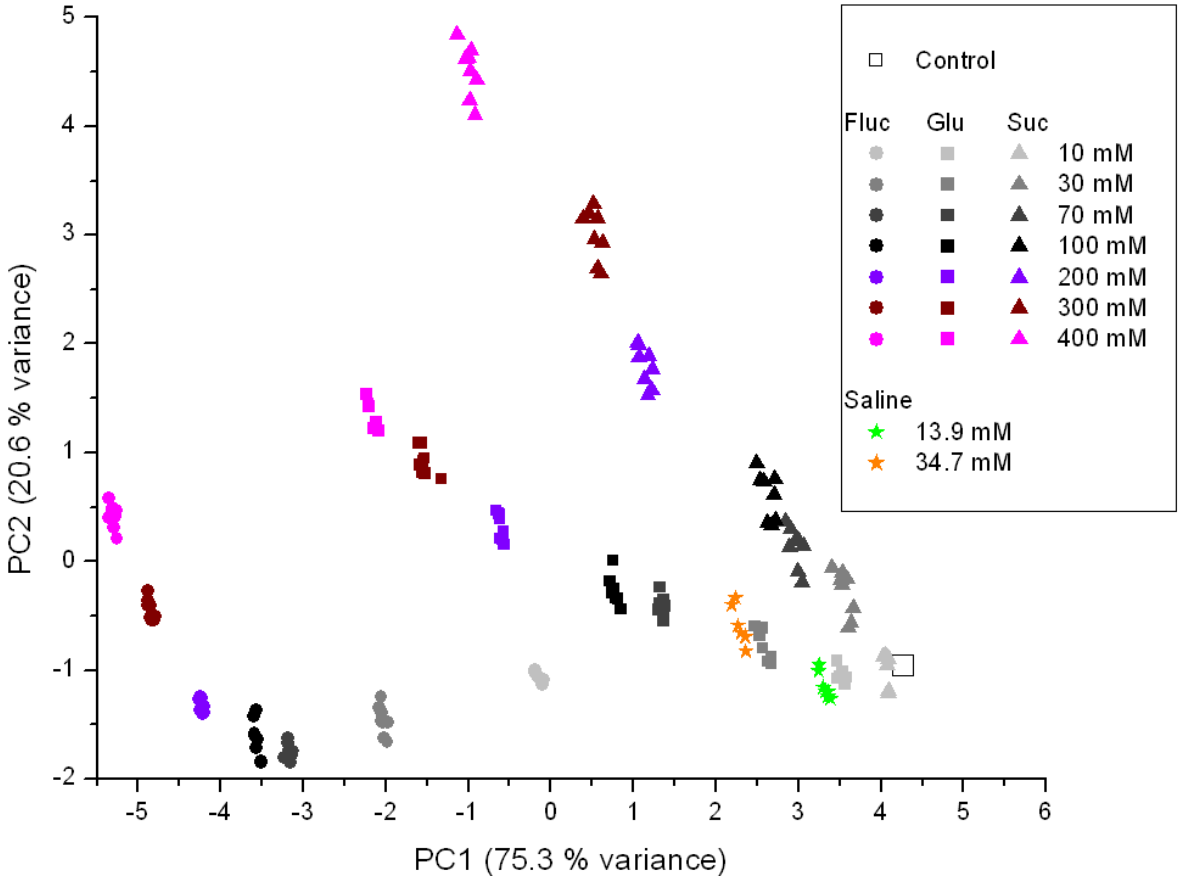

Figure 4.6. Principal component analysis (PCA) plot for real-mixture sample, saline. 11 selected ensemble probes were used to generate PCA plot (Table 2). Fruc: fructose, Glu: glucose, Suc: sucrose

4.3.4 Qualitative comparison of sugar contains in soft drinks

After getting the successful quantitative discrimination results, we applied complex mixture samples to evaluate a practical application of our system. Four commercially available soft-drinks were chosen for sugar content comparison, including Sprite, Green Tea, Starfruit, and Calamanasi Honey (Table 3). These soft-drinks contained not only distinct amount of carbohydrates, but various other ingredients. Interestingly, color-change intensities were corelated with the amount of sugar in the soft drink in general (Fig 4.7). Starfruit, which contains the highest concentration of sugar, exhibited the highest fold changes in most ensemble probes. On the other hand, soft-drinks that have lower amount of sugar showed lower fold values. It was also notable that there was noise signals due to the complexity of soft drinks. For instance, EP-10 (neutral red and 4-methylphenyl boronic acid ensemble) showed strong signal for only Green Tea.

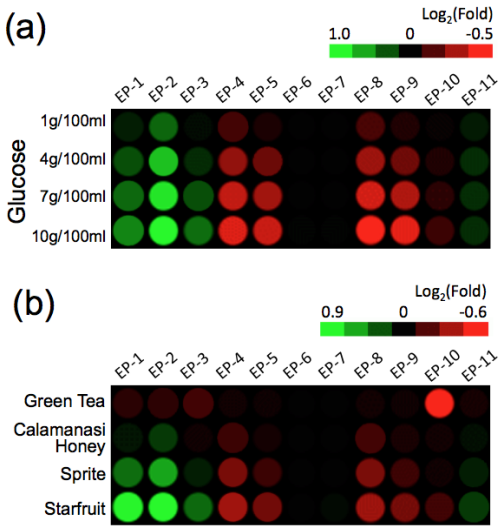

(c)

Soft Drink	Sugar Content (based on Nutrition Facts)
Starfruit	12 g/ 100 ml
Sprite	11 g/ 100 ml
Calamanasi Honey	10 g/ 100 ml
Green Tea	5 g/ 100 ml

Figure. 4.7 Heatmap plot of color change response for (a) serial concentrations of glucose solution, and (b) 10 times diluted commercial soft drinks. (c) Sugar contents of the soft drinks are based on the nutrition fact table on the bottle. Decoding information

of ensemble probes (**EP**) are summarized in Table 2, and details about soft-drink are listed in Table 3.

4.4 Conclusions

In summary, we have showed that a boronic acid derivative and pH indicator ensemble array can be used as a simple colorimetric sensor for quantitative sugar analysis. Although this sensor array does not consist of specific sugar sensors or receptors, it demonstrated dose dependent carbohydrate analysis with, boronic ester formation induced pH alteration. It was also proved that a low responsiveness of certain sugars, such as glucose and sucrose, could be enhanced by extension of boronic acid diversity. Lastly, practical carbohydrate quantization was demonstrated using medical saline solution. These results support our hypothesis that the pH alteration strategy can be applied for quantitative sugar sensing.

4.5 Experimental Procedures

4.5.1 Chemicals and reagent

The following chemicals and reagents were purchased from Sigma Aldrich: 2-biphenylboronic acid, 2-fluoro-6-methoxyphenylboronic acid, 2-(hydroxymethyl)phenylboronic acid cyclic monoester, 3-nitrophenylboronic acid, phenylboronic acid, boric acid, phosphoric acid sodium monobasic, sodium hydroxide pellets (NaOH, 99.99% purity), D-(+)-glucose min 99.5%, D-fructose 99+% and sucrose. 4-methoxybenzeneboronic acid and 4-methylbenzeneboronic acid were purchased from Alfa Aesar. The spectroscopy grade of dimethyl sulfoxide (DMSO, 99.9% purity) was purchased from Across. De-ionized water was prepared using the Picosystem (filtering system) from Hydro service and supplied company. Phosphate buffer (50 mM, pH 7.5) was prepared using phosphoric acid by titrating with NaOH solution. pH indicators were purchased from Chem Service, Sigma, Fluka, Kodak, Janssen and Aldrich. The saline solution was collected from the National University Hospital Pharmacy in Singapore. (Contents: NaCl -77.0 mM, glucose -277.5 mM)

4.5.2 Instruments and computer software

Polystyrene 384-well plates (clear flat bottom) were purchased from Greiner. All UV-VIS spectrum data were recorded from 350 nm to 750 nm using plate reader (Molecular Device; Spectra Max Plus 384). Principal component analyses were performed using Pipeline Pilot Student Edition v6.1 and R 2.3.1, and principal component analyses graphs were visually obtained using Miner 3D Professional.

4.5.3 Preparation of standard solutions and mixture samples

The pH indicator solutions (10 ~ 100 mM) were prepared by measuring appropriate amounts (in grams) of the solid forms of the solutions and then dissolving in DMSO. The DMSO solution was then diluted in de-ionized water. The list of the dye solutions and their respective concentrations can be found in Table S1. Phosphate buffer solution (50 mM, pH 7.5) was prepared using phosphoric acid by titrating with NaOH solution. The solutions of

the boronic and boric acids were prepared in the above phosphate buffer solution. Solutions of the carbohydrates were prepared in de-ionized water. For quantitative saline test, 1x saline solution was first neutralised with NaOH. Then, the solutions were diluted 4 times and 10 times using deionised water.

4.5.4 Array preparation and data acquisition

One dye and one boronic acid pair are considered as an ensemble probe. First, each solution of a pH indicator (25 μL) and boronic acid (25 μL) were prepared at corresponding concentration and place in 384 plate. Then, 2x sugar solutions (20 mM ~ 800 mM, 50 μL) were added 10 min before absorbance measurement. The absorbance spectra between 350 nm and 750 nm were recorded by the plate reader, at 10 nm interval. In order to evaluate the reproducibility of data, same experiments were repeated on another day. The absorbance spectra of the plate were then measured and the fold change value calculated using the previously reported procedure[1].

If the intensity of the analyte test is I_0 and that of the control is I_0, the fold-change, F, can be expressed as follows [Eq. (1)]:

$$F = \frac{I'_0}{I_0} \qquad \text{…… Eq. (1)}$$

For the second class of dyes, there are two absorbance max peaks: one for control (λ_1) and a new peak that appeared in the test solution (λ_2). The effective fold-change can be calculated as follows [Eq. (2)]:

$$F = \left(\frac{I_1}{I_2}\right)\left(\frac{I'_2}{I'_1}\right) \qquad \text{…… Eq. (2)}$$

Table 4.1. Absorbance maximum wavelengths of pH indicators and assay conditions. Detail data acquisition and process protocols were previously reported.

ID of pH indicator	Dye name	λ_{max} (nm)	λ_1 (nm)	λ_2 (nm)	Concentration (mM)	DMSO (%)
1	Methyl orange		460	510	0.07	0.70
2	Alizarin yellow R		370	420	0.50	0.50
3	Eriochrome blue black R		550	510	0.30	3.00
4	Aniline blue black	620			0.04	0.40
5	Congo red		500	570	0.07	0.70
6	Evans blue	590			0.07	0.70
7	Brilliant yellow		400	500	0.05	0.50
8	Dibromofluorescein	500			0.02	0.2
9	Phloxine B	540			0.03	0.3
10	Neutral red		530	450	0.07	0.7
11	Alizarin		430	530	0.42	4.20
12	Alizarin red S (ARS)		420	520	0.42	4.20
13	Amaranth (acid red 27)		520	460	0.25	2.50
14	Trypan blue	590			0.05	0.5
15	Biebrich scarlet	510			0.12	1.20
16	Ponceau S	520			0.05	0.50
17	Victoria Blue B	610			0.05	0.50
18	Eosin bluish	520			0.03	0.30
19	Bromophenol blue		590	440	0.05	0.50
20	Chlorophenol red		430	570	0.08	0.40
21	Rose Bengal	550			0.05	0.50
22	Thymol blue		430	600	0.22	2.20
23	Ethyl violet	590			0.02	0.2
24	Cresol red		430	600	0.22	2.20
25	Metanil yellow	430			0.12	1.20
26	4-Phenylazoaniline		370	490	0.13	1.30

27	Erythrosin B		530	550	0.01	0.10
28	Ethyl orange		470	510	0.12	1.20
29	Bromocresol green		620	440	0.17	1.70
30	Resazurin		600	530	0.12	1.20
31	Nitrazine Yellow		460	590	0.06	0.60
32	Bromothymol Blue		430	620	0.15	1.50
33	m-Cresol Purple		430	570	0.25	2.50
34	Pyrocatechol violet		440	610	0.20	2.00
35	Xylenol orange		430	570	0.15	1.50
36	2',7'-Dichlorofluorescein		500	490	0.05	0.50
37	Bromochlorophenol Blue		590	440	0.03	0.30
38	Quinaldine red	500			0.07	0.70
39	Methyl red		520	430	0.02	0.20

.

Table 4.2. Selected pH indicator and boronic acid pairs.

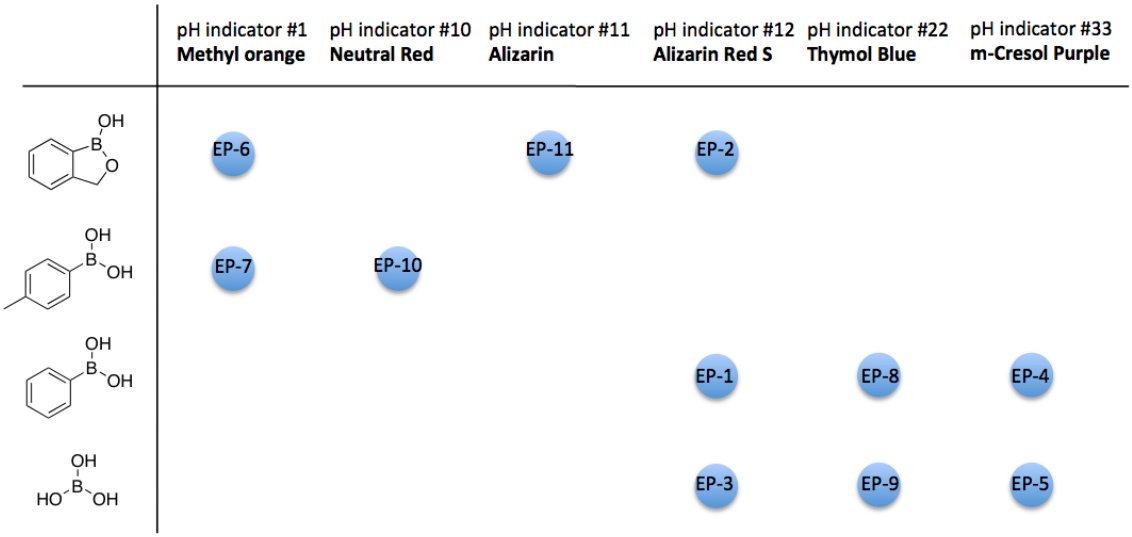

Table 4.3. Details of commercial soft drinks.

Name of the soft Drinks	Nutrient (per 100ml)		Ingredients
Starfruit	Protein	0.0g	Water, extracts of starfruit, vitamin C, Citric acid, salt, refined sugar
	Total fat	0.0g	
	Cholesterol	0.0mg	
	Total carbohydrate	12.0 g	
	Dietary fibre	0.0g	
	Sugar	12g	
	Sodium	62.0mg	
	vitamin C	5%	
Pokka Green Tea	Protein	0.0g	Water, freshly boiled jasmine green tea, sucrose, flavouring, ascorbic acid
	Total fat	0.0g	
	Cholesterol	0mg	
	Carbohydrate	6.0g	
	Total sugar	6.0g	
	Dietary fibre	0.0g	
	Sodium	6.0mg	
	Tea polyphenols	30.0mg	
Calamansi Honey Lemon	Protein	0.0g	Water, sugar, Concentrated

Juice Drink	Total fat	0.1g	juice (calamansi, lemon) and honey
	Cholesterol	0mg	
	Carbohydrate	10.7 g	
	Dietary fibre	0.0g	
	Sodium	3.0mg	
	Vitamin C	3.4mg	
sprite	Protein	0.0g	Carbonated water, sugar, citric acid, flavourings and preservative (sodium benzoate) Permitted food additives of non-animal origin
	Total fat	0.0g	
	Carbohydrate	11.0g	

4.6 References

1. Dennis, J. W., Nabi, I. R., and Demetriou, M. (2009) Metabolism, cell surface organization, and disease. *Cell 139*, 1229-41.

2. Brand-Miller, J., McMillan-Price, J., Steinbeck, K., and Caterson, I. (2009) Dietary glycemic index: health implications. *Journal of the American College of Nutrition 28 Suppl*, 446S-449S.

3. Goren, H. J. (2005) Role of insulin in glucose-stimulated insulin secretion in beta cells. *Current diabetes reviews 1*, 309-30.

4. Rohrscheib, M., Tzamaloukas, A. H., Ing, T. S., Siamopoulos, K. C., Elisaf, M. S., and Murata, H. G. (2005) Serum potassium concentration in hyperglycemia of chronic dialysis. *Advances in peritoneal dialysis. Conference on Peritoneal Dialysis 21*, 102-5.

5. James**,** T. D., Linnane, P. , and Shinkai, S.(1996) Fluoresent saccharide receptors: A sweet solution to the design, assembly and evaluation of boronic acid derived PET sensors. *Chem. Commun.* 281-88.

6. Yoon, J., and Czarnik, A. W. (1992) Fluorescent chemosensors of carbohydrates. A means of chemically communicating the binding of polyols in water based on chelation-enhanced quenching *114*, 5874-75.

7. Nagai, Y., Kobayashi, K., Toi, H., and Aoyama, Y. (1993) Stabilization of Sugar-Boronic Esters of Indolylboronic Acid in Water via Sugar–Indole Interaction: A Notable Selectivity in Oligosaccharides *B Chem. Soc. Jpn.*, **66**, 2965.

8. Pal, A., Berube, M., and Hall, D. G. (2010) Design, synthesis, and screening of a library of peptidyl bis(boroxoles) as oligosaccharide receptors in water: identification of a receptor for the tumor marker TF-antigen disaccharide. *Angew Chem Int Ed Engl 49*, 1492-5.

9. Zhang, T. Z., and Anslyn, E. V. (2006) A colorimetric boronic acid based sensing ensemble for carboxy and phospho sugars *Org. Lett.*, ***8***, 1649-52

10. Tong, A. J., Yamauchi, A., Hayashita, T., Zhang, Z. Y., Smith, B. D., and Teramae, N. (2001) Boronic acid fluorophore/beta-cyclodextrin complex sensors for selective sugar recognition in water. *Analytical chemistry 73*, 1530-6.

11. Schiller, A., Wessling, R. A., and Singaram, B. (2007) A fluorescent sensor array for saccharides based on boronic Acid appended bipyridinium salts. *Angew Chem Int Ed Engl 46*, 6457-9.

12. Gamsey, S., Baxter, N. A., Sharrett, Z., Cordes, D. B., Olmstead, M. M., Wessling R. A., and Singaram, B. (2006) The effect of boronic acid-positioning in an optical glucose-sensing ensemble *Tetrahedron62*, 6321.

13. Gamsey, S., Miller, A., Olmstead, M. M., Beavers, C. M., Hirayama, L. C., Pradhan, S., Wessling, R. A., and Singaram, B. (2007) Boronic acid-based bipyridinium salts as tunable receptors for monosaccharides and alpha-hydroxycarboxylates. *Journal of the American Chemical Society 129*, 1278-86.

14. Lee, J. W., Lee J. S., and Y. T. Chang, Colorimetric Identification of Carbohydrates by a pH Indicator/pH Change Inducer Ensemble (2006) *Angew. Chem. Int. Edit. 45*, 6485-87.15. Kim, Y., Hilderbrand, S. A., Weissleder, R., and Tung, C. H. (2007) Sugar sensing based on induced pH changes. *Chem Commun* 2299-301.

16. Musto, C. J., Lim, S. H., and Suslick, K. S. (2009) Colorimetric detection and identification of natural and artificial sweeteners. *Analytical chemistry 81*, 6526-33.

17. Lim, S. H., Musto, C. J., Park, E., Zhong, W., and Suslick, K. S. (2008) A colorimetric sensor array for detection and identification of sugars. *Organic letters 10*, 4405-8.

18. Springsteen G., and Wang, B. H. (2002) A Detailed Examination of Boronic Acid-Diol Complexation*Tetrahedron, 58*, 5291-300.19. Badugu, R., Lakowicz, J. R., and Geddes, C. D. (2004) Noninvasive continuous monitoring of physiological glucose using a monosaccharide-sensing contact lens. *Analytical chemistry 76*, 610-8.

20.Lee, J. W., Lee, J. S., Kang, M., Su, A. I., and Chang, Y. T. (2006) Visual artificial tongue for quantitative metal-cation analysis by an off-the-shelf dye array. *Chemistry 12*, 5691-6.

Chapter 5

5.1 Conclusion

In recent years, fluorescent molecules have been the key source for optical sensor development. A conventional target oriented approach provides the mechanistic details of the interaction between analytes and sensor molecules. However this case-by case study is limited in scope as well as in speed for developing new sensors. In contrast to the traditional target oriented approach, the diversity oriented fluorescent library approach can be used to discover selective probes rapidly when they are screened systematically against multiple analytes from small molecules to macro molecules in a high throughput manner.

To enlarge our potential bio imaging probe tool box, a fluorescent scaffold, xanthone was selected for diversity oriented library synthesis which has not been previously explored as a bio imaging probe. 80 CX compounds were synthesized using click chemistry with a series of available alkynes. Adaptation of the solid phase chemistry provides highly pure CX compounds without any further purification. A diverse range of fluorescent properties was observed for all the final compounds. In all the cases, an almost nonfluorescent xanthone azide was converted to highly fluorescent CX scaffold after performing the click chemistry. The CX compounds were further diversified to CXAC and CXCA compounds by using a simple but powerful solid phase activated ester chemistry. The high purity of these daughter libraries (CXAC and CXCA) demonstrate the further possibilities of making new xanthone libraries using acid and acid chloride diversities. These xanthone library compounds are biocompatible in terms of easy cell penetration and low cytotoxicity. Utilising a high throughput fluorescent image based screening of the compounds against mESC and MEF, a unique

imaging probe, CDb8 (compound of designation blue 8), capable of selectively staining mESC was identified. This is the first example of a blue fluorescent molecule which selectively stains mESC over MEF and other differentiated cells. CDb8 could be a useful imaging probe for biological study as it does not have any colour limitations when multicolour overlapping is required with standard green fluorescent protein or yellow fluorescent protein.

With an aim to evaluate xanthones photophysical properties more systematically, we have synthesized other sets of xanthone library (AX) using acid chloride diversity. For the rapid and efficient synthesis of AX library, the solid phase methodology was successfully applied. Similar to CX, the AX library compounds were also diversified to their corresponding acetyl (AXAC) and chloroacetyl (AXCA) derivatives. AX, AXCA and AXAC compounds shows blue fluorescent (λ_{em}= 495 nm) with an average excitation at 370 nm wavelength.

In chapter 2, we have successfully synthesized blue fluorescent xanthone libraries and applied them in bio imaging for the development of stem cell selective blue fluorescent probe.

In chapter 3, we have discussed the synthesis of first FRET based fluorescent libraries. Coupling AX and CX compounds with suitable bodipy derivatives, we have synthesized three FRET libraries-CXBD, AXBD and AXBY. In this project, we have developed a solid phase methodology for the simple and efficient synthesis of these FRET libraries. While AXBD and CXBD compounds emits green fluorescence (λ_{em}= 520 nm), the AXBY compounds usually show yellow fluorescence ((λ_{em}= 590 nm) upon excitation at 360 nm wavelength. In order to understand the basic photo physical properties of our synthesized FRET libraries, the full spectral characterizations were carried out. Surprisingly, these compounds behaves as mega stock shift dyes with the

energy transfer efficiency from donor to acceptor over 95 %. In summary, this chapter mainly covers the synthesis and evolutions of the photophysical properties of the FRET libraries.

In the chapter 2, we mainly focused on the synthesis and development of optical sensors for the selective detection of analytes. However, in the chapter 4, we implemented the idea of combinatorial sensing strategy and altered our sensing concept from selective detection to the discrimination of analytes. Utilising the concept of combinatorial sensor architecture, we developed an artificial tongue by using colorimetric pH indicators and boronic acids ensemble array for the discrimination of three different sugars- glucose, fructose and sucrose quantitatively. In this design, one particular probe was not sensitive or specific enough to discriminate the sugars. However, the combined response from the dye array provides an indicative fingerprint to discriminate glucose, fructose and sucrose quantitatively. This artificial tongue was also used to quantify the glucose level in real sample saline . This result reveals the power of the combinatorial sensing approach to discriminate highly cross-reactive analytes.

5.2. Future perspectives

(1) Bio imaging research is limited by the shortage of suitable probes. To accelerate the discovery of new bio imaging probes, we have developed a new chemical toolbox containing fluorescent dyes with diverse structural, chemical and spectral properties. As the design of these sets of fluorescent dyes is unbiased towards any particular analyte, screening of these dyes against variety of analytes can be used to develop new in vitro sensors and live cell imaging probes. Our simple but efficient solid phase methodology may be applied to design and synthesize new fluorescent libraries.

(2) In order to observe the FRET phenomenon, a substantial overlap between the emission wavelength of donor and the excitation wavelength of acceptor is required. This energy overlap supports a smooth energy transfer from donor to acceptor. This energy transfer in such systems could occur either through bonds or through-space[1]. The FRET efficiency also depends on the proximity between the donor and acceptor[2]. Although research has been carried out to evaluate the workings of FRET, the exact mechanism of FRET is still unclear. There is a lot of controversy over whether FRET occurs through space or through bond energy transfer. However after evaluation of the photo physical properties of CXBD, AXBD and AXBY libraries, we assume that FRET does not occur through a single mechanism. A suitable computational study of this large and versatile sets of FRET compounds would help us to evaluate the detail mechanism of the FRET phenomenon.

(3) We have successfully developed the artificial tongue based on the concept of colorimetric dye array to discriminate highly cross-reactive samples like sugars. However, these colorimetric dyes have lower sensitivity when compared to the fluorescent dyes. In order to improve the sensitivity of the artificial tongue, we could move forward to use fluorescent dyes instead of colorimetric dyes. After getting highly

sensitive fluorescent dyes, our main focus will be on the analysis of real samples containing highly complex mixtures of analytes. This artificial tongue project could further extend the quality control of different foods and drinks including drinking water.

5.3 References

1. Jiao, G. S., Thoresen, L. H., and Burgess, K. (2003) Fluorescent, through-bond energy transfer cassettes for labeling multiple biological molecules in one experiment. *Journal of the American Chemical Society 125*, 14668-9.

2. Wu, L., Loudet, A., Barhoumi, R., Burghardt, R. C., and Burgess, K. (2009) Fluorescent cassettes for monitoring three-component interactions in vitro and in living cells. *Journal of the American Chemical Society 131*, 9156-7.